

WASM: Minerals, Energy and Chemical Engineering

**Natural Metal/Oxides for Catalytic Oxidation of Persistent Organic
Pollutants (POPs) in Contaminated Water and Soil**

ZhengXin Yao
0000-0002-3391-6475

**This thesis is presented for the Degree of
Doctor of Philosophy (Chemical Engineering)
of
Curtin University**

November 2021



WA School of Mines: Minerals, Energy and Chemical Engineering

FACULTIES OF SCIENCE AND ENGINEERING

**Natural metal/oxides for catalytic oxidation of persistent
organic pollutants (POPs) in contaminated water and soil**

ZhengXin Yao

0000-0002-3391-6475

**This thesis is presented for the Degree of
Doctor of Philosophy of Curtin University**

Supervisor:

Prof. Shaobin Wang

Prof. Shaomin Liu

Prof. Hongqi Sun

Prof. Hussein Znad

November 2021



Declaration

To the best of my knowledge and belief this thesis contains no material previously published by any other person except where due acknowledgment has been made.

This thesis contains no material which has been accepted for the award of any other degree or diploma in any university.

Signature: _____ (ZhengXin Yao)

Date: _____



Acknowledgement

First of all, I would like to express my most sincere thanks to my supervisor Prof. Shaobin Wang. Prof. Wang is the guide to my doctoral subject. He is always so approachable and patiently answers the problems I encountered in my research.

Equally, I owe my most enthusiastic gratitude to supervisor Prof. Shaomin Liu. Prof. Liu gives me all those constructive suggestions about my research from day one of my Ph.D. study. Prof. Liu encouraged me and helped me a lot to complete the final stage of my Ph.D. period in my most difficult time. I feel quite lucky and proud to be his student.

Prof. Hongqi Sun offers me the inspiration and warm encouragement. It is Prof. Sun who supervised me how to design the experiments. I am very grateful to Prof. Sun for helping me establishing scientific research awareness.

I am also very grateful to Dr. Lihong Liu, an outstanding female researcher. She is very kind and gives me great help in academic and daily life.

At the same time, I would like to thank Dr. Xiaoguang Duan. As the post-doctor fellow of our team, he unites our group and helps us to carry out experiments, giving us many academic and daily guidance. In addition, I would like to extend my most sincere gratitude to Dr. Wenjie Tian and Dr. Huayang Zhang, as the senior ones in the group, they give me tremendous help in my research. Similarly, Dr. Chen Wang, Dr. Jian Kang, Dr. Xiaochen Guo, Dr. Qi Yang, Dr. Hao Tian, and Dr. Yazi Liu also give me many suggestions on the academic path. Besides, I would like to express my deep gratitude to my colleagues for their generous help during the research process: Jiaquan Li, Xinyuan Xu, Hong Wu, Kai Wang, Jinqiang Zhang, Claudia Li, Dr. Liang Zhao, Prof. Lingbao Xing, Dr. Yu Yin, and ShiShu Zhu. And Hillary Christensen Zhen Hui Ho is an excellent undergraduate student who helped me carry out some experiments and achieved good results.

Ning Han and Pengyun Liu are my best friends, and their company is an important reason I can come throughout my Ph.D. career. I also want to thank my friends during my Ph.D.: Fuping Li, Xin Pang, Qiqing Shen, Mingyang Li, Dr. Sui Boon Liaw, Dr. Min Ao, Xiaojie Li, Qiaoran Liu, Yingping Pang, Jinxiu Cao, Wenran Gao, Wei Chen,



Prof. Ruchuan Jiang, Prof. Qiqing Song. At the same time, I would like to express my gratitude to Prof. Di Li for his academic assistance.

For the technicians, I would like to thank Dr. Roshanak Doroushi and Xiao Hua for their substantial support in the experiments. In addition, I would like to thank Elaine Miller, Veronica Avery, Dr. Matthew Rowles, and Kelly Merigot for their help in the tests.

I want to express my deepest love to my partner Ruofei Chen. Without her, I could not persevere in adversity and complete this thesis. Thank you very much for your company in life and academic guidance.

I am very grateful to my parents for bringing me to this world and raising me up. Meanwhile, I would like to thank my uncle and aunt for enlightening me in my academic career. During my Ph.D. period, I lost my grandfather (father's father) and grandmother (mother's mother), and the only surviving grandmother (father's mother) also suffered a severe accident resulting in a comminuted fracture and underwent joint replacement surgery. Fortunately, after a long recovery training, she has recovered part of her mobility. In addition, to all the unnamed family members who helped me grow up, thank you for all support and care you give me. Love you all.

I really appreciate my mentors', colleagues', friends' and families' help and understanding when I was in trouble, without them I could not survive. This thesis not only condenses my efforts, but also condenses the kindness and help of each of them. Thank Gods for letting me have such a wonderful Ph.D. career.



Abstract

The severe environmental pollution in modern society urgently calls for efficient protocols for environmental remediation. Sulfate radical based advanced oxidation processes (SR-AOPs) are proved a promising eco-friendly technology for in situ treatment of refractory organics or persistent organic pollutants (POPs), with advantages including mild degradation conditions, high efficiency, wide application range and little secondary pollution. Peroxymonosulfate (PMS)-based advanced oxidation processes (AOPs) have emerged as a novel wastewater treatment strategy due to production of reactive oxygen species (ROSs) with high redox potential. PMS could be activated by various synthetic catalysts containing transition metals such as Co, Fe, Ni, Ag, Cu and Mn. However, the application of this remediation technology is largely constrained by the high material cost due to the complex synthetic processes of these transitional or precious metals or non-metal catalysts used for PMS activation. Whereas the high cost of persulfate activation is a "bottleneck" restricting the promotion of SR-AOPs. This remediation technology will be greatly advanced if the widely available natural minerals can be used directly as the catalyst. In this PhD project, natural minerals consisting of transition metal elements were employed as the substitute for conventional synthetic metal catalysts and proven to be effective for PMS activation in organic degradation in aqueous and soil environment, which may enable large scale applications to markedly reduce the processing cost and have great development potential and broad prospects. Manganese ore and bauxite were investigated for their catalytic performance in PMS activation for the oxidative degradation of organic pollutants including phenol, methylene blue (MB), rhodamine B (RB) and tetrabromobisphenol A (TBBPA). Experimental results indicate that these ores show an excellent catalytic activity during the oxidation processes, manifesting the wide applicability towards the removal of different types of pollutants. The degradation rate using the tested manganese ore/PMS system increased with the reaction temperature and pH value of the initial solution. These ore particles were characterized by X-ray diffraction (XRD), Brunauer–Emmett–Teller (BET), X-ray photoelectron spectroscopy (XPS), and scanning electron microscope (SEM) techniques. Iron oxides, manganese oxide and cobalt oxides have been identified as excellent catalysts for PMS activation. Furthermore, electron paramagnetic resonance (EPR) spectra reveal that ore/PMS is a



radical-based system where sulfate and hydroxyl radicals with strong oxidative potentials contribute to the degradation of organic pollutants. In addition, the concentration of metals in treated water meets the WHO and EU standards for drinking water, verifying this catalytic system is environmentally safe. Catalyst/ Al_2O_3 hollow fibre composites were prepared in the research as a synthetic catalyst, and was used to compare the efficiency and cost with the natural catalysts. In the comparison of efficiency and financial viability, natural ores show great advantages. This work also investigated manganese ore (MO) /peroxymonosulfate-based advanced oxidation processes (AOPs) as in-situ remediation technology to degrade organic pollutants in soil. The experiments were conducted in a home-made liquid-solid reactor. The tetrabromobisphenol A (TBBPA) removal efficiency was systematically studied with varying pollutant amount, sand volume, natural ore catalyst loading dosage and water washing flow rate. Results show that TBBPA in the sand wash water could be effectively degraded by this MO/PMS system with extremely low cost in comparison with synthetic catalysts containing transition metals. This study advances the fundamental understanding of metal ore catalysts and promotes their application in practical environment remediation.



Table of Contents

Declaration.....	i
Acknowledgement	ii
Abstract.....	iv
Table of Contents.....	vi
Chapter 1. Introduction.....	1
1.1 Background of persistent organic pollutants.....	1
1.2 Research objectives.....	4
1.3 Thesis organization.....	5
References.....	6
Chapter 2. Literature review.....	10
2.1 Introduction.....	10
2.2 Advanced oxidation processes.....	11
2.2.1 Ozone oxidation.....	12
2.2.2 Catalytic wet air oxidation.....	12
2.2.3 Photochemical oxidation.....	13
2.2.4 Sonochemical oxidation.....	13
2.2.5 Electrochemical oxidation.....	13
2.2.6 Fenton and Fenton-like oxidation method.....	14
2.3 Peroxymonosulfate based oxidation technology.....	15
2.3.1 Physical activation of peroxymonosulfate.....	16
2.3.2 Chemical activation of peroxymonosulfate.....	17
2.4 Metal catalysts for peroxymonosulfate activation.....	18
2.4.1 Conventional metal catalysts.....	18
2.4.2 Natural metal ore catalysts.....	19
2.5 Conclusions.....	20



References.....	21
Chapter 3. Natural manganese ore for efficient removal of organic pollutants via catalytic peroxymonosulfate advanced oxidation.....	31
Abstract.....	31
3.1 Introduction.....	32
3.2 Experimental Section.....	33
3.3 Results and Discussion.....	35
3.4 Conclusions.....	42
References.....	43
Chapter 4 Reactive oxygen species-induced degradation of organic contaminants by peroxymonosulfate activation over natural bauxite ore.....	48
Abstract.....	48
4.1 Introduction.....	49
4.2 Experimental Sections.....	50
4.3 Results and Discussions.....	52
4.4 Conclusions.....	58
References.....	59
Chapter 5. Efficient removal of organic pollutants by ceramic hollow fibre supported composite catalyst.....	62
Abstract.....	62
5.1 Introduction.....	63
5.2 Experimental Section.....	64
5.3 Results and Discussions.....	68
5.4 Conclusions.....	83
References.....	85
Chapter 6 Catalytic performance of natural metal ore in peroxymonosulfate activation for soil remediation and its financial feasibility.....	90
Abstract.....	90
6.1 Introduction.....	91



6.2 Experimental Section	93
6.3 Results and Discussion	95
6.4 Conclusions.....	102
References.....	103
Chapter 7 Conclusions and recommendations	105
7.1 Conclusions.....	105
7.2 Perspectives and suggestions for future research.....	106
Appendix I: Attribution Tables	108
Appendix II: Copyright Permission Statements	109



Chapter 1. Introduction

1.1 Background of persistent organic pollutants

The rapid development of industrialization and urbanization in modern society has greatly improved the quality of human life, whereas it meanwhile has increased the emission of man-made pollutants from booming human activities to an unprecedented level,[8, 9] which far exceeds the self-purification capacity of natural ecosystems.[3, 4] Then the consequent serious pollution of air, soil and water across the world has become a leading risk factor for human survival. The resulting humanitarian disasters are numerous. In term of water environment, water pollution has made billions of people unable to obtain safe water worldwide,[5] which may bring about infectious diseases (cholera, malaria, dysentery, diarrhoea, hepatitis A, etc.) and exacerbate malnutrition especially childhood stunting.[10] As a result, over one million deaths are caused by unsafe water sources each year.[11, 12] Therefore, the United Nations (UN) has included access to safe water in the Millennium Development Goals.[6, 7] As shown in Figure 2.1, low-income countries have become the worst-hit area of unsafe water. Furthermore, around one in four people worldwide lack access to safe drinking water at present.[13] In view of the ever-increasing water demand and ever-deteriorating water system, there is still a long way to achieve the Sustainable Development Goals (SDGs) Target 6 to ‘Ensure availability and sustainable management of water and sanitation for all by 2030’. The ever-deteriorating environmental pollution poses serious threats to human survival. Hence, the development of advanced environment remediation and recovery technologies is of great necessity.

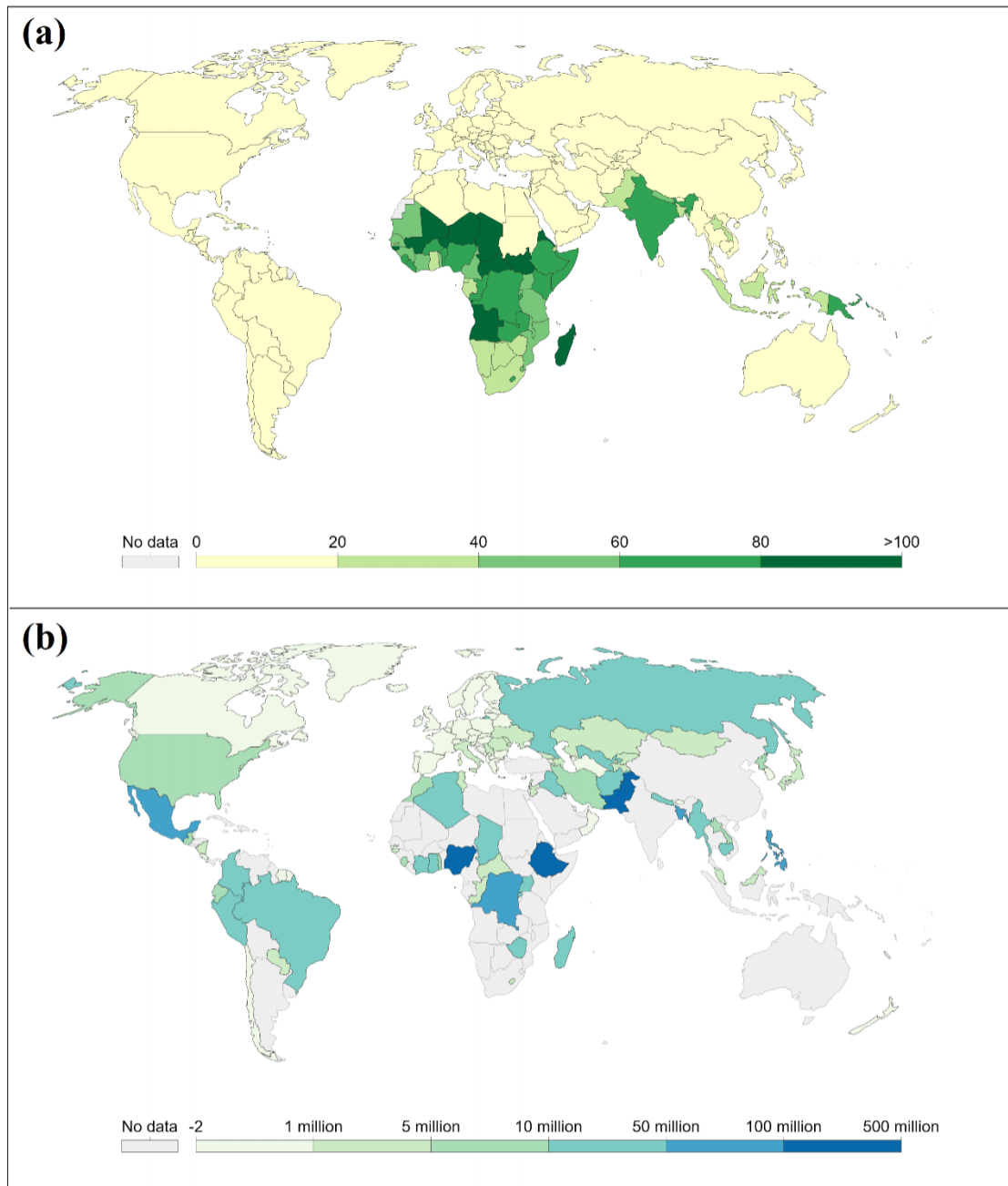


Figure 1.1. (a) Death rates from unsafe water sources (measured as the number of deaths per 100,000 individuals).[12] (b) Number of people without access to safe drinking water.[13]

Among a variety of contaminants, persistent organic pollutants (POPs), a type of substances normally used for industrial or pesticide purposes such as aldrin, chlordane, hexachlorobenzene (HCB) and polychlorinated biphenyls (PCBs), have attracted growing public attention since the second half of the last century.[14, 15] POPs first aroused widespread concern as Rachel Carson described the problem of reducing birds



and other animal species ascribed to pesticides use in her book *Silent Spring* in 1962. In response to the ever-increasing food demand caused by the population explosion since the Industrial Revolution, a large number of pesticides and fertilizers were used in the agricultural production process due to the limitations of people's recognition at that time, which consist of certain kinds of POPs like dichlorodiphenyltrichloroethane (DDT).[16, 17] Most POPs are highly toxic or even carcinogenic and difficult to decompose in the natural environment. They can exist in the environment for a long time, migrate to all corners of the earth, and accumulate through the food chain, leading to harmful effects on the environment and human health. Noteworthy that for human beings at the top of the biological chain, the accumulated toxicity inside the body is more than 70,000 times larger than the original, leading to premature aging, deformity or even death. [18-20] Therefore, POPs have been widely concerned by environmental and health departments. Specially, under the auspices of the United Nations Environment Programme (UNEP), the Stockholm Convention on Persistent Organic Pollutants has entered into force since 2004 to urge the elimination of POPs.[16, 17]

Therefore, researchers are struggling to solve the problem of POPs pollution through physical, chemical and biological methods. In recent decades, advanced oxidation processes (AOPs) have drawn extensive interest and been proved a promising technology for in-situ environment remediation. Several oxidants such as ozone (O_3), hydrogen peroxide (H_2O_2), peroxomonosulfate (PMS) and peroxydisulfate (PDS) can be employed in AOPs to produce reactive species like superoxide, hydroxyl and sulfate radicals, which are of strong oxidative potentials and capable of decomposing organic contaminants.[31, 32] Specially, sulfate radical based AOPs (SR-AOPs) systems can achieve a higher oxidative potential and a broad applicable pH value range.[33]

Based on the literature, metal oxides play an important role in SR-AOPs as the catalysts for the activation of persulfates to generate sulfate radicals.[34, 35] Transition metals and their compounds, containing metals such as Co, Fe, Ni, Ag, Cu and Mn, well known for the superior homogeneous and heterogeneous catalytic activity, have been proven to be highly effective catalysts to activate PMS.[36, 37] However, these metal catalysts do not exist in nature but need complex synthetic processes and hence are too expensive to be employed in a large-scale application.

Therefore, the search for other more economical and accessible catalysts is of great necessity. A feasible alternative to conventional metal catalysts is natural ores. Previous



research demonstrated that minerals contain transition metals and their compounds for instance iron, cobalt and manganese ores have great potential for the degradation of organic pollutants via advanced oxidation reactions.[38, 39] In addition, Western Australia is the main mining area in Australia and abundant in mineral deposits such as magnetite, bauxite and ferromanganese, most of which contain various transition metal elements.[40] Moreover, the low cost and abundance provide these natural ores with incomparable advantages against synthetic catalysts. Therefore, the locally produced cheap natural minerals, which contain transitional elements, could be used as the substitutes for expensive synthetic metal catalysts to explore the feasibility of large-scale in situ processing of PMS has become a possible research direction.

1.2 Research objectives

The purpose of this research is to investigate the feasibility of using natural metal ore catalysts instead of synthetic ones for the heterogeneous activation of peroxomonosulfate (PMS) to degrade persistent organic pollutants in aqueous and soil environment, and to discover the prospects of this catalytic system for large-scale application in in-situ remediation projects. At the same time, this research also aims to explore the mechanisms involved in natural metal ore/persulfate catalytic system. The specific objectives of this research are as follows.

1. Collecting and preparing several natural metal ore and synthetic catalysts for research.
2. Utilizing the selected natural ore samples as a heterogeneous catalyst for the activation of PMS to decompose organic pollutants such as rhodamine B (RB), tetrabromobisphenol A (TBBPA), quinclorac, etc.
3. Determining the active sites of natural ore catalyst for PMS activation and the reaction mechanism in catalytic oxidation process.
4. Evaluating the performance of natural ore and synthetic metal catalysts in organics degradation and comparing their advantages and disadvantages.
5. Studying the feasibility of natural ore catalyst with superior catalytic activity and stability for in situ remediation of contaminated soil and water.



1.3 Thesis organization

This thesis is composed of seven chapters, including introduction, literature review, results and discussions (four chapters), conclusions and perspectives for future studies.

Chapter 1 — Introduction — provides a concise description about the background and treatment methods of POPs. In addition, the research objectives and organization structure of this thesis are present in this chapter as well.

Chapter 2 — Literature review — gives a comprehensive summary of the main research history and progress on POPs and AOPs. Besides, the current research status of synthetic catalysts and natural minerals in persulfates activation are also described.

Chapter 3 — Natural manganese ore catalyst for effective removal of organic pollutants via peroxymonosulfate based advanced oxidation. — investigates the performance of manganese ore catalysts in PMS activation for the oxidative degradation of POPs as well as the effect of reaction conditions and catalytic mechanisms involved.

Chapter 4 — Reactive oxygen species-induced degradation of organic contaminants by peroxymonosulfate activation over natural bauxite ore. — investigates the catalytic activity, impact factors and reaction mechanisms of bauxite/PMS system during the oxidative degradation of organic pollutants.

Chapter 5 — Efficient removal of organic pollutants by ceramic hollow fibre supported composite catalyst. (*Sustainable Materials and Technologies*, 2019; 20, e00108.) — evaluates the catalytic performance of the synthetic $\text{TiO}_2/\text{Al}_2\text{O}_3$ composite hollow fiber in PMS based advanced oxidation of organic pollutants.

Chapter 6 — Catalytic performance of natural metal ore in peroxymonosulfate activation for soil remediation and its financial feasibility. — studies the applicability of natural metal ore/PMS catalytic system towards the removal of organic pollutants in soil environment and discuss the financial feasibility of this system.

Chapter 7 — Conclusions and perspectives — summarizes the main findings of this work and provides suggestions for follow-up research in related fields.



References

1. Dunnet, G., *Oil pollution and seabird populations*. Philosophical Transactions of the Royal Society of London. B, Biological Sciences, 1982. **297**(1087): p. 413-427.
2. Bränvall, M.-L., et al., *Four thousand years of atmospheric lead pollution in northern Europe: a summary from Swedish lake sediments*. Journal of Paleolimnology, 2001. **25**(4): p. 421-435.
3. Xueqin, M., *A Historical Study on the Environmental Pollution and Prevention of the Western Countries Since the Industrial Revolution [J]*. World History, 2000. **6**: p. 20.
4. Fouquet, R. and P.J. Pearson, *A thousand years of energy use in the United Kingdom*. The Energy Journal, 1998. **19**(4).
5. Jury, W.A. and H.J. Vaux Jr, *The emerging global water crisis: managing scarcity and conflict between water users*. Advances in agronomy, 2007. **95**: p. 1-76.
6. Onda, K., J. LoBuglio, and J. Bartram, *Global access to safe water: accounting for water quality and the resulting impact on MDG progress*. International journal of environmental research and public health, 2012. **9**(3): p. 880-894.
7. Gleick, P.H., *Global freshwater resources: soft-path solutions for the 21st century*. Science, 2003. **302**(5650): p. 1524-1528.
8. Candelone, J.P., et al., *Post-Industrial Revolution changes in large-scale atmospheric pollution of the northern hemisphere by heavy metals as documented in central Greenland snow and ice*. Journal of Geophysical Research: Atmospheres, 1995. **100**(D8): p. 16605-16616.
9. Nriagu, J.O., *A history of global metal pollution*. Science, 1996. **272**(5259): p. 223-223.
10. Prüss-Ustün, A., et al., *Burden of disease from inadequate water, sanitation and hygiene for selected adverse health outcomes: An updated analysis with a focus on low- and middle-income countries*. International Journal of Hygiene and Environmental Health, 2019. **222**(5): p. 765-777.
11. Murray, C.J.L., et al., *Global burden of 87 risk factors in 204 countries and territories, 1990–2019: a systematic analysis for the Global Burden of Disease Study 2019*. The Lancet, 2020. **396**(10258): p. 1223-1249.



12. Stanaway, J.D., et al., *Global, regional, and national comparative risk assessment of 84 behavioural, environmental and occupational, and metabolic risks or clusters of risks for 195 countries and territories, 1990–2017: a systematic analysis for the Global Burden of Disease Study 2017*. The Lancet, 2018. **392**(10159): p. 1923-1994.
13. (UNICEF), W.H.O.W.a.t.U.N.C.s.F., *Progress on household drinking water, sanitation and hygiene 2000-2020: Five years into the SDGs*. 2021.
14. Wania, F. and D. Mackay, *Peer reviewed: tracking the distribution of persistent organic pollutants*. Environmental science & technology, 1996. **30**(9): p. 390A-396A.
15. Kelce, W.R., et al., *Persistent DDT metabolite p, p'-DDE is a potent androgen receptor antagonist*. Nature, 1995. **375**(6532): p. 581-585.
16. Kolok, A.S., *POPs and Silent Spring*, in *Modern Poisons*. 2016, Springer. p. 123-130.
17. Paull, J., *Rachel Carson, a voice for organics-the first hundred years*. Elementals: Journal of Bio-Dynamics Tasmania, 2007. **86**: p. 37-41.
18. Beard, J. and A.R.H.R. Collaboration, *DDT and human health*. Science of the total environment, 2006. **355**(1-3): p. 78-89.
19. Qing Li, Q., et al., *Persistent organic pollutants and adverse health effects in humans*. Journal of Toxicology and Environmental Health, Part A, 2006. **69**(21): p. 1987-2005.
20. Damstra, T., et al., *Persistent organic pollutants: potential health effects?* Journal of Epidemiology & Community Health, 2002. **56**(11): p. 824-825.
21. Jones, K.C. and P. De Voogt, *Persistent organic pollutants (POPs): state of the science*. Environmental pollution, 1999. **100**(1-3): p. 209-221.
22. Vallack, H.W., et al., *Controlling persistent organic pollutants—what next?* Environmental Toxicology and Pharmacology, 1998. **6**(3): p. 143-175.
23. Verma, S. and S. Jayakumar, *Impact of forest fire on physical, chemical and biological properties of soil: A review*. proceedings of the International Academy of Ecology and Environmental Sciences, 2012. **2**(3): p. 168.
24. Kumar, A., et al., *Review on bioremediation of polluted environment: a management tool*. International journal of environmental sciences, 2011. **1**(6): p. 1079-1093.
25. Shishir, T., N. Mahbub, and N. Kamal, *Review on bioremediation: a tool to resurrect the polluted rivers*. Pollution, 2019. **5**(3): p. 555-568.



26. Zhao, C., et al., *Application of coagulation/flocculation in oily wastewater treatment: A review*. Science of The Total Environment, 2020: p. 142795.
27. Obotey Ezugbe, E. and S. Rathilal, *Membrane technologies in wastewater treatment: a review*. Membranes, 2020. **10**(5): p. 89.
28. Kyzas, G.Z. and K.A. Matis, *Methods of arsenic wastes recycling: Focus on flotation*. Journal of Molecular Liquids, 2016. **214**: p. 37-45.
29. Ahmed, M.B., et al., *Progress in the biological and chemical treatment technologies for emerging contaminant removal from wastewater: a critical review*. Journal of hazardous materials, 2017. **323**: p. 274-298.
30. Lofrano, G., et al., *Chemical and biological treatment technologies for leather tannery chemicals and wastewaters: A review*. Science of the Total Environment, 2013. **461**: p. 265-281.
31. Salimi, M., et al., *Contaminants of emerging concern: a review of new approach in AOP technologies*. Environmental monitoring and assessment, 2017. **189**(8): p. 1-22.
32. Guan, R., et al., *Principle and application of hydrogen peroxide based advanced oxidation processes in activated sludge treatment: A review*. Chemical Engineering Journal, 2018. **339**: p. 519-530.
33. Yang, Q., et al., *Recent advances in photo-activated sulfate radical-advanced oxidation process (SR-AOP) for refractory organic pollutants removal in water*. Chemical Engineering Journal, 2019. **378**: p. 122149.
34. Giannakis, S., K.-Y.A. Lin, and F. Ghanbari, *A review of the recent advances on the treatment of industrial wastewaters by Sulfate Radical-based Advanced Oxidation Processes (SR-AOPs)*. Chemical Engineering Journal, 2020: p. 127083.
35. Guerra-Rodríguez, S., et al., *Assessment of sulfate radical-based advanced oxidation processes for water and wastewater treatment: a review*. Water, 2018. **10**(12): p. 1828.
36. Sukhomlinov, D., et al., *Distribution of Ni, Co, precious, and platinum group metals in copper making process*. Metallurgical and Materials Transactions B, 2019. **50**(4): p. 1752-1765.
37. Ghanbari, F. and M. Moradi, *Application of peroxymonosulfate and its activation methods for degradation of environmental organic pollutants*. Chemical Engineering Journal, 2017. **310**: p. 41-62.



38. Yang, G.C., Y.-H. Chiu, and C.-L. Wang, *Integration of electrokinetic process and nano-Fe₃O₄/S₂O₈²⁻ oxidation process for remediation of phthalate esters in river sediment*. *Electrochimica Acta*, 2015. **181**: p. 217-227.
39. Fe₃O₄, M., *carbon sphere/cobalt composites for catalytic oxidation of phenol solutions with sulfate radicals for industrial wastewater treatment* Wang, Yuxian; Sun, Hongqi; Ang, Ha Ming; Tade, Moses O.; Wang, Shaobin. *Chemical Engineering Journal (Amsterdam, Netherlands)*, 2014. **245**: p. 1-9.
40. Maxwell, P., *The end of the mining boom? A Western Australian perspective*. *Mineral Economics*, 2018. **31**(1): p. 153-170.

Every reasonable effort has been made to acknowledge the owners of copyright material. I would be pleased to hear from any copyright owner who has been omitted or incorrectly acknowledged.



Chapter 2. Literature review

2.1 Introduction

Environmental pollution issues have raised a global concern. Noteworthy that with the rapid development of human society, the amount of harmful substances released by human activities into the environment since the industrial revolution has far exceeded the sum of the previous thousands of years of human history. The pollution of the environment has reached an unprecedented level, which poses serious risk to the ecosystem and human health.[1-4] Among a variety of contaminants, persistent organic pollutants (POPs) have aroused great concern all over the world. POPs pollution, along with the ozone hole and the greenhouse effect, are regarded as the three major environmental issues that affect human survival and health in the 21st century. POPs have the characteristics of persistence, long-distance migration, bioaccumulation and high toxicity.[5] Especially in modern society, large quantities of POPs pollutants are discharged with the rapid pace of industrialization and urbanization, which has caused serious pollution to the atmosphere, water and soil.

In order to safeguard human health and ecological safety from POPs, several treatment methods have been investigated to remove them from the environment or convert them into low-toxic or even non-toxic matter, including bioremediation, physical aggregation, and chemical reaction. [6-8] Bioremediation methods like activated sludge method and biofilm method are low cost options, whereas the biological treatment cycle takes long and the ability to eliminate highly toxic and refractory pollutants is limited.[9-11] Physical methods such as air flotation, coagulation, adsorption and membrane filtration can easily enrich the harmful substances from one phase to another, but further treatment processes are required and the applicability is fairly restricted by equipment and other conditions.[12-14] Meanwhile, chemical methods for instance oxidation and reduction can effectively decompose the pollutants, and present high efficiency as well as superior applicability towards diverse pollutants.[15, 16] Especially advanced oxidation processes (AOPs), which utilize superoxides to generate reactive species of high oxidative potentials and can totally break down most organic pollutants, have been proved a promising strategy for in-situ environment remediation.



In this study, several representative organic pollutants were selected for further investigation. Methylene blue (MB) is a blue dye that has a wide range of applications in textile printing and other industries. As an aniline substance, its amino group is connected to the aromatic ring. Because of its high melting point and structural stability, methylene blue is difficult to degrade in the natural environment.[17] Studies show that MB would exert certain harmful effects on the human body, including but not limited to vomiting, skin irritation, and respiratory diseases.[18] Rhodamine B (RB) is also a kind of dye, mainly used in scientific research or as a herbicide marker in industrial production.[19] It is classified as a carcinogen, and the contact with skin or eyes may also cause neurotoxic damage. Similarly, due to the high stability and non-biodegradability, rhodamine B exists widely as a xenobiotic in the biological world.[20, 21] Phenol has been gradually widely used in petrochemical and medicine industry since being discovered in the 19th century, and it is commonly employed as a representative of aromatic organic compounds in the field of organics degradation research.[22-24] Tetrabromobisphenol A (TBBPA) is normally used as a flame retardant in circuit boards. Although a small amount of exposure would not cause serious diseases, studies have shown that it may result in some cell dysfunctions, so it has been tracked by the EU environmental protection agency.[25-28]

2.2 Advanced oxidation processes

Advanced oxidation technology, also known as deep oxidation technology, is a highly efficient environmental remediation method characterized by the generation of hydroxyl radicals ($\cdot\text{OH}$) with high redox potential (1.8–2.7 V).[29, 30] During the oxidation process, a large number of hydroxyl radicals are produced as an intermediate product, which can induce the continuation of subsequent chain reactions.[31] AOPs can tackle most organic pollutants including intractable organics like macromolecules with poor biodegradability, and oxidize them into low-toxic or non-toxic small molecular substances, without producing secondary pollution.[32, 33] Especially, AOPs have great advantages in the treatment of environmental hormone pollutants and other trace harmful chemical substances.[34-36] Besides, as a kind of physical-chemical treatment process, AOPs could be easily controllable. In summary, AOPs can completely mineralize or decompose most organic matter and have broad application prospects in environment remediation.[33, 37] By utilizing various superoxides for instance air, oxygen (O_2), ozone (O_3) and hydrogen peroxide (H_2O_2), active hydroxyl



radicals can be produced in physical and chemical processes such as high temperature and high pressure, electricity, sound, light irradiation and catalysts.[38-41] According to the manners of generating free radicals and the different reaction conditions, AOPs can be mainly classified into ozone oxidation, catalytic wet air oxidation (CWAO), photochemical oxidation, sonochemical oxidation, electrochemical oxidation, Fenton and Fenton-like oxidation and so on.[30, 42, 43]

2.2.1 Ozone oxidation

The ozone oxidation method achieves the degradation of organic pollutants through two ways: direct reaction and indirect reaction.[44] The former refers to the direct reaction between pollutants and ozone, which has strong selectivity and generally attacks organics with double bonds such as unsaturated aliphatic hydrocarbons and aromatic hydrocarbon compounds.[45] The latter, with a broader applicable range, undergoes oxidation reaction between pollutants and hydroxyl radicals derived from ozone.[46] Although the ozone oxidation method has a strong ability to decolorize and remove organic pollutants, this method still has great restrictions in wastewater treatment. It has a high operating cost and cannot rapidly achieve a complete degradation in a low dose.[47] Moreover, the intermediate products formed may prevent the oxidation process of ozone.[46]

2.2.2 Catalytic wet air oxidation

The catalytic wet air oxidation method is developed on the basis of the wet air oxidation (WAO) method since the mid-1980s.[48] The CWAO method uses oxygen or air as the oxidizing agent to achieve the oxidative decomposition of the organic pollutants and ammonia through hydroxyl radicals generated under the condition of high temperature, high pressure and catalyst in the liquid phase.[49] Compared with the WAO method, the CWAO method can markedly reduce the oxidation temperature and pressure as well as increase the oxidative degradation capacity via the utilization of catalytic agents.[50] However, its industrial application is still restricted by the complex reacting conditions and the large investment of equipment system.[51] Researchers have found that suitable catalysts can greatly reduce the reaction requirements. In recent years, the study on catalysts especially heterogeneous catalysts has become a hot spot in the field of CWAO research.[49, 50, 52]



2.2.3 Photochemical oxidation

The photochemical oxidation method produces hydroxyl free radicals under ultraviolet (UV) light irradiation, including photo-excited oxidation and photocatalytic oxidation.[53] The photo-excited oxidation method mainly employs H_2O_2 , O_3 , O_2 or air as the oxidant to generate hydroxyl radicals under the action of light radiation; the photocatalytic oxidation method generates hydroxyl radicals by the oxidant under the excitation of light and the catalytic action of the catalysts represented by TiO_2 . [54, 55] However, due to the limitation of the reaction conditions, the photochemical method will produce a variety of aromatic organic intermediates during treating process, resulting in incomplete degradation of the organic substances.[56] Besides, the utilization rate of light energy is relatively low, and the expensive catalyst used is easy to deactivate and difficult to recycle, which may restrict the practical application of this technology to a certain extent.[57, 58] Currently, the immobilization of TiO_2 has become the focus of photocatalysis research, and scholars have studied the replacement of TiO_2 powder with TiO_2 film or composite catalyst film.[59, 60] In addition, the photocatalytic membrane reactor that couples the photocatalytic technology with the membrane separation technology can effectively trap the suspended catalyst, and hence improve the separation and recovery of the catalyst.[61]

2.2.4 Sonochemical oxidation

The sonochemical oxidation method mainly utilizes ultrasonic with a frequency range of 16 kHz–1 MHz to produce ultrasonic cavitation in the solution, forming high-concentration hydroxyl radicals under instantaneous local high temperature and high pressure in a small area to achieve rapid degradation of organic pollutants.[62, 63] Ultrasonic processing alone has a poor treatment effect towards organics with high hydrophilicity and low volatility, and cannot realize a complete removal of total organic carbon (TOC) content.[64] Besides, its cost is fairly high. Therefore, ultrasonic oxidation technology is often combined with other oxidation technologies to reduce the processing costs and improve the purification capacity.[65, 66]

2.2.5 Electrochemical oxidation

The electrochemical oxidation method mainly relies on the oxidative effect of hydroxyl radicals produced using electrochemically active anode materials and direct current.[67] Typically, the solution or suspension of organic substances is placed in an electrolytic



cell, and hydroxyl radicals are generated by the discharge of water molecules on the anode surface to break down the organic matter adsorbed on the anode. [68] Noteworthy that the electroactive anode surface can play a variety of conversion functions including adsorption, catalysis and oxidation during the treatment process. Hence, the selection of appropriate electrode material is the key to ensure the smooth oxidative degradation of pollutants. [69] In the process of electrochemical oxidation, the main competitive side reaction is the water splitting (i.e. oxygen escape) that occurs on the anode surface and its vicinity. Therefore, in order to promote the electrochemical oxidation reaction and improve the efficiency, a high oxygen escape overpotential of the anode is required. [70] Besides, the stability and corrosion resistance in wastewater is required as well. [71] Applicable anode materials found by researchers include graphite, Ti/Pt, Ti/PbO₂ and Ti/SnO₂-Sb composite electrodes. [72] This electrolytic oxidation approach does not involve chemical oxidants and can minimize the emission of wastes, whereas the electricity consumption cost is quite high. [73, 74]

2.2.6 Fenton and Fenton-like oxidation method

Broadly speaking, the Fenton oxidation method is a technology that uses catalysts, light radiation or electrochemistry to generate hydroxyl radicals from H₂O₂ to treat organic contaminants. [75] The conventional Fenton method is generally carried out under the condition of pH 2–5, utilizing the chain reaction between Fe²⁺ and H₂O₂ to generate hydroxyl radicals to further oxidize organics removal. At the same time, Fe²⁺ being oxidized into Fe³⁺ would bring about coagulation precipitation, which may jointly contribute to the removal of contaminants. [76] This method can rapidly degrade organic matter on account of the fast decomposition rate of H₂O₂, whereas it cannot fully mineralize organics and might produce intermediate products, which may form complexes with Fe³⁺ or compete with the generation route of hydroxyl radicals. [77, 78] Meanwhile, the application of conventional Fenton reagent is also restricted by the low utilization rate of H₂O₂ and the pH limit, and the treated water may be colored due to the high concentration of Fe²⁺ in the system. [79, 80] Further, researchers have introduced photoelectric and electrochemical effects into the Fenton reaction system as well as studied the replacement of Fe²⁺ using homogeneous catalysts (e.g. Fe³⁺ and Mn²⁺) and heterogeneous catalysts (e.g. graphite, iron powder, iron and manganese oxide minerals). [81-84] These methods can significantly enhance the oxidative degradation ability of Fenton system towards organic pollutants, and are called Fenton-



like oxidation. Besides, it has been found that adding complexing agents for instance ethylene diamine tetraacetic acid (EDTA) and oxalate ($C_2O_4^{2-}$) to the Fenton system could increase the removal rate of organic matter.[85, 86] As an improvement to the conventional Fenton reagent, the Fenton-like oxidation method has greater development potential.

Researchers have continued to make progress on advanced oxidation technology. Noteworthy that sulfate radical-based advanced oxidation processes (SR-AOPs) using persulfates such as peroxymonosulfate (PMS, or oxone) and peroxydisulfate (PDS) are recently developed for the oxidation treatment of refractory organic pollutants.[87, 88] Besides hydroxyl radicals (redox potential: 1.8–2.7 V), SR-AOPs can also generate sulfate radicals ($SO_4^{\cdot-}$, redox potential: 2.5–3.1 V) with a stronger oxidizing ability as another reactive species to degrade pollutants. Meanwhile, the lifetime of sulfate radicals ($t_{1/2} = 30\text{--}40 \mu\text{s}$) is longer than that of hydroxyl radicals ($t_{1/2} < 1.0 \mu\text{s}$), which affords an excellent mass transfer to pollutants and free radical utilization efficiency.[87, 89, 90] Hence, SR-AOPs have attracted intensive attention.

2.3 Peroxymonosulfate based oxidation technology

Peroxymonosulfate is a white non-toxic solid powder with good solubility in water. On account of its solid form and low volatility, PMS is easier to transport and store than liquid H_2O_2 . Actually, PMS can be regarded as a derivative of H_2O_2 , in which a hydrogen atom is replaced by a sulfonic acid group ($-SO_3^-$) to form HSO_5^- . It has an asymmetric structure ($H-O-O-SO_3^-$), with the distance of O-O bond of 1.497 Å and the bond energy of 377 kJ/mol. Compared with PDS and H_2O_2 , PMS is more susceptible to being stimulated by external factors due to the structural asymmetry, generating sulfate radicals and hydroxyl radicals via electron transfer. Moreover, unlike the traditional Fenton reaction that requires acidic conditions, PMS based oxidation technology can effectively work in a wide pH range. At present, the commonly used PMS agent in experimental study is oxone ($KHSO_5 \cdot 0.5KHSO_4 \cdot 0.5K_2SO_4$), of which the solubility is larger than 250 g/L and the aqueous solution is acidic.[91] As a triple salt, oxone is more stable and safer in operation process.

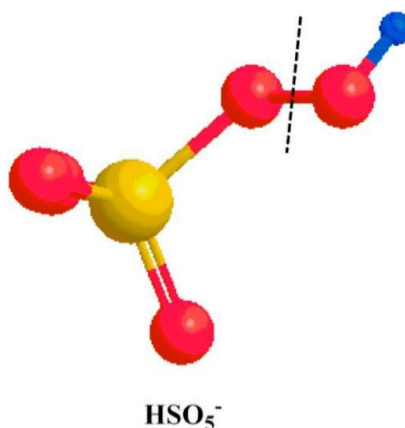


Figure 2.1. The structure of PMS. Yellow color is the sulfur atom, and the red color is the oxygen atom. Dashed line represents the fission position of O-O bond for the formation of sulfate radicals.[92]

2.3.1 Physical activation of peroxymonosulfate

The activation of PMS can be achieved through physical and chemical approaches. Physical activation methods, mostly used as an auxiliary means, utilize external energy such as heat, ultrasonic and light irradiation to break the O-O bond in the PMS to promote the generation of sulfate radicals and hydroxyl radicals.

Heating activation is the main method used in early PMS research.[93] Asif et al. found that up to 60% of algogenic organic matter could be removed via the thermal activating PMS system.[94] Heating activation is a simple method, whereas it is not realistic for normal temperature wastewater and natural water environment treated in situ, so heating activation generally appears as an auxiliary means to activate PMS. Considering the goal of reaching carbon neutrality, this activation mode requiring high energy consumption and high carbon emissions is contrary to the core concept of environmental protection.

Ultraviolet light can also activate PMS to a certain extent, achieving the degradation of organic pollutants with a simultaneous disinfection effect. Ultraviolet light activation of PMS is rarely investigated in experiments and generally studied in combination with photocatalysis.[95] Yang et al. found that although UV itself can degrade azo dye acid orange 7, the degradation efficiency was increased by nearly half once introducing PMS, indicating that UV light can effectively activate PMS to degrade organic pollutants in water. [96]

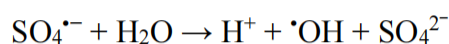
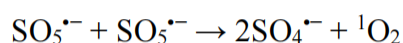
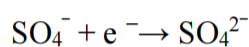
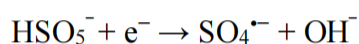
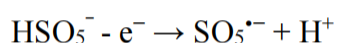


Ultrasound can be used as an auxiliary means to promote the activation of PMS and produce more free radicals. The main parameters include the sound intensity and the sound frequency. In the study of Yin et al., the ultrasonic activating PMS system was used to conduct the catalytic degradation of sulfamethazine. After introducing ultrasound, the efficiency of the ultrasound/PMS system was increased to nearly nine times that of PMS alone and ninety times that of ultrasound alone, with over 99% of contaminants removed within 30 mins. This system could operate effectively in the pH range of 3 to 11. They found that the removal efficiency continues to increase with the ultrasonic power, and the increase gradually slows down, which might be limited by the concentration of hydroxyl radicals in the system.[97] Research by Liu et al. shows that ultrasound can significantly increase the degradation efficiency in PMS system without obvious negative effects.[98]

2.3.2 Chemical activation of peroxymonosulfate

Chemical activation methods mainly utilize transition metal oxides and other inorganic substances like carbon materials for PMS activation to produce sulfate radicals and hydroxyl radicals.

A variety of oxides that includes transition metals such as Mn, Co, and Fe, are reported to have an excellent ability for PMS activation.[99-101] The activation is accomplished by the electron transfer between PMS and metals via the redox cycle as below.[102-104]



Besides, carbon materials such as graphene, activated carbon and carbon nanotubes can effectively activate PMS. Due to the different carbon structure, these materials exhibit different catalytic properties in persulfate activation.[105] Duan et al. found that reduced graphene oxide/PMS system could oxidatively degrade phenol completely within 150 min. [106, 107] Carbon nanotubes (CNTs) can be regarded as graphene coils, while their catalytic performance is much better than graphene. Both single-walled



carbon nanotubes (SWCNTs) and multi-walled carbon nanotubes (MWCNTs) can activate persulfate to oxidize and degrade organic pollutants (especially phenolic compounds), but it is difficult to oxidize and degrade organic substances with electron-withdrawing groups such as nitrobenzene and benzoic acid.[108] In addition, the catalytic activity of CNTs is related to their types. For example, SWCNTs has a higher phenol degradation reaction activity than MWCNTs, which is due to the difference in the specific surface area and active sites.[109] Activated carbon, a simple industrial product with high porosity and specific surface area, is regarded as a cheap substitute for graphene and carbon nanotubes.[108, 110] Although activated carbon has shown acceptable catalytic performance, its degradation efficiency is still too low compared with graphene and carbon nanotubes, so it is often used as a sustainable substrate material in practice.[111, 112]

2.4 Metal catalysts for peroxymonosulfate activation

2.4.1 Conventional metal catalysts

Transition metals and their compounds, well known for the superior homogeneous and heterogeneous catalytic activity, have been proven to be highly effective catalysts to activate PMS.[113, 114] Transition metals generally refer to metal elements in the d-block of the periodic table, which have a partially filled d sub-shell and can form oxides of multiple valence states.[115, 116]

In previous studies, PMS activation was achieved by various synthetic catalysts containing transition metals such as Co, Fe, Ni, Ag, Cu and Mn.[114, 117, 118] Among these metals, cobalt is considered to have the highest catalytic activity against PMS activation, while silver has a relatively low activity.[100, 119] CoO, CoO₂, Co₂O₃, CoO(OH) and Co₃O₄ have all been verified effective to activate PMS and degrade organics.[99] Among them, cobalt oxide and cobalt tetroxide have been studied more broadly due to their good stability, solubility and activation efficiency, exhibiting a good degradation effect on phenolic substances like bisphenol A and parachlorophenol as well as commercial dyes.[120-123] The research on cobalt tetroxide is more advanced. Besides traditional dyes, it can also effectively degrade sulfisoxazole, antibiotics amoxicillin, chloramphenicols and other antibiotics in PMS system.[124-126] Additionally, Co₃O₄ shows a good activity for phenol photodegradation with PMS.[127, 128]



Besides cobalt catalysts, iron catalysts are another hotspot in the field of PMS research due to their relatively low price, which mainly relies on the effect of ferrous and ferric ions that derived from various iron oxide.[89] The catalytic degradation system of cobalt and PMS has a removal rate of nearly 90% for 2,4-dichlorophenoxyacetic acid (2,4-D) within one hour, while the same study shows that ferrous ions can also reach similar capability but with their concentration about one hundred times higher than cobalt ions.[129] Bisphenol A, phenol and rhodamine B are the most common pollutants in the study of iron oxides/PMS system. It was also discovered that phthalate esters (PAEs) could be degraded by $\text{Fe}_3\text{O}_4/\text{S}_2\text{O}_8^{2-}$. [130, 131] Although their performance is lower than that of cobalt catalysts, the cost-effectiveness of iron catalysts is much higher due to the low price. Mixed oxides composed of iron and other metals have demonstrated more efficient degradation ability. [132-134]

Meanwhile, manganese catalysts have been developed for PMS activation. The catalytic activity of the divalent manganese-based materials exhibits excellent stability in a wide temperature range, which basically remains the original state under PMS oxidation after calcination at 600 °C. [135-138] The performance of magnetic $\text{MnO}_2/\text{ZnFe}_2\text{O}_4$ hybrid materials were also employed for catalytic oxidation of organic pollutants. [139-143]

2.4.2 Natural metal ore catalysts

Conventional synthetic metal catalysts are limited by the high cost for a large scale application. [144] In recent years, natural minerals containing transition metal elements such as cobalt ore, iron ore and manganese ore have been studied as the substitutes for synthetic catalysts, demonstrating great potential for organics degradation with PMS system. [145] The low price and abundance of natural ores provides them with incomparable advantages against to these synthetic catalysts. [146]

Iron ranks the fourth most abundant element on the earth and constitutes 5.6 wt% of the crust. [147] As the most economically exploitable ore, commercial iron ore can be mainly categorized into hematite (Fe_3O_4) and hematite (Fe_2O_3). [148, 149] Generally, natural iron ore contains an iron content of 20–30 wt%, and the direct shipping ore (DSO) contains an iron content of 56–62 wt%. [150] Other substandard ore will go through mineral processing to meet the standard of export. [151] Australia especially Western Australia is rich in iron ore. Australia owes the world's largest Economic



Demonstrated Resources (EDR) iron ore at 51, 545 Mt, which accounts for around 28% of worldwide EDR iron ore.[148, 152] A study shows that vanadium-titanium magnetite could effectively degrade bisphenol A via PMS system, while the mineral used is of high grade, which contains iron content of over 30% with the silicon content of merely 4%.[153]

Manganese is the twelfth most abundant element in the Earth's crust and the fourth most widely used metal in commercial products.[128, 154] Almost 300 minerals contains manganese and it is often found with iron, for example, iron ore and bauxite.[155] In other words, manganese is not a free element that exists on its own. Although many minerals containing manganese have been discovered in various geological settings, only several are economically significant.[156] In total, there are three mines in operation and one tailings re-treatment plant in Australia, which produce around 7 million tons manganese ore each year and ranks second in the world.[157, 158]

Besides, approximately thirty cobalt-bearing minerals have been found while a small amount of cobalt can be found in over one hundred kinds of other minerals.[159] China is the dominant producer of cobalt while Australia is ranked number nine in worldwide cobalt production. Cobalt element occurs naturally in two main forms that are Arsenide $\text{Co}(\text{As}_2)$ and cobalt sulfarsenide (CoAsS).[160]

2.5 Conclusions

PMS based advanced oxidation technology is an environmentally friendly treatment method developed in recent years for refractory organics like POPs, which can mineralize organic pollutants into harmless substances. It has advantages including mild degradation conditions, high efficiency, wide application range, and little secondary pollution. Whereas the high processing cost of PMS activation using synthetic catalysts is a "bottleneck" restricting its promotion to a large scale. More recently, natural minerals constituted by transition metal elements have been studied as the substitutes for conventional synthetic metal catalysts and proved effective for PMS activation in organics degradation, which may enable manufactories to markedly reduce the cost. Currently, there is still very limited research on the application of natural metal ore catalysts in PMS system. Considering the great development potential and prospects, related investigation is of great importance to accelerate the industrial application of natural minerals in environment remediation.



References

1. Dunnet, G., *Oil pollution and seabird populations*. Philosophical Transactions of the Royal Society of London. B, Biological Sciences, 1982. **297**(1087): p. 413-427.
2. Bränvall, M.-L., et al., *Four thousand years of atmospheric lead pollution in northern Europe: a summary from Swedish lake sediments*. Journal of Paleolimnology, 2001. **25**(4): p. 421-435.
3. Xueqin, M., *A Historical Study on the Environmental Pollution and Prevention of the Western Countries Since the Industrial Revolution [J]*. World History, 2000. **6**: p. 20.
4. Fouquet, R. and P.J. Pearson, *A thousand years of energy use in the United Kingdom*. The Energy Journal, 1998. **19**(4).
5. Fang, J., et al., *Spatial and temporal trends of the Stockholm Convention POPs in mothers' milk -- a global review*. Environ Sci Pollut Res Int, 2015. **22**(12): p. 8989-9041.
6. Jones, K.C. and P. De Voogt, *Persistent organic pollutants (POPs): state of the science*. Environmental pollution, 1999. **100**(1-3): p. 209-221.
7. Wania, F. and D. Mackay, *Peer reviewed: tracking the distribution of persistent organic pollutants*. Environmental science & technology, 1996. **30**(9): p. 390A-396A.
8. Vallack, H.W., et al., *Controlling persistent organic pollutants—what next?* Environmental Toxicology and Pharmacology, 1998. **6**(3): p. 143-175.
9. Verma, S. and S. Jayakumar, *Impact of forest fire on physical, chemical and biological properties of soil: A review*. proceedings of the International Academy of Ecology and Environmental Sciences, 2012. **2**(3): p. 168.
10. Kumar, A., et al., *Review on bioremediation of polluted environment: a management tool*. International journal of environmental sciences, 2011. **1**(6): p. 1079-1093.
11. Shishir, T., N. Mahbub, and N. Kamal, *Review on bioremediation: a tool to resurrect the polluted rivers*. Pollution, 2019. **5**(3): p. 555-568.
12. Zhao, C., et al., *Application of coagulation/flocculation in oily wastewater treatment: A review*. Science of The Total Environment, 2020: p. 142795.
13. Obotey Ezugbe, E. and S. Rathilal, *Membrane technologies in wastewater treatment: a review*. Membranes, 2020. **10**(5): p. 89.
14. Kyzas, G.Z. and K.A. Matis, *Methods of arsenic wastes recycling: Focus on flotation*. Journal of Molecular Liquids, 2016. **214**: p. 37-45.
15. Ahmed, M.B., et al., *Progress in the biological and chemical treatment technologies for emerging contaminant removal from wastewater: a critical review*. Journal of hazardous materials, 2017. **323**: p. 274-298.
16. Lofrano, G., et al., *Chemical and biological treatment technologies for leather tannery chemicals and wastewaters: A review*. Science of the Total Environment, 2013. **461**: p. 265-281.
17. Schirmer, R.H., et al., *Lest we forget you—methylene blue....* Neurobiology of aging, 2011. **32**(12): p. 2325. e7-2325. e16.
18. Ginimuge, P.R. and S. Jyothi, *Methylene blue: revisited*. Journal of anaesthesiology, clinical pharmacology, 2010. **26**(4): p. 517.



19. Fisher, P., *Review of using Rhodamine B as a marker for wildlife studies*. Wildlife Society Bulletin, 1999: p. 318-329.
20. Al-Buriah, A.K., et al., *Elimination of rhodamine B from textile wastewater using nanoparticle photocatalysts: A review for sustainable approaches*. Chemosphere, 2021: p. 132162.
21. Bhat, S.A., et al., *Highly efficient catalytic reductive degradation of Rhodamine-B over Palladium-reduced graphene oxide nanocomposite*. Chemical Physics Letters, 2020. **754**: p. 137724.
22. Kulkarni, S.J. and J.P. Kaware, *Review on research for removal of phenol from wastewater*. International journal of scientific and research publications, 2013. **3**(4): p. 1-5.
23. Mohammadi, S., et al., *Phenol removal from industrial wastewaters: a short review*. Desalination and Water Treatment, 2015. **53**(8): p. 2215-2234.
24. Schmidt, R.J., *Industrial catalytic processes—phenol production*. Applied Catalysis A: General, 2005. **280**(1): p. 89-103.
25. Deng, J., et al., *Hazardous substances in indoor dust emitted from waste TV recycling facility*. Environmental science and pollution research, 2014. **21**(12): p. 7656-7667.
26. Suh, K.S., et al., *Tetrabromobisphenol A induces cellular damages in pancreatic β -cells in vitro Part A Toxic/hazardous substances & environmental engineering*. 2017.
27. Choi, E.M., et al., *Exposure to tetrabromobisphenol A induces cellular dysfunction in osteoblastic MC3T3-E1 cells Part A Toxic/hazardous substances & environmental engineering*. 2017.
28. Pittinger, C.A. and A.M. Pecquet, *Review of historical aquatic toxicity and bioconcentration data for the brominated flame retardant tetrabromobisphenol A (TBBPA): effects to fish, invertebrates, algae, and microbial communities*. Environmental Science and Pollution Research, 2018. **25**(15): p. 14361-14372.
29. Wang, W., et al., *Different activation methods in sulfate radical-based oxidation for organic pollutants degradation: Catalytic mechanism and toxicity assessment of degradation intermediates*. Science of The Total Environment, 2021: p. 145522.
30. Ma, D., et al., *Critical review of advanced oxidation processes in organic wastewater treatment*. Chemosphere, 2021: p. 130104.
31. Wang, J.L. and L.J. Xu, *Advanced oxidation processes for wastewater treatment: formation of hydroxyl radical and application*. Critical reviews in environmental science and technology, 2012. **42**(3): p. 251-325.
32. Fiaz, A., D. Zhu, and J. Sun, *Environmental fate of tetracycline antibiotics: degradation pathway mechanisms, challenges, and perspectives*. Environmental Sciences Europe, 2021. **33**(1): p. 1-17.
33. Luo, H., et al., *Application of iron-based materials in heterogeneous advanced oxidation processes for wastewater treatment: A review*. Chemical Engineering Journal, 2021. **407**: p. 127191.
34. Schröder, P., et al., *Status of hormones and painkillers in wastewater effluents across several European states—considerations for the EU watch list concerning estradiols and diclofenac*. Environmental Science and Pollution Research, 2016. **23**(13): p. 12835-12866.



35. Gogoi, A., et al., *Occurrence and fate of emerging contaminants in water environment: a review*. Groundwater for Sustainable Development, 2018. **6**: p. 169-180.
36. Ribeiro, A.R., et al., *An overview on the advanced oxidation processes applied for the treatment of water pollutants defined in the recently launched Directive 2013/39/EU*. Environment international, 2015. **75**: p. 33-51.
37. Zhang, X.-W., et al., *Photocatalysis activation of peroxodisulfate over the supported Fe₃O₄ catalyst derived from MIL-88A (Fe) for efficient tetracycline hydrochloride degradation*. Chemical Engineering Journal, 2021. **426**: p. 131927.
38. Mouele, E.S.M., *Degradation of persistent organic pollutants (pharmaceuticals & dyes) by combined dielectric barrier electrohydraulic discharge system and photo catalysts*. 2019.
39. Jain, P., S. Raghav, and D. Kumar, *Advanced Oxidation Technologies for the Treatment of Wastewater*. Applied Water Science: Remediation Technologies, 2021. **2**: p. 469-484.
40. Chaohui, X., et al., *Remove of ammoniacal nitrogen wastewater by ultrasound/Mg/Al₂O₃/O₃*. Chemosphere, 2021: p. 132645.
41. Gautam, P., S. Kumar, and S. Lokhandwala, *Advanced oxidation processes for treatment of leachate from hazardous waste landfill: A critical review*. Journal of Cleaner Production, 2019. **237**: p. 117639.
42. Wu, Q., H. Wang, and C. Yi, *Heterogeneous photocatalytic degradation of organic contaminant in water over high-activity Fe-TS-1 under the radiation of solar light*. Optik, 2018. **158**: p. 1460-1469.
43. Litter, M.I., *Introduction to Oxidative Technologies for Water Treatment*, in *Advanced Nano-Bio Technologies for Water and Soil Treatment*. 2020, Springer. p. 119-175.
44. Ikehata, K. and Y. Li, *Ozone-based processes*, in *Advanced Oxidation Processes for Waste Water Treatment*. 2018, Elsevier. p. 115-134.
45. Beltrán, F. and A. Rey, *Free radical and direct ozone reaction competition to remove priority and pharmaceutical water contaminants with single and hydrogen peroxide ozonation systems*. Ozone: Science & Engineering, 2018. **40**(4): p. 251-265.
46. Rekhate, C.V. and J. Srivastava, *Recent advances in ozone-based advanced oxidation processes for treatment of wastewater-A review*. Chemical Engineering Journal Advances, 2020: p. 100031.
47. Hussain, M., M.S. Mahtab, and I.H. Farooqi, *The applications of ozone-based advanced oxidation processes for wastewater treatment: A review*. Advances in environmental research, 2020. **9**(3): p. 191-214.
48. Zhang, Y. and Y. Wang. *Application and Improvement of Wet Oxidation Technology*. in *IOP Conference Series: Earth and Environmental Science*. 2020. IOP Publishing.
49. Kumari, M. and A.K. Saroha, *Performance of various catalysts on treatment of refractory pollutants in industrial wastewater by catalytic wet air oxidation: A review*. Journal of environmental management, 2018. **228**: p. 169-188.
50. Zhou, L., et al., *Phenolic compounds removal by wet air oxidation based processes*. Frontiers of Environmental Science & Engineering, 2018. **12**(1): p. 1-20.



51. Wang, P., et al., *Nano-hybrid bimetallic Au-Pd catalysts for ambient condition-catalytic wet air oxidation (AC-CWAO) of organic dyes*. Separation and Purification Technology, 2020. **233**: p. 115960.
52. Rocha, R.P., M.F.R. Pereira, and J.L. Figueiredo, *Metal-free carbon materials as catalysts for wet air oxidation*. Catalysis Today, 2020. **356**: p. 189-196.
53. Yang, J., M. Zhu, and D.D. Dionysiou, *What is the role of light in persulfate-based advanced oxidation for water treatment?* Water Research, 2021. **189**: p. 116627.
54. Liu, H., C. Wang, and G. Wang, *Photocatalytic advanced oxidation processes for water treatment: Recent advances and perspective*. Chemistry—An Asian Journal, 2020. **15**(20): p. 3239-3253.
55. Wang, K., et al., *Perovskite Oxide Catalysts for Advanced Oxidation Reactions*. Advanced Functional Materials, 2021: p. 2102089.
56. Wu, C., et al., *Photosonochemical degradation of phenol in water*. Water Research, 2001. **35**(16): p. 3927-3933.
57. Ferguson, C.T. and K.A. Zhang, *Classical Polymers as Highly Tunable and Designable Heterogeneous Photocatalysts*. ACS Catalysis, 2021. **11**(15): p. 9547-9560.
58. Li, X., et al., *Micro/macrostructure and multicomponent design of catalysts by MOF-derived strategy: Opportunities for the application of nanomaterials-based advanced oxidation processes in wastewater treatment*. Science of The Total Environment, 2021: p. 150096.
59. Tung, T.X., et al., *Removing humic acid from aqueous solution using titanium dioxide: A review*. Polish Journal of Environmental Studies, 2018. **28**(2): p. 529-542.
60. Wang, Y.-H., et al., *A Review on the Pathways of the Improved Structural Characteristics and Photocatalytic Performance of Titanium Dioxide (TiO₂) Thin Films Fabricated by the Magnetron-Sputtering Technique*. Catalysts, 2020. **10**(6): p. 598.
61. Koe, W.S., et al., *An overview of photocatalytic degradation: photocatalysts, mechanisms, and development of photocatalytic membrane*. Environmental Science and Pollution Research, 2020. **27**(3): p. 2522-2565.
62. Savun-Hekimoğlu, B. *A review on sonochemistry and its environmental applications. in Acoustics*. 2020. Multidisciplinary Digital Publishing Institute.
63. Cao, H., et al., *Sonochemical degradation of poly-and perfluoroalkyl substances-a review*. Ultrasonics Sonochemistry, 2020: p. 105245.
64. Anandan, S., V.K. Ponnusamy, and M. Ashokkumar, *A review on hybrid techniques for the degradation of organic pollutants in aqueous environment*. Ultrasonics sonochemistry, 2020. **67**: p. 105130.
65. Dheyab, M.A., et al., *Mechanisms of effective gold shell on Fe₃O₄ core nanoparticles formation using sonochemistry method*. Ultrasonics sonochemistry, 2020. **64**: p. 104865.
66. Wood, R.J., J. Lee, and M.J. Bussemaker, *A parametric review of sonochemistry: control and augmentation of sonochemical activity in aqueous solutions*. Ultrasonics sonochemistry, 2017. **38**: p. 351-370.
67. Brito, L.R., et al., *Removal of antibiotic rifampicin from aqueous media by advanced electrochemical oxidation: Role of electrode materials, electrolytes and real water matrices*. Electrochimica Acta, 2021. **396**: p. 139254.



68. Serrano, K.G., *Indirect electrochemical oxidation using hydroxyl radical, active chlorine, and peroxodisulfate*, in *Electrochemical water and wastewater treatment*. 2018, Elsevier. p. 133-164.
69. Shestakova, M. and M. Sillanpää, *Electrode materials used for electrochemical oxidation of organic compounds in wastewater*. *Reviews in Environmental Science and Bio/Technology*, 2017. **16**(2): p. 223-238.
70. Lu, Q. and F. Jiao, *Electrochemical CO₂ reduction: Electrocatalyst, reaction mechanism, and process engineering*. *Nano Energy*, 2016. **29**: p. 439-456.
71. Mandal, P., B.K. Dubey, and A.K. Gupta, *Review on landfill leachate treatment by electrochemical oxidation: drawbacks, challenges and future scope*. *Waste Management*, 2017. **69**: p. 250-273.
72. Tasic, Z., V. Gupta, and M. Antonijevic, *The mechanism and kinetics of degradation of phenolics in wastewaters using electrochemical oxidation*. *Int. J. Electrochem. Sci*, 2014. **9**(7): p. 3473-3490.
73. Martínez-Huitle, C.A. and M. Panizza, *Electrochemical oxidation of organic pollutants for wastewater treatment*. *Current Opinion in Electrochemistry*, 2018. **11**: p. 62-71.
74. Martinez-Huitle, C.A. and S. Ferro, *Electrochemical oxidation of organic pollutants for the wastewater treatment: direct and indirect processes*. *Chemical Society Reviews*, 2006. **35**(12): p. 1324-1340.
75. Brillas, E., *A review on the photoelectro-Fenton process as efficient electrochemical advanced oxidation for wastewater remediation. Treatment with UV light, sunlight, and coupling with conventional and other photo-assisted advanced technologies*. *Chemosphere*, 2020. **250**: p. 126198.
76. Mishra, N.S., et al., *A review on advanced oxidation processes for effective water treatment*. *Current World Environment*, 2017. **12**(3): p. 470.
77. Nidheesh, P.V., R. Gandhimathi, and S.T. Ramesh, *Degradation of dyes from aqueous solution by Fenton processes: a review*. *Environmental Science and Pollution Research*, 2013. **20**(4): p. 2099-2132.
78. Matavos-Aramyan, S. and M. Moussavi, *Advances in Fenton and Fenton based oxidation processes for industrial effluent contaminants control-a review*. *Int. J. Environ. Sci. Nat. Resour*, 2017. **2**(4): p. 1-18.
79. Bokare, A.D. and W. Choi, *Review of iron-free Fenton-like systems for activating H₂O₂ in advanced oxidation processes*. *Journal of hazardous materials*, 2014. **275**: p. 121-135.
80. Diya'uddeen, B.H., A.A. AR, and W.W. Daud, *On the limitation of Fenton oxidation operational parameters: a review*. *International Journal of Chemical Reactor Engineering*, 2012. **10**(1).
81. Neves, L.C., et al., *Phytotoxicity indexes and removal of color, COD, phenols and ISA from pulp and paper mill wastewater post-treated by UV/H₂O₂ and photo-Fenton*. *Ecotoxicology and Environmental Safety*, 2020. **202**: p. 110939.
82. Zhu, Y., et al., *A critical review on metal complexes removal from water using methods based on Fenton-like reactions: Analysis and comparison of methods and mechanisms*. *Journal of Hazardous Materials*, 2021: p. 125517.
83. Poza-Nogueiras, V., et al., *Current advances and trends in electro-Fenton process using heterogeneous catalysts—a review*. *Chemosphere*, 2018. **201**: p. 399-416.



84. Ganiyu, S.O., M. Zhou, and C.A. Martinez-Huitle, *Heterogeneous electro-Fenton and photoelectro-Fenton processes: a critical review of fundamental principles and application for water/wastewater treatment*. Applied Catalysis B: Environmental, 2018. **235**: p. 103-129.
85. De Luca, A., *Fenton and Photo-Fenton like at neutral pH for the removal of emerging contaminants in water and wastewater effluents*. 2016.
86. Hamd, W.S. and J. Dutta, *c0011 Heterogeneous photo-Fenton reaction and its enhancement upon addition of chelating agents 11*. 2020.
87. Giannakis, S., K.-Y.A. Lin, and F. Ghanbari, *A review of the recent advances on the treatment of industrial wastewaters by Sulfate Radical-based Advanced Oxidation Processes (SR-AOPs)*. Chemical Engineering Journal, 2021. **406**: p. 127083.
88. Jia, D., et al., *A review of Manganese (III)(Oxyhydr) Oxides use in advanced oxidation processes*. Molecules, 2021. **26**(19): p. 5748.
89. Xiao, S., et al., *Iron-mediated activation of persulfate and peroxymonosulfate in both homogeneous and heterogeneous ways: a review*. Chemical Engineering Journal, 2020. **384**: p. 123265.
90. Xiong, Z., et al., *Synthesis strategies and emerging mechanisms of metal-organic frameworks for sulfate radical-based advanced oxidation process: A review*. Chemical Engineering Journal, 2021. **421**: p. 127863.
91. Xu, L., et al., *Mechanistic studies on peroxymonosulfate activation by g-C₃N₄ under visible light for enhanced oxidation of light-inert dimethyl phthalate*. Chinese Journal of Catalysis, 2020. **41**(2): p. 322-332.
92. Wang, J. and S. Wang, *Activation of persulfate (PS) and peroxymonosulfate (PMS) and application for the degradation of emerging contaminants*. Chemical Engineering Journal, 2018. **334**: p. 1502-1517.
93. Ahn, Y.-Y., et al., *Chloride-Mediated Enhancement in Heat-Induced Activation of Peroxymonosulfate: New Reaction Pathways for Oxidizing Radical Production*. Environmental Science & Technology, 2021. **55**(8): p. 5382-5392.
94. Asif, M.B., et al., *Allogenic organic matter fouling alleviation in membrane distillation by peroxymonosulfate (PMS): Role of PMS concentration and activation temperature*. Desalination, 2021. **516**: p. 115225.
95. Matafonova, G. and V. Batoev, *Recent advances in application of UV light-emitting diodes for degrading organic pollutants in water through advanced oxidation processes: A review*. Water research, 2018. **132**: p. 177-189.
96. Yang, S., et al., *Degradation efficiencies of azo dye Acid Orange 7 by the interaction of heat, UV and anions with common oxidants: persulfate, peroxymonosulfate and hydrogen peroxide*. Journal of hazardous materials, 2010. **179**(1-3): p. 552-558.
97. Yin, R., et al., *Enhanced peroxymonosulfate activation for sulfamethazine degradation by ultrasound irradiation: performances and mechanisms*. Chemical Engineering Journal, 2018. **335**: p. 145-153.
98. Liu, J., et al., *Ultrasound irradiation enhanced heterogeneous activation of peroxymonosulfate with Fe₃O₄ for degradation of azo dye*. Ultrasonics sonochemistry, 2017. **34**: p. 953-959.



99. Hu, P. and M. Long, *Cobalt-catalyzed sulfate radical-based advanced oxidation: A review on heterogeneous catalysts and applications*. Applied Catalysis B: Environmental, 2016. **181**: p. 103-117.
100. Kohantorabi, M., G. Moussavi, and S. Giannakis, *A review of the innovations in metal-and carbon-based catalysts explored for heterogeneous peroxymonosulfate (PMS) activation, with focus on radical vs. non-radical degradation pathways of organic contaminants*. Chemical Engineering Journal, 2021. **411**: p. 127957.
101. Huang, J. and H. Zhang, *Mn-based catalysts for sulfate radical-based advanced oxidation processes: A review*. Environment international, 2019. **133**: p. 105141.
102. Ali, J., et al., *Modulating the redox cycles of homogenous Fe (III)/PMS system through constructing electron rich thiomolybdate centres in confined layered double hydroxides*. Chemical Engineering Journal, 2021. **408**: p. 127242.
103. Zhang, J., et al., *Surface dual redox cycles of Mn (III)/Mn (IV) and Cu (I)/Cu (II) for heterogeneous peroxymonosulfate activation to degrade diclofenac: Performance, mechanism and toxicity assessment*. Journal of Hazardous Materials, 2021. **410**: p. 124623.
104. Chai, C., et al., *Photoinduced g-C₃N₄-promoted Mn²⁺/Mn³⁺/Mn⁴⁺ redox cycles for activation of peroxymonosulfate*. Journal of Solid State Chemistry, 2019. **277**: p. 466-474.
105. Gao, Y., et al., *Degradation of antibiotic pollutants by persulfate activated with various carbon materials*. Chemical Engineering Journal, 2021: p. 132387.
106. Duan, X., et al., *Occurrence of radical and nonradical pathways from carbocatalysts for aqueous and nonaqueous catalytic oxidation*. Applied Catalysis B: Environmental, 2016. **188**: p. 98-105.
107. Duan, X., et al., *Unveiling the active sites of graphene-catalyzed peroxymonosulfate activation*. Carbon, 2016. **107**: p. 371-378.
108. Huang, W., et al., *Activation of persulfate by carbonaceous materials: A review*. Chemical Engineering Journal, 2021: p. 129297.
109. Lee, H., et al., *Activation of persulfates by carbon nanotubes: oxidation of organic compounds by nonradical mechanism*. Chemical Engineering Journal, 2015. **266**: p. 28-33.
110. Wang, Y., et al., *Efficient removal of acetochlor pesticide from water using magnetic activated carbon: Adsorption performance, mechanism, and regeneration exploration*. Science of The Total Environment, 2021. **778**: p. 146353.
111. Zhao, Q., et al., *Metal-free carbon materials-catalyzed sulfate radical-based advanced oxidation processes: a review on heterogeneous catalysts and applications*. Chemosphere, 2017. **189**: p. 224-238.
112. Chu, C., et al., *Cooperative pollutant adsorption and persulfate-driven oxidation on hierarchically ordered porous carbon*. Environmental science & technology, 2019. **53**(17): p. 10352-10360.
113. Sukhomlinov, D., et al., *Distribution of Ni, Co, precious, and platinum group metals in copper making process*. Metallurgical and Materials Transactions B, 2019. **50**(4): p. 1752-1765.



114. Ghanbari, F. and M. Moradi, *Application of peroxymonosulfate and its activation methods for degradation of environmental organic pollutants*. Chemical Engineering Journal, 2017. **310**: p. 41-62.
115. Chandel, M. and G.C. Jain, *Toxic effects of transition metals on male reproductive system: A review*. J Environ Occup Sci ● Oct-Dec, 2014. **3**(4): p. 205.
116. Beaumier, E.P., et al., *Modern applications of low-valent early transition metals in synthesis and catalysis*. Nature Reviews Chemistry, 2019. **3**(1): p. 15-34.
117. Lin, K.-Y.A., B.-J. Chen, and C.-K. Chen, *Evaluating Prussian blue analogues $M^{II}_3 [M^{III} (CN)_6]_2$ ($M^{II} = Co, Cu, Fe, Mn, Ni$; $M^{III} = Co, Fe$) as activators for peroxymonosulfate in water*. Rsc Advances, 2016. **6**(95): p. 92923-92933.
118. Pouran, S.R., A.A.A. Raman, and W.M.A.W. Daud, *Review on the application of modified iron oxides as heterogeneous catalysts in Fenton reactions*. Journal of Cleaner Production, 2014. **64**: p. 24-35.
119. Hou, J., et al., *Recent advances in cobalt-activated sulfate radical-based advanced oxidation processes for water remediation: A review*. Science of The Total Environment, 2021: p. 145311.
120. Wang, Q., et al., *Rapid synthesis of amorphous CoO nanosheets: Highly efficient catalyst for parachlorophenol degradation by peroxymonosulfate activation*. Separation and Purification Technology, 2021. **263**: p. 118369.
121. Oguzie, K.L., et al., *Oxidative degradation of Bisphenol A in aqueous solution using cobalt ion-activated peroxymonosulfate*. Journal of Molecular Liquids, 2020. **313**: p. 113569.
122. Shukla, P., et al., *Cobalt exchanged zeolites for heterogeneous catalytic oxidation of phenol in the presence of peroxymonosulphate*. Applied Catalysis B: Environmental, 2010. **99**(1-2): p. 163-169.
123. Zhang, B., et al., *Comparison of the catalytic performances of different commercial cobalt oxides for peroxymonosulfate activation during dye degradation*. Chemical Research in Chinese Universities, 2017. **33**(5): p. 822-827.
124. Xu, H., et al., *Heterogeneous activation of peroxymonosulfate by a biochar-supported Co_3O_4 composite for efficient degradation of chloramphenicols*. Environmental Pollution, 2020. **257**: p. 113610.
125. Guo, W., et al., *Degradation of antibiotics amoxicillin by Co_3O_4 -catalyzed peroxymonosulfate system*. Environmental progress & sustainable energy, 2013. **32**(2): p. 193-197.
126. Liu, L., et al., *The efficient degradation of sulfisoxazole by singlet oxygen (1O_2) derived from activated peroxymonosulfate (PMS) with Co_3O_4 - SnO_2 /RSBC*. Environmental Research, 2020. **187**: p. 109665.
127. Wang, Y., et al., *Photochemical degradation of phenol solutions on Co_3O_4 nanorods with sulfate radicals*. Catalysis Today, 2015. **258**: p. 576-584.
128. Wang, Y., et al., *3D-hierarchically structured MnO_2 for catalytic oxidation of phenol solutions by activation of peroxymonosulfate: structure dependence and mechanism*. Applied Catalysis B: Environmental, 2015. **164**: p. 159-167.
129. Bandala, E.R., et al., *Degradation of 2, 4-dichlorophenoxyacetic acid (2, 4-D) using cobalt-peroxymonosulfate in Fenton-like process*. Journal of Photochemistry and Photobiology A: Chemistry, 2007. **186**(2-3): p. 357-363.



130. Yang, G.C., Y.-H. Chiu, and C.-L. Wang, *Integration of electrokinetic process and nano-Fe₃O₄/S₂O₈²⁻ oxidation process for remediation of phthalate esters in river sediment*. *Electrochimica Acta*, 2015. **181**: p. 217-227.
131. Fe₃O₄, M., *carbon sphere/cobalt composites for catalytic oxidation of phenol solutions with sulfate radicals for industrial wastewater treatment* Wang, Yuxian; Sun, Hongqi; Ang, Ha Ming; Tade, Moses O.; Wang, Shaobin. *Chemical Engineering Journal (Amsterdam, Netherlands)*, 2014. **245**: p. 1-9.
132. Nguyen, N.T.T., et al., *Degradation of aqueous organic pollutants using an Fe₂O₃/WO₃ composite photocatalyst as a magnetically separable peroxymonosulfate activator*. *Separation and Purification Technology*, 2021. **267**: p. 118610.
133. Wang, J., et al., *SiO₂ mediated templating synthesis of γ-Fe₂O₃/MnO₂ as peroxymonosulfate activator for enhanced phenol degradation dominated by singlet oxygen*. *Applied Surface Science*, 2021. **560**: p. 149984.
134. Yang, J., et al. *Study on Preparation and Properties of Fe₂O₃/Al₂O₃/CeO₂/ZrO₂ Material*. in *IOP Conference Series: Materials Science and Engineering*. 2018. IOP Publishing.
135. Liu, Q., et al., *Size-tailored porous spheres of manganese oxides for catalytic oxidation via peroxymonosulfate activation*. *The Journal of Physical Chemistry C*, 2016. **120**(30): p. 16871-16878.
136. Wang, Y., et al., *Synthesis of magnetic core/shell carbon nanosphere supported manganese catalysts for oxidation of organics in water by peroxymonosulfate*. *Journal of colloid and interface science*, 2014. **433**: p. 68-75.
137. Wang, Y., et al., *The role of Mn-doping for catalytic ozonation of phenol using Mn/γ-Al₂O₃ nanocatalyst: Performance and mechanism*. *Journal of Environmental Chemical Engineering*, 2016. **4**(3): p. 3415-3425.
138. Wang, Y., et al., *New insights into heterogeneous generation and evolution processes of sulfate radicals for phenol degradation over one-dimensional α-MnO₂ nanostructures*. *Chemical Engineering Journal*, 2015. **266**: p. 12-20.
139. Wang, Y., et al., *Facile synthesis of hierarchically structured magnetic MnO₂/ZnFe₂O₄ hybrid materials and their performance in heterogeneous activation of peroxymonosulfate*. *ACS applied materials & interfaces*, 2014. **6**(22): p. 19914-19923.
140. Yao, Y., et al., *Facile synthesis of Mn₃O₄-reduced graphene oxide hybrids for catalytic decomposition of aqueous organics*. *Industrial & Engineering Chemistry Research*, 2013. **52**(10): p. 3637-3645.
141. Saputra, E., et al., *Different crystallographic one-dimensional MnO₂ nanomaterials and their superior performance in catalytic phenol degradation*. *Environmental science & technology*, 2013. **47**(11): p. 5882-5887.
142. Yao, Y., et al., *Magnetic ZnFe₂O₄-C₃N₄ hybrid for photocatalytic degradation of aqueous organic pollutants by visible light*. *Industrial & Engineering Chemistry Research*, 2014. **53**(44): p. 17294-17302.
143. Liang, H., et al., *Excellent performance of mesoporous Co₃O₄/MnO₂ nanoparticles in heterogeneous activation of peroxymonosulfate for phenol degradation in aqueous solutions*. *Applied Catalysis B: Environmental*, 2012. **127**: p. 330-335.



144. Vahdat, S.M., et al., *Organocatalytic synthesis of α -hydroxy and α -aminophosphonates*. Tetrahedron Letters, 2008. **49**(46): p. 6501-6504.
145. Newton, M.D., *Electronic structure analysis of electron-transfer matrix elements for transition-metal redox pairs*. The Journal of Physical Chemistry, 1988. **92**(11): p. 3049-3056.
146. Van der Ploeg, F., *Natural resources: Curse or blessing?* Journal of Economic Literature, 2011. **49**(2): p. 366-420.
147. Selinus, O., et al., *Essentials of medical geology*. 2013: Springer.
148. Britt, A., et al., *Australia's identified mineral resources 2014*. Geoscience Australia, Canberra, 2015: p. 4.
149. Murad, E. and J. Cashion, *Iron oxides*, in *Mössbauer Spectroscopy of Environmental Materials and their Industrial Utilization*. 2004, Springer. p. 159-188.
150. Association, A.I.O., *Iron Ore*. 1965.
151. Everett, J.E., *Iron ore handling procedures enhance export quality*. Interfaces, 1996. **26**(6): p. 82-94.
152. Prior, T., et al., *Resource depletion, peak minerals and the implications for sustainable resource management*. Global Environmental Change, 2012. **22**(3): p. 577-587.
153. Lai, L., H. Zhou, and B. Lai, *Heterogeneous degradation of bisphenol A by peroxymonosulfate activated with vanadium-titanium magnetite: Performance, transformation pathways and mechanism*. Chemical Engineering Journal, 2018. **349**: p. 633-645.
154. Glasser, F.P., *The system MnO-SiO₂*. American Journal of Science, 1958. **256**(6): p. 398-412.
155. Krauskopf, K.B., *Separation of manganese from iron in sedimentary processes*. Geochimica et Cosmochimica Acta, 1957. **12**(1-2): p. 61-84.
156. Post, J.E., *Manganese oxide minerals: Crystal structures and economic and environmental significance*. Proceedings of the National Academy of Sciences, 1999. **96**(7): p. 3447-3454.
157. ORE, I., *2011 Minerals Yearbook*. US Geological Survey, 2013.
158. Mudd, G.M., *The environmental sustainability of mining in Australia: key mega-trends and looming constraints*. Resources Policy, 2010. **35**(2): p. 98-115.
159. Horn, S., et al., *Cobalt resources in Europe and the potential for new discoveries*. Ore Geology Reviews, 2020: p. 103915.
160. Weight, D. *Ores Containing Cobalt*. 2017 [cited 2018 24 April]; Available from: <https://www.cobaltinstitute.org/ores-containing-cobalt.html>.

Every reasonable effort has been made to acknowledge the owners of copyright material. I would be pleased to hear from any copyright owner who has been omitted or incorrectly acknowledged.



Chapter 3. Natural manganese ore for efficient removal of organic pollutants via catalytic peroxymonosulfate advanced oxidation

Abstract

Sulfate radical-based advanced oxidation processes (SR-AOPs) using persulfates like peroxymonosulfate (PMS) are a superior strategy for in situ degradation of persistent organic pollutants (POPs) in water environment. However, the application of this remediation technology is largely constrained by the high material cost due to the complex synthetic processes of these precious metal or non-metal catalysts used for PMS activation. This remediation technology will be greatly advanced if the widely available natural minerals can be used as the catalyst. In this work, manganese ore was investigated for its catalytic performance in PMS activation for the oxidative degradation of organic pollutants including phenol, methylene blue (MB), rhodamine B (RB) and tetrabromobisphenol A (TBBPA). Experimental results indicate that manganese ore shows an excellent catalytic activity during the oxidation processes, manifesting its wide applicability towards the removal of different types of pollutants. The degradation rate using this manganese ore/PMS system increased with the reaction temperature and pH value of the initial solution. Furthermore, electron paramagnetic resonance (EPR) spectra reveal that manganese ore/PMS is a radical-based system where sulfate and hydroxyl radicals with strong oxidative potentials contribute to the degradation of organic pollutants. In addition, the concentration of metals in treated water meets the WHO and EU standards for drinking water, verifying this catalytic system is environmentally safe. This study advances the practical application of natural manganese ore for in-situ wastewater remediation.



3.1 Introduction

Rapid global industrialization and population growth is leading to an extensive environmental pollution and water scarcity is becoming a serious global issue [1, 2]. To solve these issues, water treatment or remediation seems the most practical method. Persistent organic pollutants (POPs), a kind of contaminants notoriously known for their long-lasting and toxicity existence in the environment, require urgent treatment. [3-5] Among the various biochemical and physicochemical methods developed for POPs treatment, advanced oxidation processes (AOPs) have drawn a particular attention due to their high efficiency and broad applicability. [6, 7] Noteworthy that sulfate radical-based advanced oxidation processes (SR-AOPs) using persulfates like peroxymonosulfate (PMS) are a superior strategy for in situ degradation of POPs in water environment. [8] In previous studies, metal oxides were mainly utilized as the catalysts for the activation of PMS to generate sulfate radicals ($\text{SO}_4^{\bullet-}$, 2.5–3.1 V). [9, 10] However, these metal catalysts do not naturally exist and have to be prepared via complex synthetic processes thus are expensive for industrial applications. [11] Hence, it is necessary to search other more economical and accessible catalysts. [12-15]

Many natural materials like minerals contain transition metals and their compounds such as iron, cobalt and manganese ores demonstrate great potential for the degradation of organic pollutants via advanced oxidation reactions [15-17]. The low price and abundance provide these natural ores with incomparable advantages against synthetic catalysts. [18] Manganese is the twelfth most abundant element in the earth. [19, 20] In previous studies, various manganese oxides, including manganese monoxide, manganese dioxide and manganese trioxide, have been exhibited extremely high activity in the degradation of POPs in the PMS system. [21, 22] Natural manganese ore (MO) consists of various manganese compounds and therefore may display good catalytic performance. Specifically, there are four operating mines and one tailings re-treatment plant in Australia, producing millions of tons of manganese ore per year that worth more than one billion Australian dollars. [20, 23] Two of the four manganese mining areas are located in Western Australia, which entitles us a unique geographical advantage in this study.

In this work, a series of natural manganese ore samples were employed as the catalyst for the degradation of organic pollutants in water environment under the Fenton reaction via PMS system. The pollutants were chosen from phenol, methylene blue



(MB), rhodamine B (RB) and tetrabromobisphenol A (TBBPA). The influence of PMS concentration on pollutant degradation was explored. The impacts of temperature and initial pH value of the solution on removal efficiency were also studied, which may provide some useful information on that the catalytic activity variation of manganese ore for PMS activation under different environmental conditions. Furthermore, electron paramagnetic resonance (EPR) and selective radical quenching experiments were conducted to demonstrate the catalytic mechanism in manganese ore/PMS system.

3.2 Experimental Section

Chemicals and Materials. The manganese ore (MO) was supplied by Karara Mining Ltd., Australia and OM Manganese Pty. Ltd., Australia. The composition of the received ore was provided by mining companies as shown in Table 3.1. Two batches of commercial testing ore samples were obtained from the same mine, while each batch contains four samples, successively labeled as Mn-1 to Mn-8. Prior to the experiments, the ore samples were washed with an ultrasonic cleaner, filtered and then dried overnight. Afterwards, the samples were ground into powder and sieved with a particle size of 50–60 μm for subsequent tests.

Table 3.1. The composition of manganese ore (MO) as received.

Composition	Formula	Content (wt%)
Braunite	$4\text{MnO}_3 \cdot 3\text{MnO}_2 \cdot \text{SiO}_2$	30%
Psilomelane	$\text{Ba} \cdot \text{Mn} \cdot \text{Mn}_8\text{O}_{16}(\text{OH})$	30%
Pyrolusite	MnO_2	30%
Quartz	SiO_2	10%

Phenol ($\geq 99.0\%$), methylene blue ($\geq 99.0\%$), rhodamine B ($\geq 97.0\%$), tetrabromobisphenol A ($\geq 97.0\%$), 5,5 dimethyl-1-pyrroline (DMPO, $\geq 99.0\%$) and 2,2,6,6-tetramethyl-4-piperidinol (TMP, $\geq 99.0\%$) were purchased from Sigma-Aldrich, Australia. Ultrapure water was manufactured via an Agilent water purification system. For further use, the targeted contaminants were diluted by a certain amount of ultrapure water to reach the designed concentration. Specifically, due to the low solubility of TBBPA under standard pH condition, sodium hydroxide was added into the solution to adjust the pH value to 11.



Characterization of Materials. The crystal structure of selected manganese ore was characterized by powder X-ray diffraction (XRD, Bruker D8 Advance) using Cu K α radiation at 40 kV and 30 mA with the step size and time of 0.02° (2 θ) and 0.01 s, respectively. The surface morphology of ore sample was probed using a scanning electron microscope (SEM, FEI Sirion 200) coupled with energy disperse spectroscopy (EDS). The textural properties of sample were measured by N₂ adsorption at 77 K with a surface area analyzer (Micromeritics TriStar II Plus), and the specific surface area and pore size distribution were estimated via the Brunauer–Emmett–Teller (BET) method and Barrett–Joyner–Halenda (BJH) method, respectively. Besides, the surface chemical composition of manganese ore was determined through X-ray photoelectron spectroscopy (XPS, Thermo Escalab 250) under Al K α X-ray. The deconvolution of obtained XPS spectra was carried out via Voigt functions with a 30% Lorentzian component after baseline subtraction using Shirley method.

Catalytic Activity Tests. The catalytic performance of manganese ore samples was evaluated for catalytic oxidation of organics with PMS, and phenol, methylene blue, rhodamine B and tetrabromobisphenol A were selected as the targeted contaminants. The adsorption and catalytically oxidative degradation tests were conducted in a thermostatic water bath with mechanical stirring throughout the reaction to maintain homogeneous solution condition. To initialize the oxidation, a certain amount of PMS and ore catalyst were simultaneously added to the solution of targeted pollutant (20 ppm). During the reaction, 1 mL of solution was periodically withdrawn, filtered by 0.45 μ m PEFT membrane, and then immediately mixed with 0.5 mL of methanol to quench the oxidation. In the case of phenol, the mixture was analyzed with an ultrahigh performance liquid chromatograph (UHPLC, Thermo Fisher Scientific UltiMate 3000) with a UV detector set at 270 nm. While the concentration of MB, TBBPA and RB was measured by a JASCO UV-visible spectrophotometer at 664, 464 and 554 nm, respectively.[24] Besides, EPR was applied to detect the free radicals during the activation of PMS, which was performed on a Bruker EMX-E spectrometer using DMPO and TMP as spin-trapping agents. The test conditions were as follows: centerfield, 3510 G; sweep width, 100 G; modulation frequency, 100 GHz. Moreover, the concentration of trace metal elements was detected by an inductively coupled plasma-mass spectrometry (ICP-MS, PerkinElmer, Elan DRC-e) equipment.



3.3 Results and Discussion

The catalytic performance of MO on phenol degradation is exhibited in Figure 3.1. Given that adsorption often occurs during AOPs processes, the adsorption ability of MO samples was estimated as well.

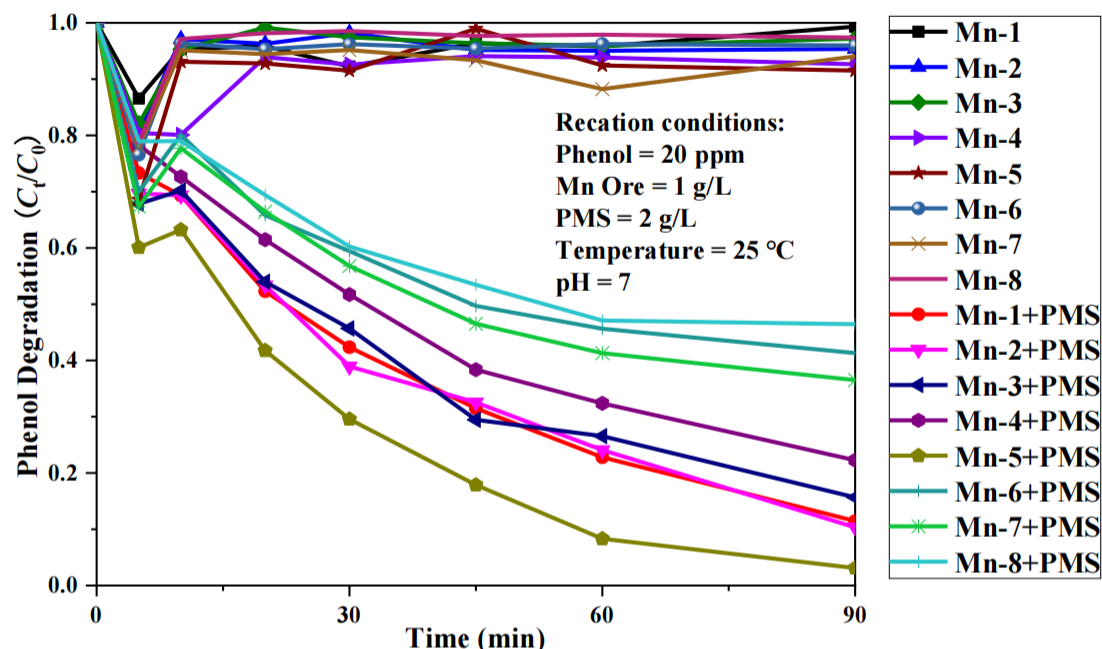


Figure 3.1. Degradation of phenol over manganese ore catalysts.

As shown in Figure 3.1, an obvious adsorption-desorption process appeared in the first 15 minutes. However, the equilibrium adsorption capacity of MO is constrained by the limited specific surface area ($12.6 \text{ m}^2/\text{g}$), with the highest adsorptive removal achieved by sample Mn-5 around 10%. In the case of PMS involvement, phenol removal became much more significant. Specially, phenol degradation reached above 95% in 90 minutes with Mn-5 and PMS in the solution. As PMS alone, little phenol removal was achieved [14, 25-27]; therefore, it can be deduced that the significant decline of phenol concentration was the result of MO-PMS collaborative catalytic degradation. To further investigate the effects of reaction conditions, sample Mn-5 was selected as the representative in the following study. The results of RB and TBBPA degradation at different PMS concentrations are presented in Figure 3.2.

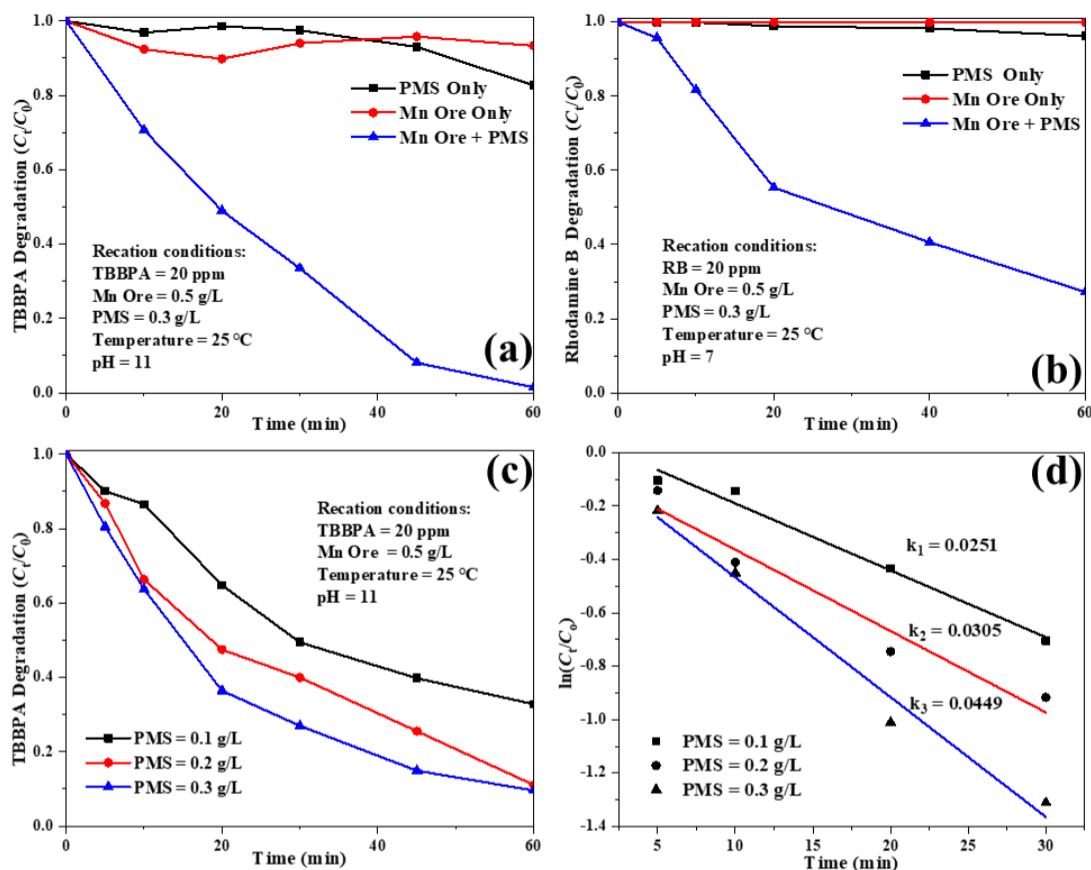


Figure 3.2. Degradation of RB and TBBPA at different PMS concentrations: (a) (c) Concentration of pollutants; (b) (d) Reaction rate constant of the first-order kinetics.

As shown in Figure 3.2 a&b, more than 50% of TBBPA and RB could be degraded through the manganese ore/PMS system within 60 mins, whereas ore or PMS individually produced insignificant effect on the degradation of pollutants. [25-27] Besides, the influence of PMS concentration (0.1, 0.2 and 0.3 g/L) on TBBPA degradation was investigated with the manganese ore of 0.5 g/L as shown in Figure 3.2c. Apparently, the reaction efficiency displays a positive correlation with the concentration of PMS, and the degradation of TBBPA ranging from 60% to 90% could be achieved within one hour. Although the curves based on 0.3 g/L and 0.2 g/L display a gap between 20 and 40 mins, the two curves intersect at 60 mins in the end of the reaction, demonstrating that a further increase of PMS concentration would not exert a significant effect on degradation when it reached a certain level. Additionally, the reaction rate constant (k , min⁻¹) of the first-order kinetics, which is generally used to indicate the speed of a chemical reaction within a period of time, [28] was calculated according to the following equation:



$$\ln(C_t/C_0) = -kt \quad (1)$$

where C_t is the current concentration of pollutants (mg/L), C_0 is the initial concentration of pollutants (mg/L), and t is the reaction time (min). As shown in Figure 3.2d, when the PMS concentration is 0.1, 0.2 and 0.3 g/L, the corresponding k value is 0.0251, 0.0305 and 0.0449 min^{-1} , respectively. Obviously, the reaction rate tends to increase significantly with the PMS concentration at the beginning of TBBPA degradation.

Meanwhile, to further understand the effect of pH value on the catalytic activity of manganese ore, MB degradation tests were conducted at different initial solution pH values (pH = 7, 9 and 10) by adding 0.1M H_2SO_4 and/or 0.1M NaOH aqueous solutions, with the concentration of PMS maintained at 0.1 g/L. As shown in Figure 3.3a, the degradation rate in this manganese ore/PMS system increased with the pH values of the initial solution. Accordingly, Figure 3.3b shows the reaction rate constant under different pH values, which increased from 0.0056 to 0.0311 min^{-1} with the pH value increasing from 7 to 10. This may be because a higher acidity means more hydrogen ions that could consume sulfate and hydroxyl radicals, and then reduce the degradation capacity for pollutants.

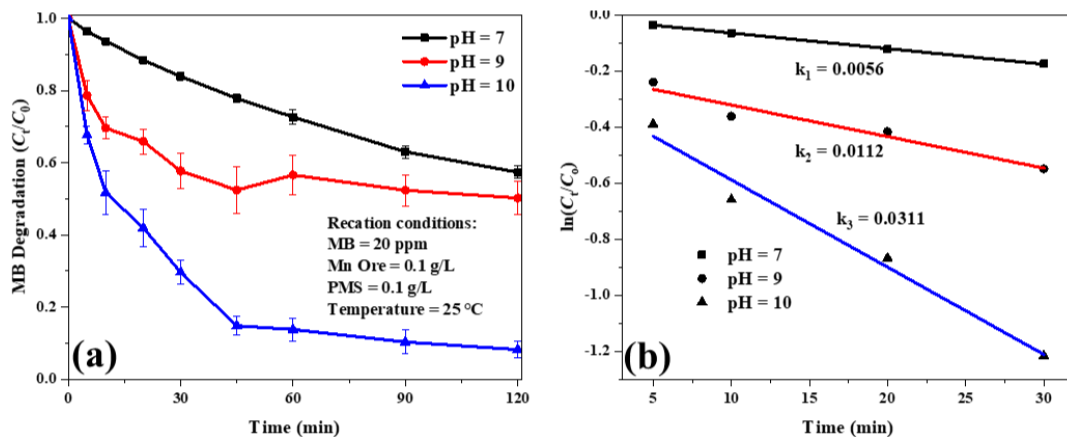


Figure 3.3. The effect of initial pH value on MB degradation: (a) Concentration of pollutants; (b) Reaction rate constant of the first-order kinetics.

Besides, the influence of reaction temperature on MB degradation was investigated as well. Since the temperature of practical sewage treatment process is generally higher than 10 °C due to exothermic reactions,[29] temperatures being examined herein are 15, 25, 35 and 45 °C, respectively. As shown in Figure 3.4a, MB decolorization rate and extent increased with the reaction temperature. The removal ratio of MB reached 37, 42 and 62 % at 15, 25 and 35 °C, respectively, and a removal rate of 83% was



achieved when the temperature was increased to 45 °C. From Figure 3.4b, the catalytic activity of this manganese ore/PMS system increased from 0.0045 to 0.0056 min⁻¹ with the temperature rising from 15 to 25 °C, indicating that the ore/PMS system has a wide temperature adaptability. The significant efficiency presented at 45 °C could be explained by the fact that high temperature would give rise to the increase of energy absorption for the O-O break-up, which would finally facilitate PMS activation.

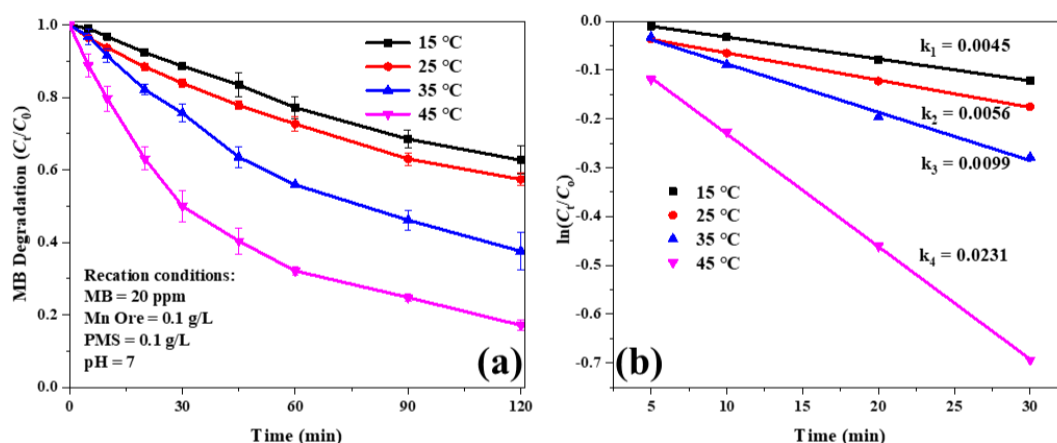


Figure 3.4. Degradation of MB at different temperatures (a) Concentration of pollutants; (b) Reaction rate constant of the first-order kinetics.

As mentioned above, the total content of manganese in ore sample was nearly 30% (Table 3.1), which consists of various manganese-containing compounds. Considering different manganese species may result in diverse catalytic efficiency, several characterization methods were adopted to explore the chemical compositions of the ore sample. The XRD patterns of Mn-5 sample are provided in Figure 3.5a, with peaks attributed to quartz (SiO_2), pyrolusite (MnO_2) and hematite (Fe_2O_3). This result verifies the fact as indicated in Table 3.1 that divalent manganese plays a dominate role in the ore. According to XPS analysis, a variety of metal elements including cobalt, iron, manganese and aluminium were found on ore surface as shown in Figure 3.5b. From Mn 2p spectrum (Figure 3.5c), two peaks located at 643.0 and 654.2 eV demonstrate the existence of MnO_2 . [30-32] Fe 2p spectrum (Figure 3.5d) shows two peaks at 711.3 and 724.6 eV, indicating the composition of Fe_2O_3 . [33-35] Co 2p spectrum (Figure 3.5e) exhibits three peaks at 779.3, 781.1 and 794.7 eV, which means that cobalt on ore surface mainly exists in the form of Co_3O_4 and CoO . [36-38]

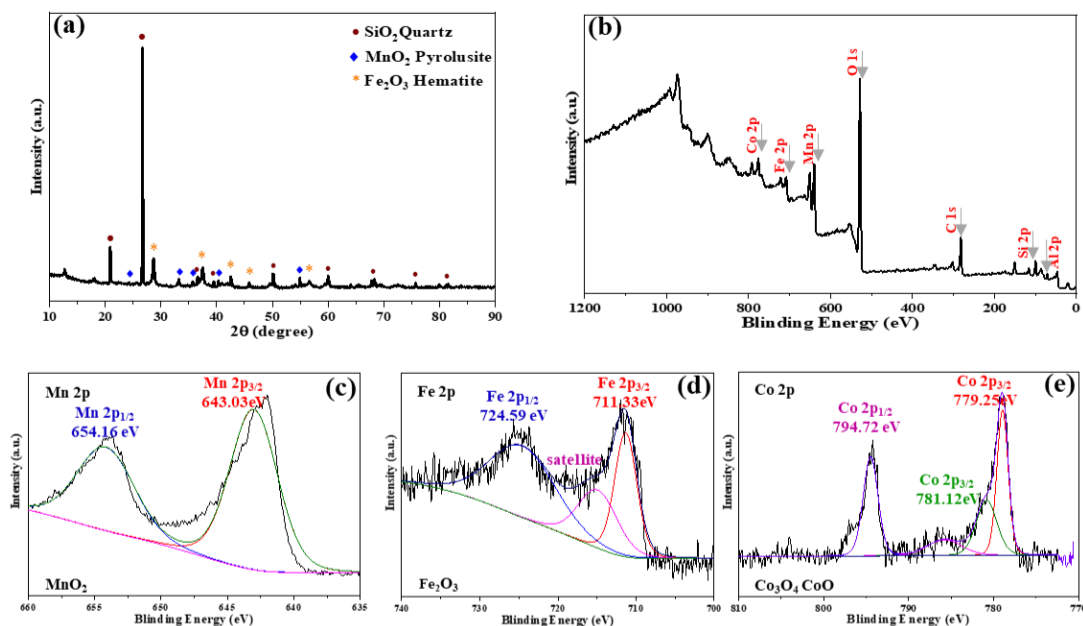


Figure 3.5. (a) XRD patterns, (b) XPS survey, (c) Mn 2p, (d) Fe 2p and (e) Co 2p spectra.

The BET specific surface area of Mn-5 sample was measured to be $12.6 \text{ m}^2/\text{g}$, with an average pore size of 7.4 nm . Figure 3.6 displays the SEM-EDS graphs of Mn-5 sample. As shown in Figure 3.6a–c, some fine particles could be observed, which might be attributed to the magnetism of ore. From Figure 3.6d–i, it can be clearly seen that manganese is the most abundant element in the ore, while a certain amount of oxygen and silicon also exist sourced from metallic oxides and silicon dioxide. Besides, a small amount of iron was also detected. It is understandable as iron ore is the largest ore resource in Australia and hence often detected together with other ore compositions.[39] In addition, a minor quantity of cobalt was detected, which may play a significant role in catalytic system as well.[40, 41] Based on these characterization results, it can be concluded that the main active ingredients of the manganese ore samples are identified as MnO_2 , Fe_2O_3 , CoO and Co_3O_4 .

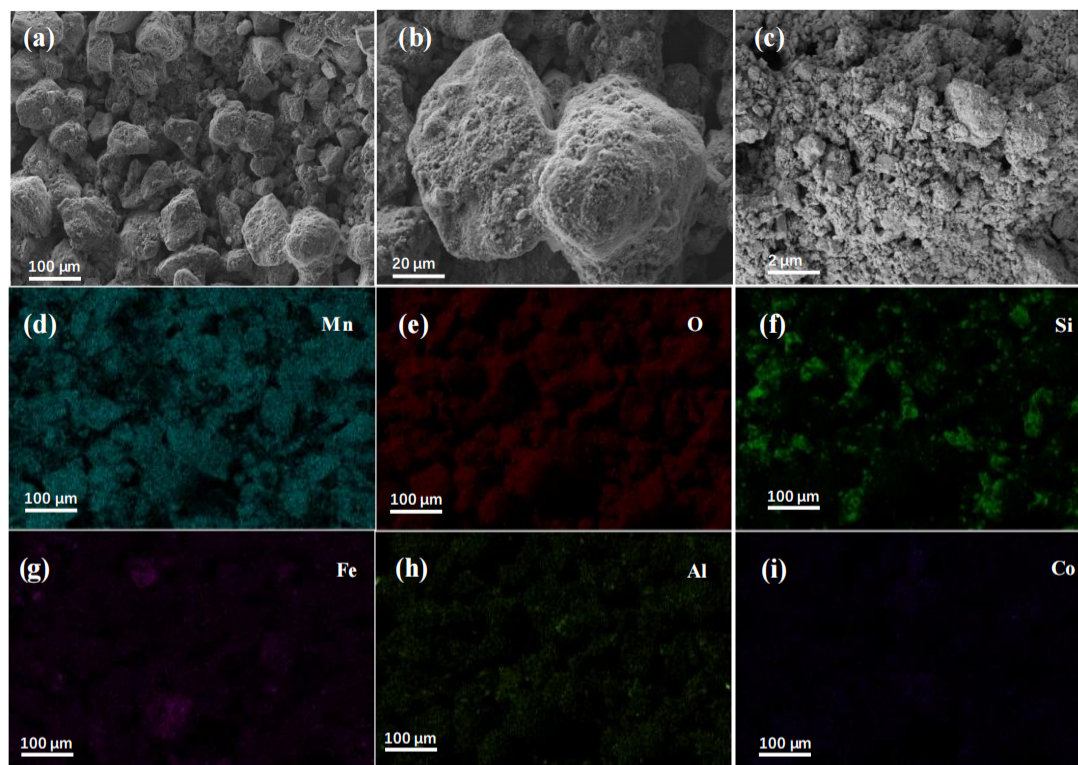
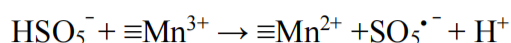
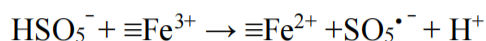


Figure 3.6. SEM-EDS images of manganese ore. SEM image: (a) 100 μm (b) 20 μm (c) 2 μm ; (e)-(j) SEM-EDS elemental mapping of selected area in (a).

In order to determine the involved reaction mechanism, in situ EPR experiments were performed to detect the radicals generated during PMS activation, and the reaction conditions are as follows: catalyst loading = 0.5 g/L, PMS loading = 0.3 g/L, pH = 7.0, DMPO = 8 mM, TMP = 0.08 mM. The results of EPR tests are provided in Figure 3.7. As shown, both $\text{DMPO-SO}_4^{\bullet-}$ and $\text{DMPO}\cdot\text{OH}$ signals (consisting of a quartet with an intensity ratio of 1:2:2:1) were observed in Mn ore/PMS composite catalyst system at the beginning of the reaction.[14] as well as $\text{TMP}\cdot\text{O}_2$ were observed in this bauxite ore/PMS composite system at the beginning of the reaction, indicating the generation of sulfate radical, hydroxyl radical and singlet oxygen during PMS activation, which may play a participant role in the catalytic oxidation process of organic pollutants. Combined with pervious study, the activation of PMS by manganese ore catalyst might follow the equations or steps as below:[42-44]



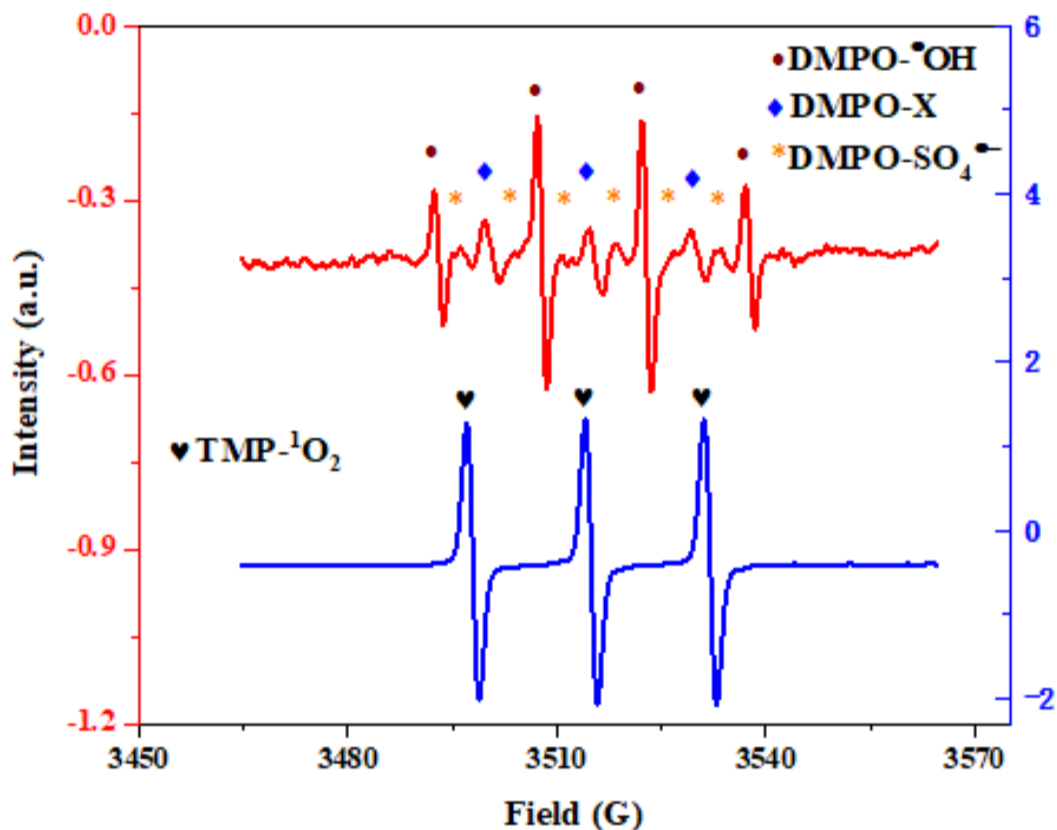
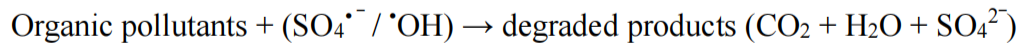
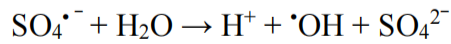
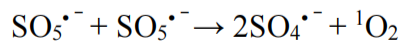
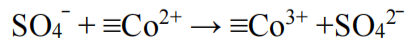


Figure 3.7. EPR spectra of PMS activation with manganese ore.

On the other hand, in order to ensure the metal content of treated water due to ore leaching meet the standard for drinking water, the residual solution was sent to ICP-MS analysis to determine the concentration of metals precipitated in the reaction. As a single standard system does not contain all these four metal elements, this study adopted two drinking water standards for comparison, i.e. WHO standard and EU standard, and the lower value was employed if the limits towards one element exist in both standards. As shown in Table 3.1, all these four indicators satisfied the requirements of the WHO and EU drinking water standards. The concentration of iron in treated solution was characterized as 0.1 mg/L, which is one-third of the standard limit value of 0.3 mg/L. The concentration of manganese ions is 0.01 mg/L, and the standard limit is five times



as that. The detected concentration of calcium ions is only 1.1 mg/L, far below the limit of 61 mg/L. And the concentration of magnesium ions is 4.2 mg/L, less than 20% of the limit value. Apparently, metal leaching in Mn ore/PMS system is quite slight, verifying this technology is environmentally safe.

Table 3.1. ICP-MS results compared with drinking water standard.

Element (mg/L)	Fe	Mg	Mn	Ca
Mn ore/PMS system with 20 ppm phenol	0.1	4.2	0.01	1.1
Drinking water standard[45, 46]	0.3	25	0.05	61

3.4 Conclusions

This study proposes an in-situ wastewater remediation strategy by directly utilizing natural manganese ore as the catalyst in PMS activation for organic pollutants removal via advanced oxidation processes. The results show that the manganese ore/PMS catalytic system performed well during the oxidative degradation of different types of contaminants including phenol, MB, RB and TBBPA. The degradation efficiency has a positive correlation with PMS concentration, whereas a further increase in PMS concentration would not exert a significant effect on degradation efficiency when it reaches a maximum level. Besides, MB degradation rate was promoted by the improved reaction temperature, and the catalytic activity of this manganese ore/PMS system is increased with the initial pH values. Based on characterization results, the main active ingredients of the manganese ore are MnO_2 , Fe_2O_3 , CoO and Co_3O_4 . EPR spectra reveal that $\text{SO}_4^{\cdot-}$, $\cdot\text{OH}$ and $^1\text{O}_2$ were generated during PMS activation process, and sulfate and hydroxyl radicals with strong oxidative potentials contribute to the catalytic degradation of organic pollutants. Moreover, ICP-MS analysis results demonstrate that the concentration of metals precipitated in the reaction is far below the limit of drinking water standard, verifying the manganese ore/PMS catalytic system is environmentally safe. This work promotes the application of cost-efficient natural manganese ore catalyst in sulfate radical-based advanced oxidation processes for environment remediation.



References

1. Singh, V.P., *Water, environment, engineering, religion, and society*. Journal of Hydrologic Engineering, 2008. **13**(3): p. 118-123.
2. Ebenstein, A., *The consequences of industrialization: evidence from water pollution and digestive cancers in China*. Review of Economics and Statistics, 2012. **94**(1): p. 186-201.
3. Jones, K.C. and P. De Voogt, *Persistent organic pollutants (POPs): state of the science*. Environmental pollution, 1999. **100**(1-3): p. 209-221.
4. Wania, F. and D. Mackay, *Peer reviewed: tracking the distribution of persistent organic pollutants*. Environmental science & technology, 1996. **30**(9): p. 390A-396A.
5. Vallack, H.W., et al., *Controlling persistent organic pollutants—what next?* Environmental Toxicology and Pharmacology, 1998. **6**(3): p. 143-175.
6. Zhi, D., et al., *Remediation of persistent organic pollutants in aqueous systems by electrochemical activation of persulfates: a review*. Journal of environmental management, 2020. **260**: p. 110125.
7. Zhao, Q., et al., *In-situ hydrogen peroxide synthesis with environmental applications in bioelectrochemical systems: a state-of-the-art review*. International Journal of Hydrogen Energy, 2021. **46**(4): p. 3204-3219.
8. Yang, Q., et al., *Recent advances in photo-activated sulfate radical-advanced oxidation process (SR-AOP) for refractory organic pollutants removal in water*. Chemical Engineering Journal, 2019. **378**: p. 122149.
9. Ding, Y., et al., *Nonradicals induced degradation of organic pollutants by peroxydisulfate (PDS) and peroxymonosulfate (PMS): Recent advances and perspective*. Science of The Total Environment, 2020: p. 142794.
10. Hou, J., et al., *Recent advances in cobalt-activated sulfate radical-based advanced oxidation processes for water remediation: A review*. Science of The Total Environment, 2021: p. 145311.
11. Hu, J., et al., *Duet Fe₃C and FeN_x Sites for H₂O₂ Generation and Activation toward Enhanced Electro-Fenton Performance in Wastewater Treatment*. Environmental Science & Technology, 2021. **55**(2): p. 1260-1269.



12. Zhou, Z., et al., *Persulfate-based advanced oxidation processes (AOPs) for organic-contaminated soil remediation: A review*. Chemical Engineering Journal, 2019. **372**: p. 836-851.
13. Sun, B., et al., *Recent advances in the removal of persistent organic pollutants (POPs) using multifunctional materials: a review*. Environmental Pollution, 2020: p. 114908.
14. Descostes, M., et al., *Use of XPS in the determination of chemical environment and oxidation state of iron and sulfur samples: constitution of a data basis in binding energies for Fe and S reference compounds and applications to the evidence of surface species of an oxidized pyrite in a carbonate medium*. Applied Surface Science, 2000. **165**(4): p. 288-302.
15. Scheringer, M., et al., *Long-range transport and global fractionation of POPs: insights from multimedia modeling studies*. Environmental Pollution, 2004. **128**(1-2): p. 177-188.
16. Andreozzi, R., et al., *Advanced oxidation processes (AOP) for water purification and recovery*. Catalysis today, 1999. **53**(1): p. 51-59.
17. Scheringer, M., et al., *Long-range transport and global fractionation of POPs: insights from multimedia modeling studies*. Environmental Pollution, 2004. **128**(1): p. 177-188.
18. Van der Ploeg, F., *Natural resources: curse or blessing?* Journal of Economic literature, 2011. **49**(2): p. 366-420.
19. Sigel, H., *Manganese in natural waters and earth's crust: Its availability to organisms*, in *Metal ions in biological systems*. 2000, CRC Press. p. 49-82.
20. Atlas, A.M., *Australian Atlas of mineral resources, mines and processing centres*. 2016.
21. Ye, P., et al., *Mechanochemical formation of highly active manganese species from OMS-2 and peroxymonosulfate for degradation of dyes in aqueous solution*. Research on Chemical Intermediates, 2019. **45**(3): p. 935-946.
22. Wang, Y., et al., *Synthesis of magnetic carbon supported manganese catalysts for phenol oxidation by activation of peroxymonosulfate*. Catalysts, 2017. **7**(1): p. 3.



23. Geoscience Australia, C.D.o.I., Science, and M.C.o. Australia, *Australian mines atlas online*. 2015, Geoscience Australia (GA), Commonwealth Department of Industry and Science
24. Tian, W., et al., *Template-free synthesis of N-doped carbon with pillared-layered pores as bifunctional materials for supercapacitor and environmental applications*. Carbon, 2017. **118**: p. 98-105.
25. Saputra, E., et al., *Manganese oxides at different oxidation states for heterogeneous activation of peroxymonosulfate for phenol degradation in aqueous solutions*. Applied Catalysis B: Environmental, 2013. **142**: p. 729-735.
26. Wu, H., et al., *Manganese oxide integrated catalytic ceramic membrane for degradation of organic pollutants using sulfate radicals*. Water research, 2019. **167**: p. 115110.
27. Yang, Y., et al., *Sustainable redox processes induced by peroxymonosulfate and metal doping on amorphous manganese dioxide for nonradical degradation of water contaminants*. Applied Catalysis B: Environmental, 2021. **286**: p. 119903.
28. Wentzell, P.D. and S. Crouch, *Comparison of reaction-rate methods of analysis for systems following first-order kinetics*. Analytical Chemistry, 1986. **58**(13): p. 2855-2858.
29. Howland, W., *Effect of temperature on sewage treatment processes*. Sewage and Industrial Wastes, 1953: p. 161-169.
30. Davoglio, R.A., et al., *Synthesis and characterization of α -MnO₂ nanoneedles for electrochemical supercapacitors*. Electrochimica Acta, 2018. **261**: p. 428-435.
31. Xie, G., et al., *The evolution of α -MnO₂ from hollow cubes to hollow spheres and their electrochemical performance for supercapacitors*. Journal of Materials Science, 2017. **52**(18): p. 10915-10926.
32. Hussain, S., et al., *Water plasma functionalized CNTs/MnO₂ composites for supercapacitors*. The Scientific World Journal, 2013. **2013**.
33. Han, T., et al., *Hydrothermal self-assembly of α -Fe₂O₃ nanorings@ graphene aerogel composites for enhanced Li storage performance*. Journal of Materials Science, 2019. **54**(9): p. 7119-7130.



34. Wang, H., et al., *Photocatalytic degradation of deoxynivalenol over dendritic-like α -Fe₂O₃ under visible light irradiation*. *Toxins*, 2019. **11**(2): p. 105.
35. Liu, Y.-T., et al., *Electrochemical activity and stability of core-shell Fe₂O₃/Pt nanoparticles for methanol oxidation*. *Journal of power sources*, 2013. **243**: p. 622-629.
36. Meng, Y., et al., *Ionic liquid-derived Co₃O₄/carbon nano-onions composite and its enhanced performance as anode for lithium-ion batteries*. *Journal of Materials Science*, 2017. **52**(22): p. 13192-13202.
37. Cheng, M., et al., *Core@ shell CoO@ Co₃O₄ nanocrystals assembling mesoporous microspheres for high performance asymmetric supercapacitors*. *Chemical Engineering Journal*, 2017. **327**: p. 100-108.
38. Qiu, B., et al., *Fabrication of Co₃O₄ nanoparticles in thin porous carbon shells from metal-organic frameworks for enhanced electrochemical performance*. *RSC advances*, 2017. **7**(22): p. 13340-13346.
39. Ye, Q., *Commodity booms and their impacts on the Western Australian economy: the iron ore case*. *Resources Policy*, 2008. **33**(2): p. 83-101.
40. Hu, P. and M. Long, *Cobalt-catalyzed sulfate radical-based advanced oxidation: a review on heterogeneous catalysts and applications*. *Applied Catalysis B: Environmental*, 2016. **181**: p. 103-117.
41. Do, S.-H., et al., *Application of a peroxymonosulfate/cobalt (PMS/Co (III)) system to treat diesel-contaminated soil*. *Chemosphere*, 2009. **77**(8): p. 1127-1131.
42. Yan, S., et al., *Natural Fe-bearing manganese ore facilitating bioelectro-activation of peroxymonosulfate for bisphenol A oxidation*. *Chemical Engineering Journal*, 2018. **354**: p. 1120-1131.
43. Liang, H., et al., *Excellent performance of mesoporous Co₃O₄/MnO₂ nanoparticles in heterogeneous activation of peroxymonosulfate for phenol degradation in aqueous solutions*. *Applied Catalysis B: Environmental*, 2012. **127**: p. 330-335.
44. Saputra, E., et al., *A comparative study of spinel structured Mn₃O₄, Co₃O₄ and Fe₃O₄ nanoparticles in catalytic oxidation of phenolic contaminants in aqueous solutions*. *Journal of colloid and interface science*, 2013. **407**: p. 467-473.



45. Kallis, G. and D. Butler, *The EU water framework directive: measures and implications*. Water policy, 2001. **3**(2): p. 125-142.
46. Edition, F., *Guidelines for drinking-water quality*. WHO chronicle, 2011. **38**(4): p. 104-8.

Every reasonable effort has been made to acknowledge the owners of copyright material. I would be pleased to hear from any copyright owner who has been omitted or incorrectly acknowledged.



Chapter 4 Reactive oxygen species-induced degradation of organic contaminants by peroxymonosulfate activation over natural bauxite ore

Abstract

Peroxymonosulfate (PMS)-based advanced oxidation processes (AOPs) have emerged as a novel wastewater treatment strategy due to production of reactive oxygen species (ROSs) with high redox potential. PMS could be activated by various synthetic catalysts containing transition metals such as Co, Fe, Ni, Ag, Cu and Mn. However, the high cost greatly limits their practical application. Bauxite is the principal ore for aluminium. It is a heterogeneous material that normally consists of Al_2O_3 , iron oxides and other impurities. This study demonstrates the capability of bauxite rock to effectively activate PMS and destroy organic pollutants in water environment. The degradation of three substrates (methylene blue, rhodamine B, and tetrabromobisphenol A) was affected by solution pH and reaction temperature. The ore particles were characterized by XRD, BET, XPS, and SEM techniques. Iron oxides have been identified as excellent catalysts for PMS activation. Electron paramagnetic resonance (EPR) experiments confirm the involvement of sulfate radical, hydroxyl radical and singlet oxygen. This research promotes the application of natural bauxite ore and sulfate radical-based advanced oxidation processes in environment remediation.



4.1 Introduction

In recent decades, public concern on environmental pollution issues has reached an unprecedented level due to the environmental crisis caused by booming human activities.[1] Among various kinds of pollutants, persistent organic pollutants (POPs) are notoriously intractable as they are normally high toxic and quite difficult to be broken down, and their bio-accumulative effects pose serious risks to the safety of the ecosystem and human beings.[2, 3] The ever-deteriorating environment is in urgent need of advanced proposals for pollution control and environment recovery.[4] Advanced oxidation processes (AOPs) are a category of green technologies that have been developed to decompose organic contaminants using superoxides to evolve various reactive oxygen species like hydroxyl radicals ($\cdot\text{OH}$) and sulfate radicals ($\text{SO}_4^{\cdot-}$). [5-7] Employing the conjugation of the transition metal elements (Co, Fe, Ag and Mn) and peroxymonosulfate (PMS) to generate sulfate radicals ($\text{SO}_4^{\cdot-}$) for pollutants oxidation is a new hotspot in the field of AOP.[8, 9] In previous studies, the degradation of organic pollutants mainly utilized man-made metal oxides as the catalyst for AOPs, whereas these metal containing catalysts are constrained by their high prices and complex synthetic processes for industrial application.[10] Herein, natural bauxite ore would be applied as a cost-efficient and environmental-friendly catalyst alternative for wastewater treatment. Bauxite is the principal ore for aluminium products. It is a heterogeneous material that contains multiple oxides including Al_2O_3 (normally 40–60%), iron oxides (normally 10–30%) like goethite ($\text{FeO}(\text{OH})$) and haematite (Fe_2O_3), and other impurities.[11-13] As iron oxides has demonstrated great potential in AOP technology for water purification and recovery,[14] the plentiful iron oxides in bauxite indicate that natural bauxite ore is a promising catalyst candidate.

On the other hand, Australia is the world's largest exporter of bauxite, accounting for more than 30% of the world market supply with more than 80% of production exported.[11] Bauxite has many commercial application, e.g., metallurgical, cement, fertiliser, abrasive, and refractory. Although the vast majority of the bauxite has been extracted for the production of aluminium metal, the metallurgical market demand for bauxite is unstable due to the impact of the economic cycle. As an institution in Australia, conducting this research is conducive to the diversified development of local products.



In this study, natural bauxite ore was employed as the catalyst for the degradation of organic pollutants under Fenton reaction via PMS system. Tetrabromobisphenol A (TBBPA), methylene blue (MB) and rhodamine B (RB) were chosen as the pollutants. The influence of reaction temperature and initial pH value on pollutants degradation process was studied, which could show the variation of the catalytic activity of bauxite ore for PMS activation under different conditions. Furthermore, electron paramagnetic resonance (EPR) and selective radical quenching experiments were conducted to determine the catalytic mechanism in bauxite ore/PMS system.

4.2 Experimental Sections

Chemicals and Materials. The bauxite ore was provided by one local mining company. The composition of the received ore was obtained from the mining company as shown in Table 4.1. Considering iron is the fourth most abundant element in the earth's crust, the rich iron content (mainly exists in the form of various iron oxides) in bauxite ore products is quite normal in the mining industry. Prior to experiments, the bauxite ore was washed by ultrapure water with an ultrasonic cleaner and then collected by filtration. Subsequently, the product was crushed and sieved to a particle size of 50–60 μm for further tests.

Table 4.1 The composition of bauxite ore as received (wt%).

Al	4–5	Ca	0.5–1.0	Mg	0.5–1.5
Fe	15–25	SiO ₂	16–20	Ni	1.0–1.5
Cr	0.8–1.2	Mn	1.0–1.5	Zn	0.04–0.05

Peroxymonosulfate (OXONE) ($\geq 42.8\%$), methylene blue ($\geq 99.0\%$), rhodamine B ($\geq 97.0\%$), tetrabromobisphenol A ($\geq 97.0\%$), 5,5 dimethyl-1-pyrroline 5,5-dimethyl-1-pyrroline N-oxide (DMPO, $\geq 99.0\%$) and 2,2,6,6-tetramethyl-4-piperidinol (TMP, $\geq 99.0\%$) were purchased from Sigma-Aldrich, Australia. Ultrapure water was manufactured via an Agilent water purification system. For further use, the targeted contaminants were diluted by a certain amount of ultrapure water to reach the designed



concentration. Specifically, due to the low solubility of TBBPA under standard pH condition, sodium hydroxide was added into the solution to adjust the pH value to 11.

Characterization of Materials. The crystal structure of selected bauxite ore was characterized by powder X-ray diffraction (XRD, Bruker D8 Advance) using Cu K α radiation at 40 kV and 30 mA with the step size and time of 0.02° (2 θ) and 0.01 s, respectively. The surface morphology of ore sample was probed using a scanning electron microscope (SEM, FEI Sirion 200) coupled with energy disperse spectroscopy (EDS). The textural properties of sample were measured by N₂ adsorption at 77 K with a surface area analyzer (Micromeritics TriStar II Plus), and the specific surface area and pore size distribution were estimated via the Brunauer–Emmett–Teller (BET) method and Barrett–Joyner–Halenda (BJH) method, respectively. Besides, the surface chemical composition of bauxite ore was determined using X-ray photoelectron spectroscopy (XPS, Thermo Escalab 250) under Al K α X-ray. The deconvolution of obtained XPS spectra was carried out via Voigt functions with a 30% Lorentzian component after baseline subtraction using Shirley method. Thermogravimetric-differential thermal analysis (TG-DTA) was recorded on a Perkin-Elmer Diamond thermal analyzer with a heating rate of 10 °C/min in air.

Catalytic Activity Tests. The catalytic performance of bauxite ore samples was evaluated for catalytic oxidation of organics with PMS. Methylene blue, rhodamine B and tetrabromobisphenol A were selected as the targeted contaminants. The adsorption and catalytically oxidative degradation tests were conducted in a thermostatic water bath with mechanical stirring throughout the reaction to maintain homogeneous solution condition. To initialize the oxidation, a certain amount of PMS and ore catalyst were simultaneously added to the solution of targeted pollutants (20 ppm). During the reaction, 1 mL of solution was periodically withdrawn, filtered by 0.45 μ m PEFT membrane, and then immediately mixed with 0.5 mL of methanol to quench the oxidation. While the concentration of MB, TBBPA and RB was measured by a JASCO UV-visible spectrophotometer at 664, 464 and 554 nm, respectively.[15] Besides, EPR was applied to detect the free radicals during the activation of PMS, which was performed on a Bruker EMX-E spectrometer using DMPO and TMP as spin-trapping agents. The test conditions were as follows: centerfield, 3510 G; sweep width, 100 G; modulation frequency, 100 GHz. Moreover, the concentration of trace metal elements



was detected by an inductively coupled plasma-mass spectrometry (ICP-MS, PerkinElmer, Elan DRC-e) equipment.

4.3 Results and Discussions

The catalytic activity tests of bauxite ore were carried out for catalytic oxidation of organic pollutants with PMS. As shown in Figure 4.1, the adsorption capacity of bauxite ore is limited. In the case of TBBPA removal, the adsorption process reached equilibrium within 30 mins and about 10% adsorption was achieved on bauxite ore (Figure 4.1a). With regard to RB, the adsorption effect is more negligible with RB concentration decline less than 5% after 210 mins (Figure 4.1b). The limited adsorption capacity of bauxite ore could be easily understood in view of its low specific surface area (characterized as $59.6 \text{ m}^2/\text{g}$). Whereas, the introduction of PMS largely improves the removal efficiency, and ore/PMS composite system is apparently more efficient than PMS only, with nearly 65% of TBBPA and 50% of RB removed respectively after 210 mins, verifying the significant role of bauxite ore in the catalytic degradation process of organic pollutants.

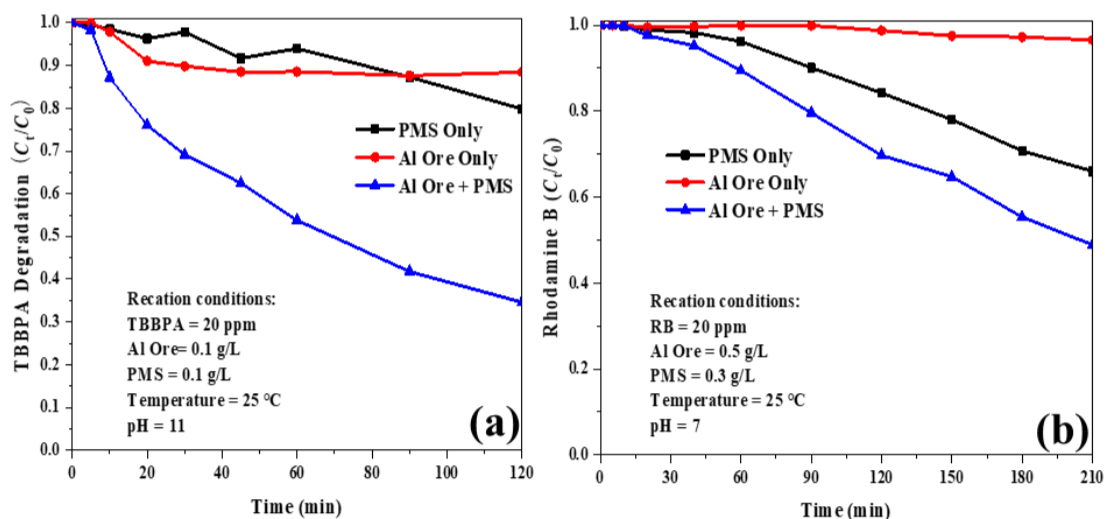


Figure 4.1 Degradation of tetrabromobisphenol A and rhodamine B over bauxite ore catalyst.

To understand the effect of pH on the catalytic activity of bauxite ore, MB degradation tests were performed at different initial pH values (pH = 7, 9 and 10) by adding 0.1M H_2SO_4 and/or 0.1M NaOH aqueous solution, and the concentration of PMS was set as 0.1 g/L. As shown in Figure 4.2a, the MB degradation rate of this bauxite/PMS system



increases with increasing pH values of initial solution. The curve of pH=10 drops much more rapidly than the others, with more than 70% MB removal achieved in 30 mins. Besides, the reaction rate constant (k , min^{-1}) of the first-order kinetics under different pH values was calculated according to Eq. 4.1. As shown in Figure 4.2b, the reaction rate constant of this bauxite/PMS system increased from 0.0057 to 0.0365 min^{-1} with the pH value rising from 7 to 10. This could be explained by that higher pH values would inhibit hydrogen ions in solution that may consume sulfate and hydroxyl radicals, and then facilitate organics degradation process.

$$\ln(C_t/C_0) = -kt \quad \text{Eq. (4.1)}$$

where C_t is the current concentration of pollutants (mg/L), C_0 is the initial concentration of pollutants (mg/L), and t is the reaction time (min).

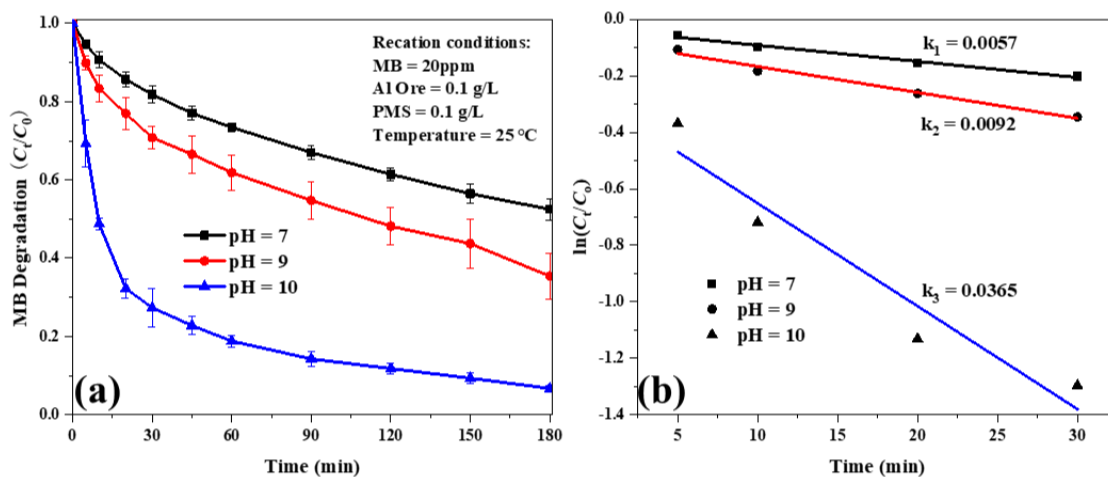


Figure 4.2 The effect of initial pH value on MB degradation: (a) Concentration of pollutants as a function of time; (b) Reaction rate constant of the first-order kinetics.

The influence of reaction temperature on MB degradation was studied as well. As shown in Figure 4.3a, MB degradation extent increased with increasing reaction temperature. The difference in removal rate between 35 °C and 45 °C is smaller than that between 25 °C and 35 °C, indicating that the enhancement in catalytic activity of this bauxite/PMS system resulting from reaction temperature increase becomes minor when the temperature reaches a certain level. The reaction rate constant of the first-order kinetics under different reaction temperatures was calculated according to Eq. 4.1. As shown in Figure 4.3b, the reaction rate constant increased from 0.0057 to 0.1293



min^{-1} with the reaction temperature rising from 25 °C to 45 °C, indicating that this bauxite/PMS system has a good applicability in normal temperature environment.

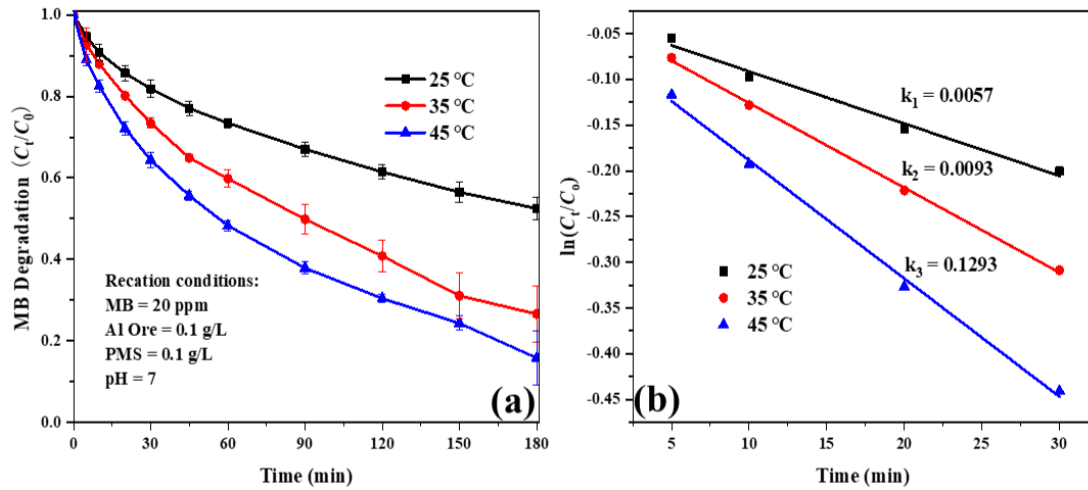


Figure 4.3 The effect of reaction temperature on MB degradation: (a) Concentration of the pollutant as a function of reaction time; (b) Reaction rate constant of the first-order kinetics.

The surface morphology of bauxite ore was detected by SEM-EDS as shown in Figure 4.4. The sieved ore particles show irregular shapes with different sizes of the same order of magnitude. According to elemental mapping results, iron and aluminium are two of the most abundant metal elements in the ore, which also contains plentiful oxygen and silicon as the result of metal oxides and silicon dioxide. Additionally, a small amount of Mn was discovered in the sample, which may also act as an effective element in the catalytic degradation of organics.[16] Based on surface area analysis, the specific surface area of bauxite ore is $59.6 \text{ m}^2/\text{g}$, and the average pore size is 4.4 nm.

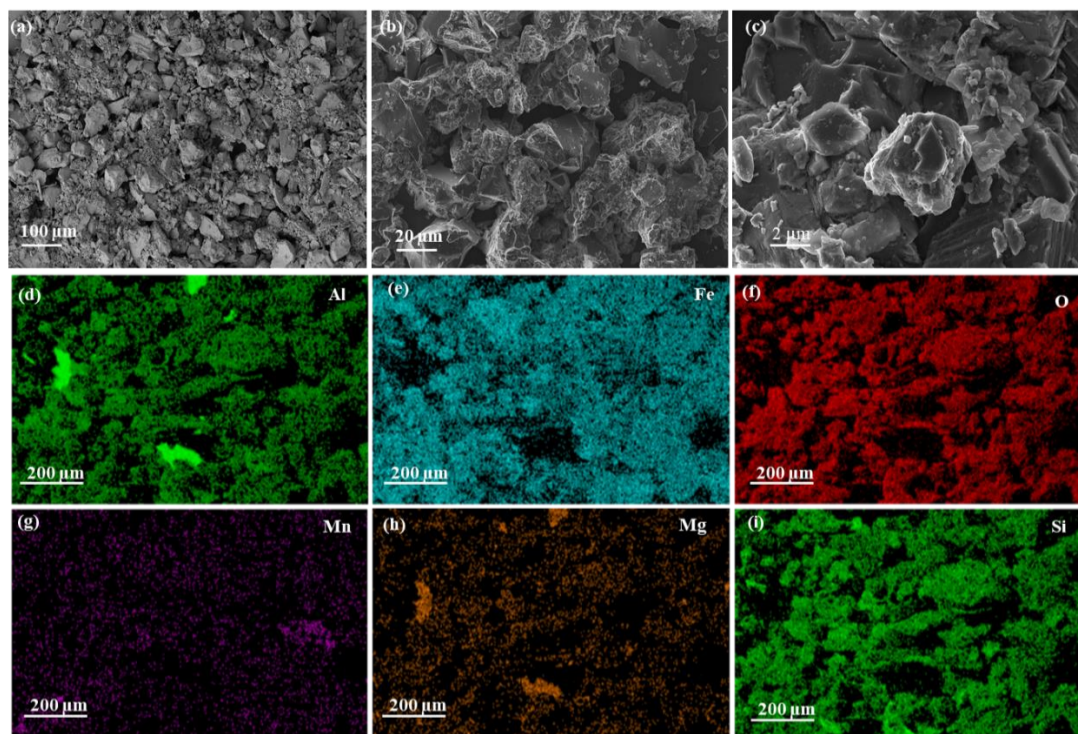


Figure 4.4 (a)–(c) SEM images and (d)–(i) SEM-EDS elemental mapping of bauxite ore.

As shown in Figure 4.5a, the XRD patterns of bauxite ore sample match with maghemite (Fe_2O_3), cacoenite ($\text{Fe}_{21}\text{Al}_{14}(\text{PO}_4)_{17}\text{O}_6(\text{OH})_{12}(\text{H}_2\text{O})_{24}$) and silicon oxide (SiO_2). The XRD results together with SEM-EDS images further verify the complicated composition of this bauxite ore as previously mentioned in Figure 4.5. According to the thermogravimetric curve as plotted in Figure 4.5b, bauxite ore exhibits a good thermal stability at the operating temperature range required for catalytic oxidation in water environment. Based on XPS survey as shown in Figure 4.5c, a variety of elements were detected such as oxygen, silicon, iron, aluminium, etc. However, the manganese element previously found via SEM-EDS mapping (Figure 4.4h) was not detected in XPS survey. This disagreement might result from the inherent heterogeneity of the ore. As shown in Figure 4.5d, Fe_2O_3 could be clearly identified from the Fe 2p spectrum. Therefore, it can be deduced that the main effective component of this bauxite ore catalyst is iron oxide.

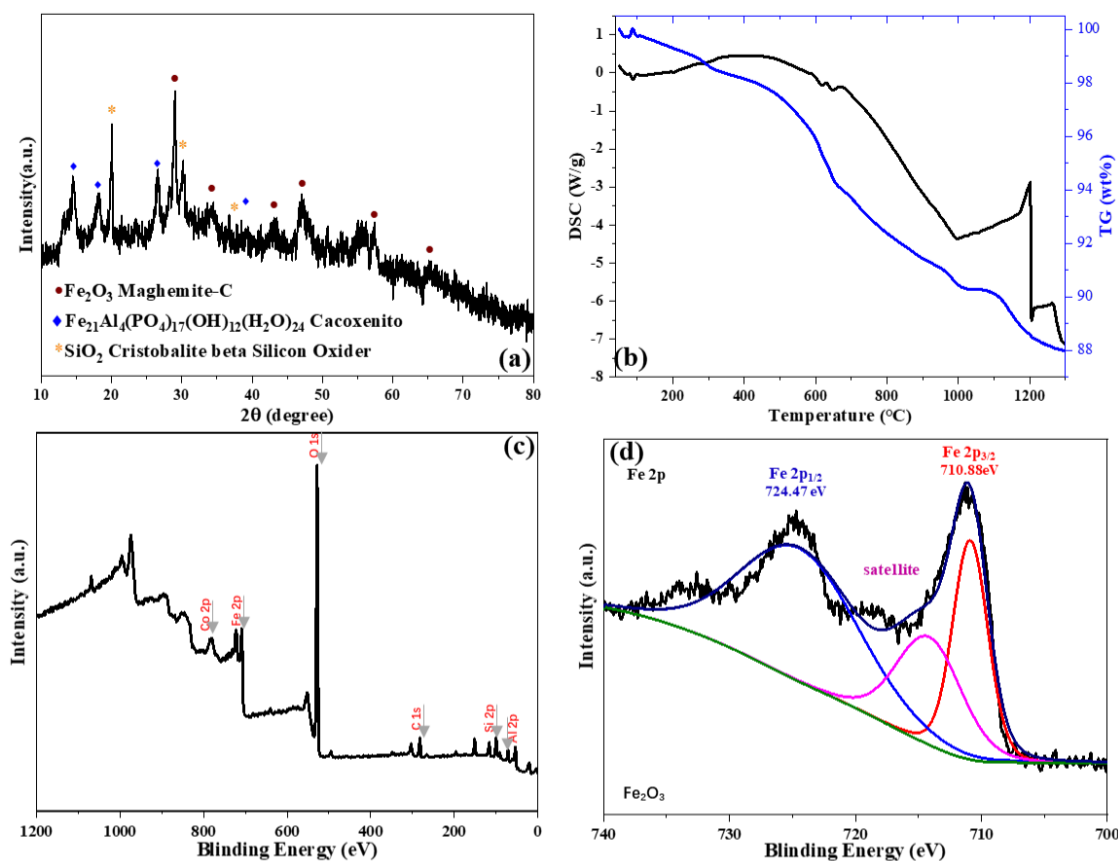
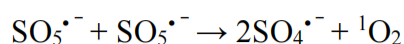
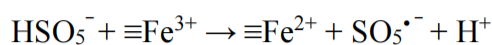


Figure 4.5 (a) XRD patterns, (b) TGA curves, (c) XPS survey and (d) Fe 2p spectra of bauxite ore.

In order to explore the reaction mechanism, in situ EPR experiments were carried out to detect the active radicals generated during PMS activation over bauxite ore. The reaction conditions were set as follows: bauxite ore catalyst loading = 0.5 g/L, PMS loading = 0.3 g/L, pH = 7.0, DMPO = 8 mM, TMP = 0.08 mM.[17] The results are shown in Figure 4.6. DMPO-SO₄^{•-} and DMPO-[•]OH signals (consisting of a quartet with an intensity ratio of 1:2:2:1)[18] as well as TMP-¹O₂ were observed in this bauxite ore/PMS composite system at the beginning of the reaction, indicating the generation of sulfate radical, hydroxyl radical and singlet oxygen during PMS activation, which may play a participant role in the catalytic oxidation process of organic pollutants. Based on pervious study, the activation of PMS by bauxite ore catalyst might follow the equations as below.[19-21]



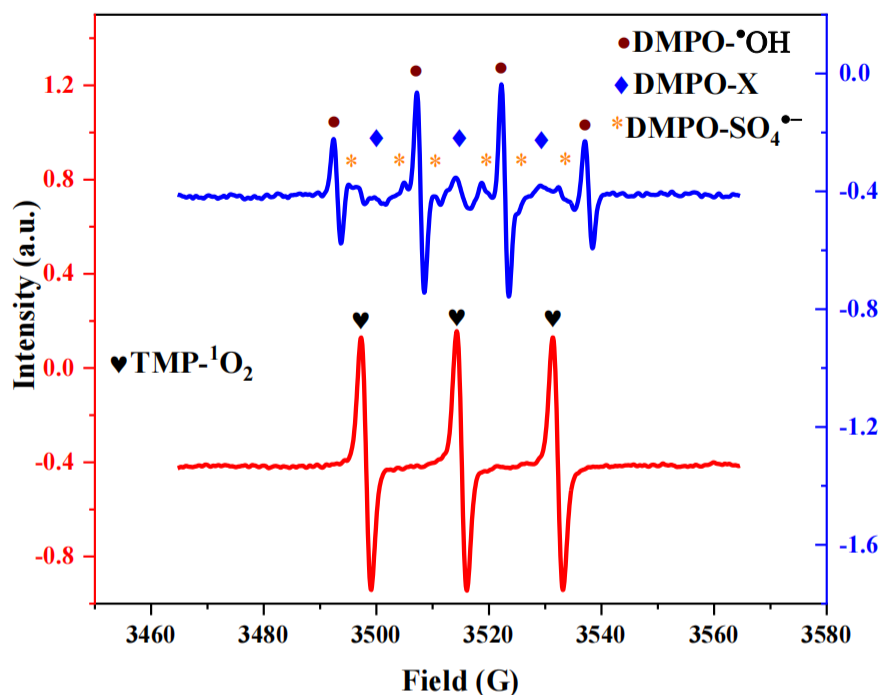
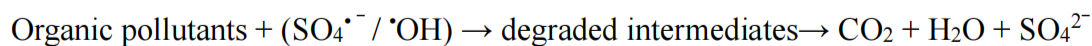
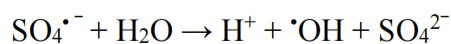


Figure 4.6 EPR spectra of PMS activation with bauxite ore.

Moreover, the residual solution was sent to ICP-MS analysis to determine the concentration of metals precipitated in the reaction. The metal content of treated water due to ore leaching meet the standard for drinking water. As shows in Table 3.1, the metal leaking in this bauxite ore/PMS system is quite slight. Except for the iron content, most indicators of treated water meet the WHO and EU standard for drinking water. Although the precipitation of iron is higher than the drinking water standard, it is still low with regard to the industrial standard. The low metal content of treated water proves that this bauxite ore/PMS catalytic system is environmentally safe and has great potential for large scale industrial application.

**Table 4.2** ICP-MS results compared with drinking water standard.

Element (mg/L)	Fe	Mg	Mn	Ca
Bauxite ore/PMS system with 20 ppm MB	0.8	7.5	0.01	3.1
Drinking water standard[22, 23]	0.3	25	0.05	61

4.4 Conclusions

The bauxite catalyst used in this study is non-refined ore powder directly provided by a mining company, which is extremely cheap in the international commodity market. In the catalytic system of bauxite ore/PMS composite, this mineral catalyst exhibits a good performance during the oxidative degradation of organic pollutants including methylene blue, rhodamine B, and tetrabromobisphenol A. The degradation efficiency has a positive correlation with the reaction temperature and solution pH. According to characterization results, the main active component of the bauxite ore is Fe_2O_3 . Sulfate radical, hydroxyl radical and singlet oxygen are generated during PMS activation process, and sulfate and hydroxyl radicals with strong oxidative potentials contribute to the catalytic degradation of organic pollutants. Besides, the low content of leaching metals in treated water verifies the bauxite ore/PMS catalytic system is environmentally safe. Although the efficiency is not as satisfactory as synthetic catalysts, the cheap price of natural bauxite ore makes it a cost-efficient catalyst alternative to synthetic catalysts. As the leading mining export country in the world, Australia has a unique advantage and great potential in this research field.



References

1. Ensing, B., et al., *Chemical involvement of solvent water molecules in elementary steps of the Fenton oxidation reaction*. *Angewandte Chemie International Edition*, 2001. **40**(15): p. 2893-2895.
2. Postel, S.L., G.C. Daily, and P.R. Ehrlich, *Human appropriation of renewable fresh water*. *Science*, 1996. **271**(5250): p. 785-788.
3. Postel, S.L., *Entering an era of water scarcity: the challenges ahead*. *Ecological applications*, 2000. **10**(4): p. 941-948.
4. Holdgate, M.W., *A perspective of environmental pollution*. 1980: CUP Archive.
5. Scheringer, M., et al., *Long-range transport and global fractionation of POPs: insights from multimedia modeling studies*. *Environmental Pollution*, 2004. **128**(1): p. 177-188.
6. Andreozzi, R., et al., *Advanced oxidation processes (AOP) for water purification and recovery*. *Catalysis today*, 1999. **53**(1): p. 51-59.
7. Zhang, T., et al., *Efficient peroxydisulfate activation process not relying on sulfate radical generation for water pollutant degradation*. *Environmental science & technology*, 2014. **48**(10): p. 5868-5875.
8. Furman, O.S., A.L. Teel, and R.J. Watts, *Mechanism of base activation of persulfate*. *Environmental science & technology*, 2010. **44**(16): p. 6423-6428.
9. Ahn, S., et al., *Disinfection of ballast water with iron activated persulfate*. *Environmental science & technology*, 2013. **47**(20): p. 11717-11725.
10. Vahdat, S.M., et al., *Organocatalytic synthesis of α -hydroxy and α -aminophosphonates*. *Tetrahedron Letters*, 2008. **49**(46): p. 6501-6504.
11. Atlas, A.M., *Australian Atlas of mineral resources, mines and processing centres*. 2016.
12. Norman, M.A., et al., *Vegetation succession after bauxite mining in Western Australia*. *Restoration Ecology*, 2006. **14**(2): p. 278-288.
13. Deng, B., et al., *Enrichment of Sc₂O₃ and TiO₂ from bauxite ore residues*. *Journal of hazardous materials*, 2017. **331**: p. 71-80.



14. Newton, M.D., *Electronic structure analysis of electron-transfer matrix elements for transition-metal redox pairs*. The Journal of Physical Chemistry, 1988. **92**(11): p. 3049-3056.
15. Tian, W., et al., *Template-free synthesis of N-doped carbon with pillared-layered pores as bifunctional materials for supercapacitor and environmental applications*. Carbon, 2017. **118**: p. 98-105.
16. Huang, K.Z. and H. Zhang, *Direct electron-transfer-based peroxymonosulfate activation by iron-doped manganese oxide (δ -MnO₂) and the development of galvanic oxidation processes (GOPs)*. Environmental science & technology, 2019. **53**(21): p. 12610-12620.
17. Han, N., et al., *Efficient removal of organic pollutants by ceramic hollow fibre supported composite catalyst*. Sustainable Materials and Technologies, 2019: p. e00108.
18. Descostes, M., et al., *Use of XPS in the determination of chemical environment and oxidation state of iron and sulfur samples: constitution of a data basis in binding energies for Fe and S reference compounds and applications to the evidence of surface species of an oxidized pyrite in a carbonate medium*. Applied Surface Science, 2000. **165**(4): p. 288-302.
19. Yan, S., et al., *Natural Fe-bearing manganese ore facilitating bioelectro-activation of peroxymonosulfate for bisphenol A oxidation*. Chemical Engineering Journal, 2018. **354**: p. 1120-1131.
20. Liang, H., et al., *Excellent performance of mesoporous Co₃O₄/MnO₂ nanoparticles in heterogeneous activation of peroxymonosulfate for phenol degradation in aqueous solutions*. Applied Catalysis B: Environmental, 2012. **127**: p. 330-335.
21. Saputra, E., et al., *A comparative study of spinel structured Mn₃O₄, Co₃O₄ and Fe₃O₄ nanoparticles in catalytic oxidation of phenolic contaminants in aqueous solutions*. Journal of colloid and interface science, 2013. **407**: p. 467-473.
22. Kallis, G. and D. Butler, *The EU water framework directive: measures and implications*. Water policy, 2001. **3**(2): p. 125-142.
23. Edition, F., *Guidelines for drinking-water quality*. WHO chronicle, 2011. **38**(4): p. 104-8.



Every reasonable effort has been made to acknowledge the owners of copyright material. I would be pleased to hear from any copyright owner who has been omitted or incorrectly acknowledged.



Chapter 5. Efficient removal of organic pollutants by ceramic hollow fibre supported composite catalyst

Abstract

Various metal-based heterogeneous catalysts for the activation of peroxymonosulfate have been explored to be highly efficient in the degradation of organic pollutants. However, the secondary contamination hindered their steps for practical application and is the key-problem to be urgently addressed. In this work, catalyst/ Al_2O_3 hollow fibre composites have been developed, which enables the elimination of the secondary contamination by immobilization of catalyst on robust supports instead of powdered catalysts. $Ag-La_{0.8}Ca_{0.2}Fe_{0.95}O_{3-\delta}/Al_2O_3$ composite hollow fibres were synthesized and showed excellent catalytic effect on methylene blue degradation by advanced oxidation process. TiO_2/Al_2O_3 composite hollow fibres were also fabricated to decompose the pollutant via photocatalysis. This study provides a potential strategy enabling ceramic hollow fibre-supported catalysts to remove organic pollutants in aqueous phase effectively, opening a new window of membrane-based catalyst for advanced oxidation in the practical application.



5.1 Introduction

Worldwide environmental deterioration has become an inevitable issue with the development of contemporary society. This reinforces the importance of developing novel and efficient strategies for water treatment. Traditional water treatment methods include sediment filtration, water softeners, activated charcoal, deionization, reverse-osmosis process, ultrafiltration, distillation, biochemical method, and ultraviolet disinfection. Recently, advanced oxidation processes (AOPs) have been explored for chemical and microbial decontamination utilizing the in site generated active radical species (e.g., $\cdot\text{OH}$ and $\text{SO}_4^{\cdot-}$) for oxidation.[1] Chemical oxidants such as ozone, hydrogen peroxide, peroxymonosulfate, and persulfate are involved in the AOP system to produce radicals with high redox potentials.[2-4] Peroxymonosulfate (PMS), the precursor of $\text{SO}_4^{\cdot-}$, is well-known as a non-toxic and cost-effective oxidant, which has been widely applied in AOPs. In order to improve the reaction rate, catalysts like metal oxides are necessary for the activation of PMS.

Perovskite oxides (ABO_3), which have been widely studied as oxygen permeation membranes, solid oxide fuel cells (SOFCs) and electrocatalysts,[5-9] have demonstrated their great potential in environmental catalysis because of their special physicochemical properties.[10-16] Very recently, perovskite oxides have been explored for AOPs,[2-4, 10, 17] however the issue of low reaction rate and narrow pH ranges are addressed.[18-19] Meanwhile, the inevitable metal leaching may be the main obstacle for further applications.[2-3] To solve this problem, catalyst support will be an effective way to fix the metal-based catalyst for aqueous-phase advanced oxidation.

Ceramic membranes have received significant attention due to their stable structure and flexible composition tailoring for various catalytic applications. Specifically, hollow fibre membranes, which possesses sub-micron pores with enhanced specific surface areas and excellent mechanical properties, are becoming the promising micro-reactors for industrial applications, such as oxygen separation,[20-22] solid oxide electrolysis cell (SOEC),[23] SOFCs,[24] clean solar panel production,[25] and methane coupling.[26] Because of the good thermal and mechanical stability, excellent chemical stability (in acidic and alkaline solutions), and high repeatability compared with other ceramic oxides, Al_2O_3 has widely used to prepare hollow fibre support.



In this work, two different methods were applied to prepare nano-catalyst/ Al_2O_3 composite hollow fibre. Firstly, perovskite oxide/ Al_2O_3 composite hollow fibre was developed *via* dip-coating method for aqueous-phase advanced oxidation. As Fe-mediated PMS decomposition was promising, we synthesized $\text{La}_{0.8}\text{Ca}_{0.2}\text{Fe}_{0.95}\text{O}_{3-\delta}$ with A-site calcium doping and B-site cation deficiency. Nano-sized silver particles can deliver the promotion of radical formation, and thus are doped in the $\text{La}_{0.8}\text{Ca}_{0.2}\text{Fe}_{0.95}\text{O}_{3-\delta}$ here. To further verify the broad applicability of this combination (nano-catalyst/ Al_2O_3 composite hollow fibre), photo-degradation was also investigated. The typical photocatalyst TiO_2 was chosen and the *in situ* growing method was applied to prepare $\text{TiO}_2/\text{Al}_2\text{O}_3$ composite hollow fibre catalyst for aqueous-phase photocatalytic reaction.

5.2 Experimental Section

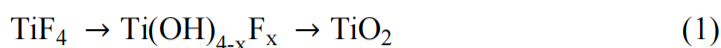
Preparation of Catalyst/ Al_2O_3 Composite Hollow Fibres

(a) Ag- $\text{La}_{0.8}\text{Ca}_{0.2}\text{Fe}_{0.95}\text{O}_{3-\delta}/\text{Al}_2\text{O}_3$ composite hollow fibre

Ag- $\text{La}_{0.8}\text{Ca}_{0.2}\text{Fe}_{0.95}\text{O}_{3-\delta}$ (LCFA) was prepared *via* a classic sol-gel method followed by calcination as reported in our previous study.[2, 27] Dip coating method was used to deposit LCFA decoration layer (from the 800 °C-calcined LCFA powder) on the surface of the Al_2O_3 hollow fibre.[14, 28-29] The thickness of the decoration layer was adjusted by varying the weight loading of the LCFA powder in the coating slurry or by adding extra dipping step(s).[14]

(b) $\text{TiO}_2/\text{Al}_2\text{O}_3$ composite hollow fibre

Metal oxide films, such as SiO_2 , [30] SnO_2 , [31] FeOOH , [32] V_2O_5 [33] and TiO_2 [34-35] can be prepared by direct chemical deposition in supersaturated solutions. Specifically, anatase TiO_2 particles can be easily generated in titanium tetrafluoride (TiF_4) aqueous solutions at relatively low temperatures. The chemical reactions of TiF_4 hydrolysis to form TiO_2 particles take place in the following steps, given in equation (1):[35]



Upon this reaction, TiO_2 deposition can be realized on various substrates with complex shapes through heterogeneous nucleation.[36] Low pH will slow down the hydrolysis of TiF_4 and thus ensuring a smooth TiO_2 coating.[37]



Here, $\text{TiO}_2/\text{Al}_2\text{O}_3$ composite hollow fibres have been prepared *via* in-situ growth. Home-made Al_2O_3 hollow fibres (outer diameter 1.5 mm, inner diameter 1.0 mm) were used as substrate supports. Hydrochloric acid (HCl), aqueous ammonia (NH_4OH), deionized water (DI water) and titanium tetrafluoride (TiF_4 , Aldrich) were used as coating solution for $\text{TiO}_2/\text{Al}_2\text{O}_3$ composite hollow fibre. HCl and NH_4OH were used to adjust the pH of deionized water from 1.01 to 2.1. TiF_4 was then dissolved in this solution to reach a concentration of 0.04 M, during which pH was changed to 1.6. Al_2O_3 hollow fibres were immersed in the solution and maintained at 60 °C for 48, 72, and 96 h. After being washed with deionized water and dried at 60 °C for 24 h, the composite hollow fibres were then annealed at 250, 450, 650 °C in air for 1.5 h at a heating rate of 2 °C/min.

Characterization

Crystal structure of the hollow fibres and the powders were characterized by powder X-ray diffraction (XRD, Bruker D8 Advance) using a Cu-K radiation. Continuous scan mode was used to collect patterns from 10° to 90° using a 0.02° step size and a 0.01 s step time. The X-ray tube potential and current were set at 40 kV and 30 mA, respectively. The morphologies of the composite hollow fibres were probed using scanning electron microscope (SEM, FEI Sirion 200). The sub-micron structure of LCFA powder was also probed using transmission electron microscope (TEM, Tecnai G2TF20 S-Twin). X-ray photoelectron spectra (XPS) were recorded using a PHI 5000 Versa Probe spectrometer with an Al-K α X-ray gun. All of the binding energies were calibrated using carbon (C 1s) at 284.6 eV as a reference. Electron paramagnetic resonance (EPR) was applied to detect the free radicals during the activation of PMS, which was performed on a Bruker EMX-E spectrometer using 5,5 dimethyl-1-pyrroline (DMPO, >99.0%) and 2,2,6,6-tetramethyl-4-piperidinol (TMP, >99.0%) as spin-trapping agents.

Evaluation of Catalyst/ Al_2O_3 Composite Hollow Fibres

In this study, methylene blue (MB) was used as the target pollutant for the evaluation of catalyst/ Al_2O_3 composite hollow fibres.

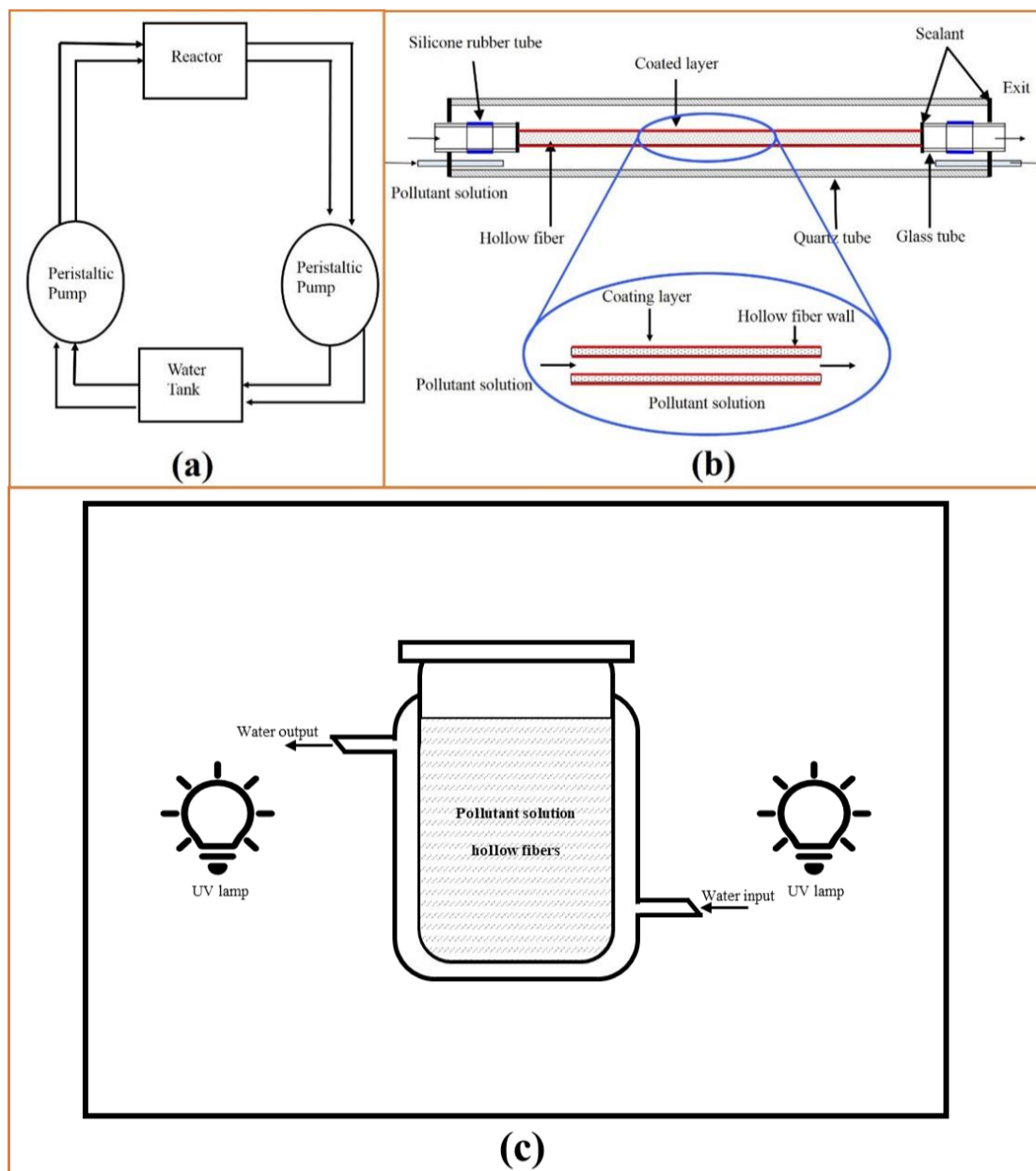


Figure 5.1. Schematic diagrams, (a) Flow diagram; (b) The home-made device; (c) Photocatalytic reactor.

The permeability of prepared fibres was evaluated by measuring the fibre flux in DI water and MB solution in a home-made device with configuration schematically shown in Figure 5.1. Samples were collected from water tank, and peristaltic pumps provide the driving force for the water cycle (Figure 5.1a). The home-made device was designed



based on hollow fibre support for aqueous-phase advanced oxidation (Figure 5.1b). The hollow fibre with the length of 30 cm was connected successively to the glass tube and silicone tube using silicone sealant (Tonsan New Materials and Technology Co., Beijing). A larger quartz tube (18 mm in diameter and 400 mm in length) was used to accommodate the hollow fibre, connected on both sides with small-diameter quartz tubes and sealed with epoxy glue. Pollutant-contained solution was fed into the shell/core side of the test module. [14, 29] the fibre flux is calculated based on the following equation:

$$J = \frac{V_0 - V_t}{A \times t} \quad (2)$$

Where J is the fibre flux, V_0 is the volume of feed solution before filtration, V_t is the volume of the feed solution at time t (1 h in this study) and A is the fibre surface area.

The adsorption capacity of the $\text{TiO}_2/\text{Al}_2\text{O}_3$ composite hollow fibres was tested by immersing the samples into MB solutions for 24 h. The concentration of MB solution was analysed by a JASCO UV-vis spectrophotometer at a wavelength of 664 nm.

Catalytic degradation of methylene blue through perovskites/PMS oxidation was evaluated in a batch reactor. The mixture of pollutant solution and perovskite oxide was kept in dark for 30 min to achieve adsorption equilibrium before adding the required amount of PMS to start the reaction. A magnetic stirrer was used to ensure a homogeneous solution throughout the reaction. At given time intervals, 2 mL of MB solution was taken out and analysed by the spectrophotometer.

The photocatalytic activities of composite hollow fibres were investigated in a 1 L Pyrex double-jacket reactor containing MB solution. The reaction temperature was maintained at 25 °C using a thermostat connected to the reactor. The photoreaction vessel was placed 30 cm away from the radiation source, which is a UV lamp with intensity $848.3 \mu\text{W}/\text{cm}^2$ ($\lambda=315\text{-}400 \text{ nm}$). The photocatalytic reaction was started by turning on the lamp after 30 min dark adsorption. The MB samples were examined by the method as above.

5.3 Results and Discussions

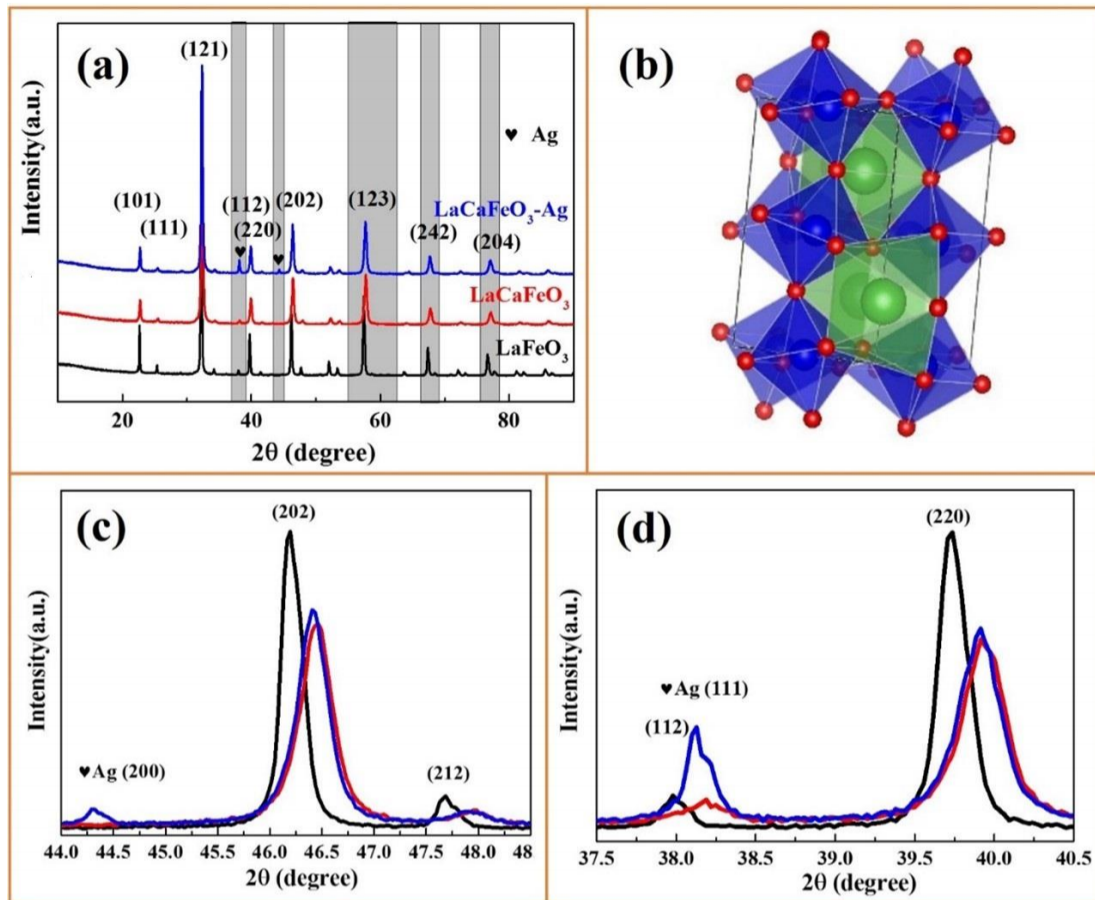


Figure 5.2. (a) Powder X-ray diffraction (XRD) patterns of $\text{LaFeO}_{3-\delta}$ (LF), $\text{La}_{0.8}\text{Ca}_{0.2}\text{Fe}_{0.95}\text{O}_{3-\delta}$ (LCF) and $\text{Ag-La}_{0.8}\text{Ca}_{0.2}\text{Fe}_{0.95}\text{O}_{3-\delta}$ (LCFA) powders; (b) Crystal structure of orthorhombic perovskite; (c) and (d) The magnified characteristic peaks of metallic Ag and perovskite.

XRD patterns of sintered $\text{LaFeO}_{3-\delta}$ (LF), $\text{La}_{0.8}\text{Ca}_{0.2}\text{Fe}_{0.95}\text{O}_{3-\delta}$ (LCF) and $\text{Ag-La}_{0.8}\text{Ca}_{0.2}\text{Fe}_{0.95}\text{O}_{3-\delta}$ (LCFA) powders were given in Figure 5.2a. The characteristic peaks of LF calcined at 800 °C agree well with the standard XRD patterns of orthorhombic perovskite phase (JCPDS PDF# 88-0641), the crystal structure of which is displayed in Figure 5.2b. Ca-doping on A-site and Fe-defecting on B-site bring little changes on crystal structure except a slight high angle migration, as shown in Figure 5.2c and d. The coordination number of A-site and B-site in ABO_3 perovskite oxide are 12 and 6, which determines the ionic radii of La^{3+} , Fe^{3+} (LS=low spin) and Fe^{3+} (HS=high spin) are 1.36, 0.55 and 0.645 Å, respectively.² Beside Fe-defecting, Ca-doping on A-site would weaken the positive electrical property, resulting in the partially valence increase of Fe on B-site to Fe^{4+} . Moreover, it also brings cations with small



radius in both Fe^{4+} and Ca^{2+} , which may lead to the shrinkage of crystal cell, thus a slight right shift could be observed comparing with XRD patterns of LF. Details of radius of various ionic states were listed in **Table 5.1**.

Table 5.1 The radius of various ionic states

Ionic	Coordination No.	Spin state	Radius (Å)
La^{3+}	XII		1.36
Fe^{3+}	VI	low spin	0.55
	VI	high spin	0.645
Fe^{4+}	VI		0.585
Ca^{2+}	XII		1.34

The characteristic peaks of *in situ* grown nanoparticles (Ag) were marked as ♥ in Figure 5.2. It is well known that the perovskite structure is closely related to the tolerance factor (t) as follows:

$$r_A + r_O = t\sqrt{2}(r_B + r_O) \quad (3)$$

Where r_A and r_B are the average radii of metal ions in A and B-site of perovskite, and r_O is the ionic radius of oxygen. The t value of LCFA could be calculated as $0.95793 < t < 0.99645$, which greatly proved that the perovskite structure could maintain well as it was in the range $0.75 \leq t \leq 1$. Meanwhile, in terms of the planes (121), (202), (112) and (220), the blue line of LCFA demonstrated the same patterns with those of LCF under room temperature, which further excluded the possibility of doping/ substituting potential of metallic Ag nanoparticles into LCF system.

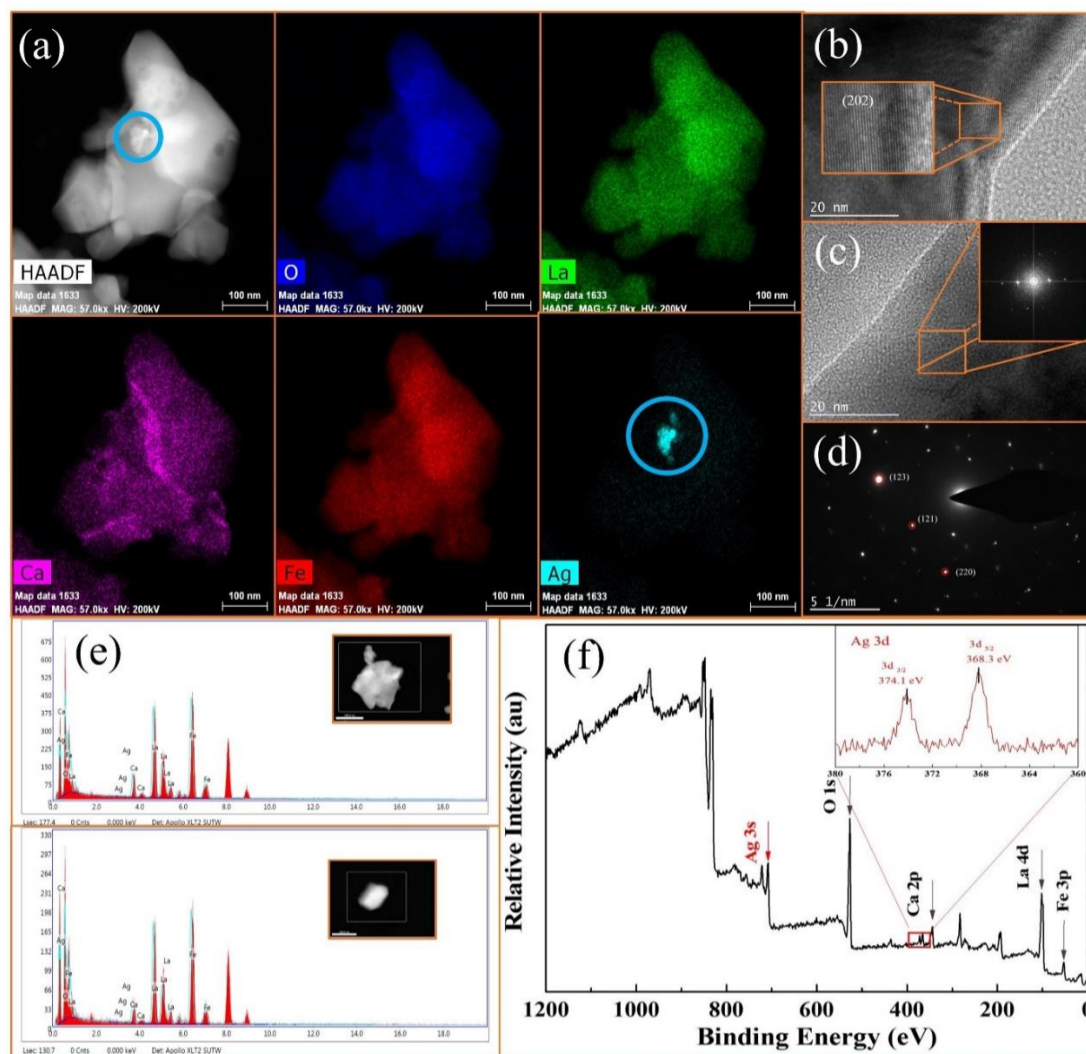


Figure 5.3. TEM images and XPS of LCFA powder sintered at 900 °C. (a) STEM and corresponding elemental maps: O, La, Ca, Fe, Ag; (b) and (c) HRTEM images with (202) plane and FFT of orthorhombic system as insets; (d) SAED pattern; (e) EDS of two particles given as insets; (f) XPS full survey spectra and magnified Ag 3d XPS spectra (inset).

LCFA powder was investigated through transmission electron microscope (TEM) and X-ray photoelectron spectroscopy (XPS). Figure 5.3a shows the scanning transmission electron microscope (STEM) and the corresponding elemental maps. It could be observed that the elements of La, Ca, Fe, and O are uniformly distributed in the sample. Nano-sized silver particles were successfully mixed into LCF system. Figure 5.3b&c show the high-resolution transmission electron microscopy (HRTEM) images with (202) plane and corresponding fast fourier transform (FFT) of orthorhombic system as insets, which indicate the orthorhombic structure of LCFA. To further identify the crystal structure, selected area electron diffraction (SAED) patterns for LCFA are

displayed in Figure 5.3d. A single-zone axis pattern could be obtained, and the formation of polycrystalline rings can be indexed as (123), (121), and (220) reflections of orthorhombic lattice marked as red circles. Furthermore, Figure 5.3e displays energy dispersive X-ray spectroscopy (EDS) of two particles given as insets, which could prove that the Ag nanoparticles are successful mixed into LCF system. The overall X-ray photoelectron spectroscopy (XPS) survey spectra verify the coexistence of La, Ca, Fe, Ag and O elements, shown in Figure 5.3f. Moreover, the magnified Ag 3d spectrum exhibits double-peak structure, 3d 3/2 and 3d 5/2, at 374.1 eV and 368.3 eV, respectively, which could further confirm the existence of metallic Ag^{0,2}

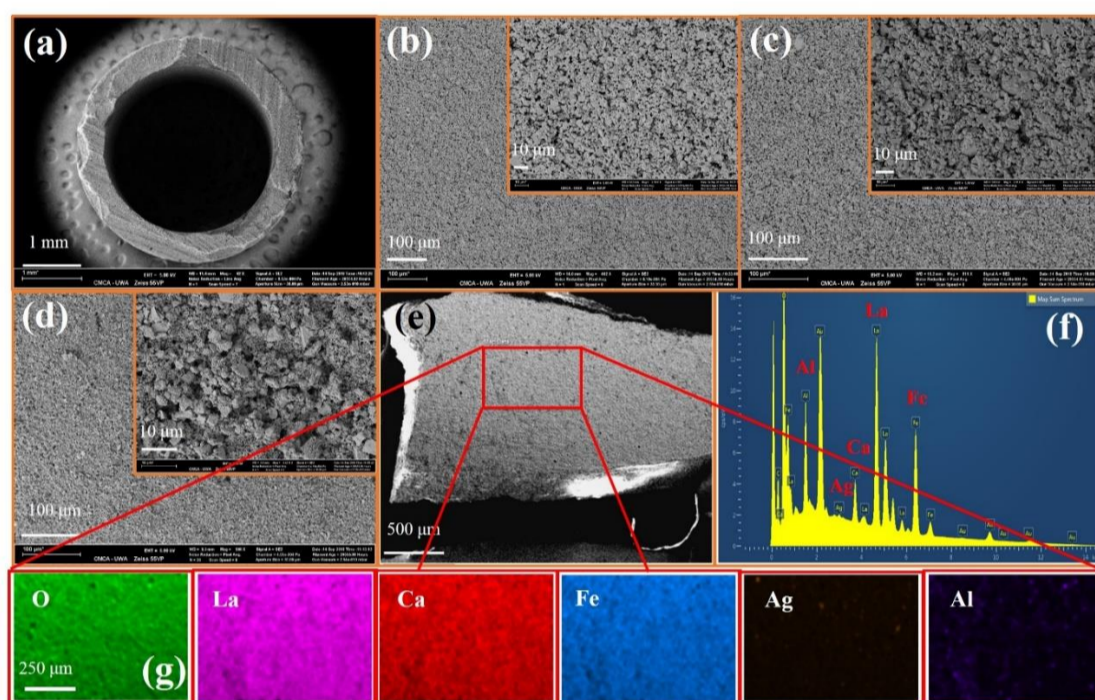


Figure 5.4. SEM micrographs of Al₂O₃ (a-c), and LCFA/Al₂O₃ (d-g) composite hollow fibres. (a) Cross section of hollow fibre; (b) Inner, and (c) Outer circumference surfaces of Al₂O₃ hollow fibre; (d and e) Outer circumference surfaces of LCFA/Al₂O₃ composite hollow fibre; (f) SEM-EDS of selected area in (e); and (g) Elemental mapping of (e).

Figure 5.4 displays the scanning electron microscopy (SEM) images of Al₂O₃ and LCFA/Al₂O₃ composite hollow fibres. Our home-made Al₂O₃ hollow fibre has 4.5 and 3.0 mm of outer and inner diameters, respectively, as shown in Figure 5.4a. Inner and outer circumference surfaces of Al₂O₃ hollow fibre were given in Figure 5.4b and c, where we can clearly see the polycrystalline grains. After dip-coating, LCFA was



deposited on both inner and outer Al_2O_3 surfaces, the porous perovskite layer could be observed in Figure 5.4d. The selected area SEM-Energy dispersive X-ray spectroscopy (EDS) and mapping of the coating layer (Figure 5.4e-g) showed the coexistence of La, Ca, Fe and Ag with Al from the fibre support, which ensured that the perovskite LCFA was successfully anchored on the surface of Al_2O_3 hollow fibre.

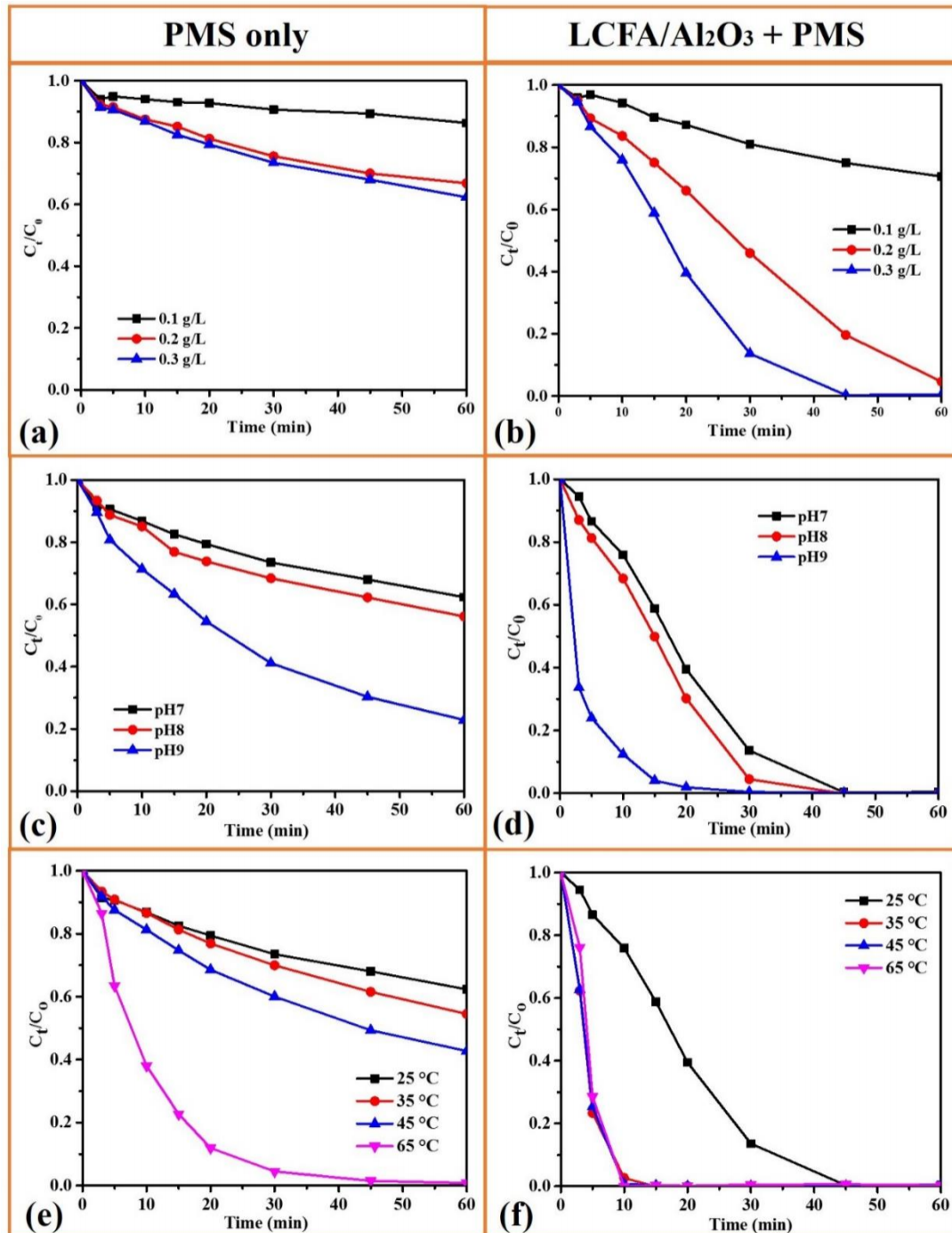


Figure 5.5. Decolourization of methylene blue at different PMS concentrations, (a) PMS only; (b) PMS and LCFA/ Al_2O_3 composite hollow fibre; Initial pH effect on MB



degradation, (c) PMS only; (d) PMS and LCFA/Al₂O₃ composite hollow fibre (Conditions: PMS 0.3 g/L, MB 20 ppm, and testing temperature 25 °C); Decolorization of MB at different temperatures, (e) PMS only; (f) PMS and LCFA/Al₂O₃ composite hollow fibre (Conditions: PMS 0.3 g/L, MB 20 ppm, and pH=7).

The effect of PMS on the LCFA/Al₂O₃ composite hollow fibre for MB degradation was investigated under different concentration of PMS (Figure 5.5a and b). The degradation efficiency displays positive correlation with concentration of PMS both with and without the catalyst, due to more contact areas between PMS, MB and catalyst with high PMS dosage. Therefore, the reaction could be initiated on more active sites to boost the reaction rate. It could only achieve 40 % degradation of MB in 1 h with PMS only at the dosage of 0.3 g/L. When the LCFA/Al₂O₃ composite hollow fibre participated in the reaction, the methylene blue could be degraded completely within 45 min using 0.3 g/L PMS. The reactions above conformed to the first-order kinetics and the reaction rate constant increased from 0.0012 to 0.0086 min⁻¹ with PMS only and from 0.0063 to 0.0490 min⁻¹ in the PMS/LCFA/Al₂O₃ composite hollow fibre system with PMS concentration rising from 0.1 to 0.3 g/L (Figure 5.6). With the existence of composite catalyst, the degradation efficiency of methylene blue was greatly improved, indicating the promising effect of the composite hollow fibre in the activation of PMS.

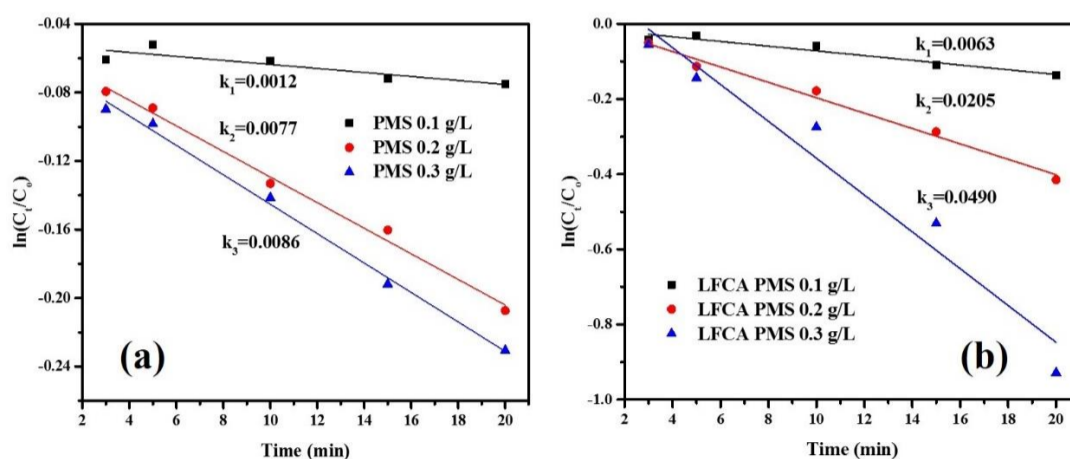


Figure 5.6. The first-order kinetics of decolorization of methylene blue at different PMS concentrations (a) PMS only; (b) PMS and LCFA/Al₂O₃ composite hollow fibre.

To understand the possible effect of pH values on organic degradation, we performed the catalytic reactions at different initial solution pH values (pH= 7, 8, and 9) by adding 0.1 M H₂SO₄ and/or 0.1 M KOH aqueous solutions. No buffered solutions were used



here in order to avoid the radical-scavenger effect of the buffer agents. It can be seen in Figure 5.5c-d that the decolourization efficiency displays positive correlation with the pH value. In the presence of LCFA, the MB could be degraded completely within 45 mins at pH=7 and 8, while within 30 mins at pH=9. The reaction rate constant rose from 0.0490 min^{-1} at pH=7 to 0.1729 min^{-1} at pH=9 (Figure 5.7a). There are two reasons for the improved catalytic performances at higher pH values: one is that the stronger alkaline condition facilitated the self-decomposition of PMS and induced more active species to attack the pollutant. The reaction rate constant with PMS only increased from 0.0086 min^{-1} at pH=7 to 0.0278 min^{-1} at pH =9 (Figure 5.7b). The other reason is that the basic environment is beneficial to the redox cycle of $\text{Fe}^{3+}/\text{Fe}^{2+}$, and thus accelerate the catalytic reaction here. [10, 38] Noteworthy, the basic condition can not only improve the reaction rate, but also maintain the surficial chemistry of the perovskite and suppress the metal leaching into the reaction solution. It suggested that the LCFA/ Al_2O_3 composite hollow fibre-PMS system is expected to avoid second contamination due to the fixation of LCFA on the support and the basic solution.

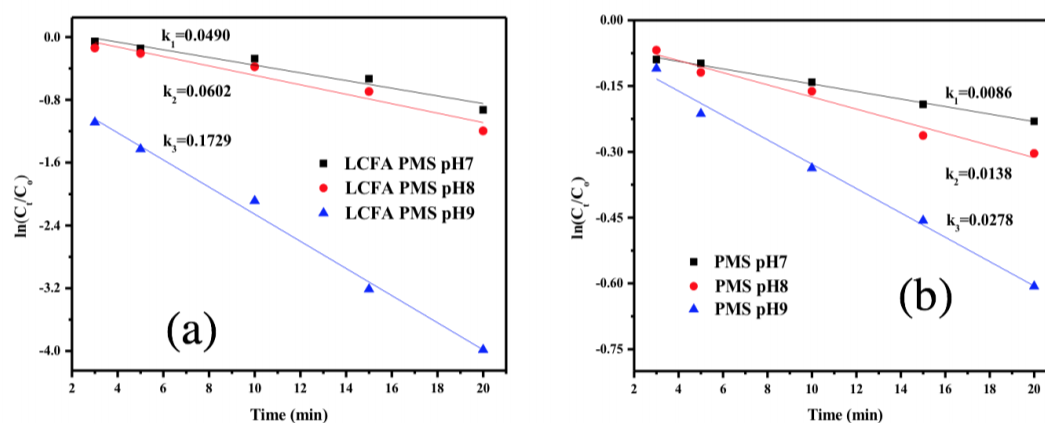


Figure 5.7. The first-order kinetics of decolourization of methylene blue under different initial pH. (a) PMS and LCFA/ Al_2O_3 composite hollow fibre; (b) PMS only. Conditions: PMS 0.3 g/L, MB 20 ppm, and testing temperature 25 °C.

The influence of reaction temperature on MB degradation was studied (Figure 5.5e&f), showing that the increasing reaction temperature exerted positive influence on the decomposition rate of the pollutant. Although the reaction rate was improved by PMS only at higher temperature, MB decolourization was still not completed even at 65 °C (Figure 5.5e). After the addition of composite catalyst, the complete degradation of MB could be achieved only in 10 min over 35 °C (Figure 5.5f). This could be explained by



that the high temperature gave rise to the increased energy absorption of O-O break-up, which would finally facilitate PMS activation.[39]

Table 5.2. Leaching effect of LCFA/Al₂O₃ composite catalyst vs time (temperature=25°C, pH=7, PMS=0.3 g/L, catalyst loading = 0.5 g/L).

Time (pH7 25°C)	Ag (mg/L)	Fe (mg/L)	Al (mg/L)	Ca (mg/L)	La (mg/L)
0 min	0.00	0.19	0.00	0.27	0.08
10 min	0.00	0.20	0.01	0.34	0.08
20 min	0.00	0.21	0.03	0.56	0.08
30 min	0.01	0.30	0.11	0.56	0.10

Table 5.3. Leaching effect of LCFA/Al₂O₃ composite catalyst vs pH (temperature=25°C, PMS=0.3 g/L, catalyst loading = 0.5 g/L).

	Ag (mg/L)	Fe (mg/L)	Al (mg/L)	Ca (mg/L)	La (mg/L)
pH9 Original	0.00	0.19	0.13	0.00	0.08
pH9 30 min	0.00	0.19	0.26	0.08	0.08
pH8 Original	0.01	0.18	0.12	0.29	0.08
pH8 30 min	0.01	0.21	0.23	0.97	0.09
pH7 Original	0.00	0.19	0.00	0.27	0.08
pH7 30 min	0.01	0.30	0.11	0.56	0.10



Table 5.4. Leaching effect of LCFA/Al₂O₃ composite catalyst vs temperature (pH=7, PMS=0.3 g/L, catalyst loading = 0.5 g/L).

	Ag (mg/L)	Fe (mg/L)	Al (mg/L)	Ca (mg/L)	La (mg/L)
65°C Original	0.09	0.00	1.18	1.74	0.02
65°C 30 min	0.12	0.22	1.60	2.04	0.05
45°C Original	0.02	0.18	0.10	1.53	0.07
45°C 30 min	0.16	0.32	1.17	3.18	0.32
25°C Original	0.00	0.19	0.00	0.27	0.08
25°C 30 min	0.01	0.30	0.11	0.56	0.10

In order to verify the elimination of secondary contamination, the leaching rate of this composite catalyst as function of temperature, pH values and temperatures was tested and summarized in Table 5.2-4. The results showed that the concentration of metal ions in the water was generally satisfied for the US-EPA environmental standards (USEPA, 1996, Fe: 0.3 mg/L; Al: 0.2 mg/L; Ca: 61 mg/L; Ag 0.1 mg/L) except for some harsh conditions such as high reaction temperature.

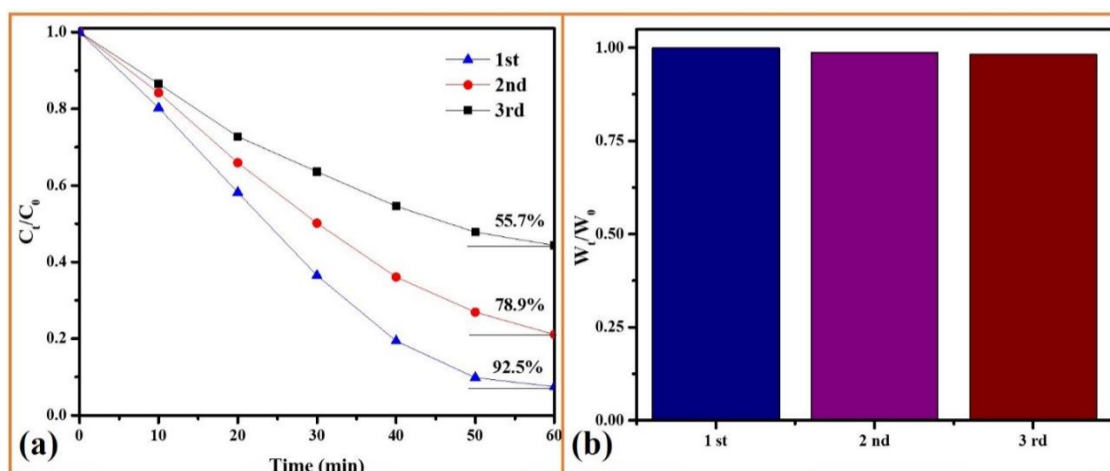


Figure 5.8. Reusability tests of LCFA/Al₂O₃ composite hollow fibre catalyst on MB degradation. (a) Degradation; (b) Mass-lose of the LCFA/Al₂O₃ composite hollow fibre. Conditions: MB solution (20 ppm), 0.1 g/L PMS, pH=7 and test temperature 25 °C.

The reusability of LCFA/Al₂O₃ composite hollow fibre catalyst on MB degradation was

also studied. After three times tests, the degradation percentage in 1 h decreased from 92.6 % to 55.7 % (Figure 5.8a), while negligible mass-lose of LCFA/Al₂O₃ composite hollow fibre could be observed (Figure 5.8b). Thus, the decrease of degradation percentage may not be caused by mass-lose of catalyst, but be induced by the surface contamination and coverage of active sites by the intermediate products. Note that the negligible mass-loss of the composite catalyst here could directly prove that this hollow fibre-based composite catalyst would greatly enable the elimination of secondary contamination, opening a new window of membrane-based catalyst for advanced oxidation.

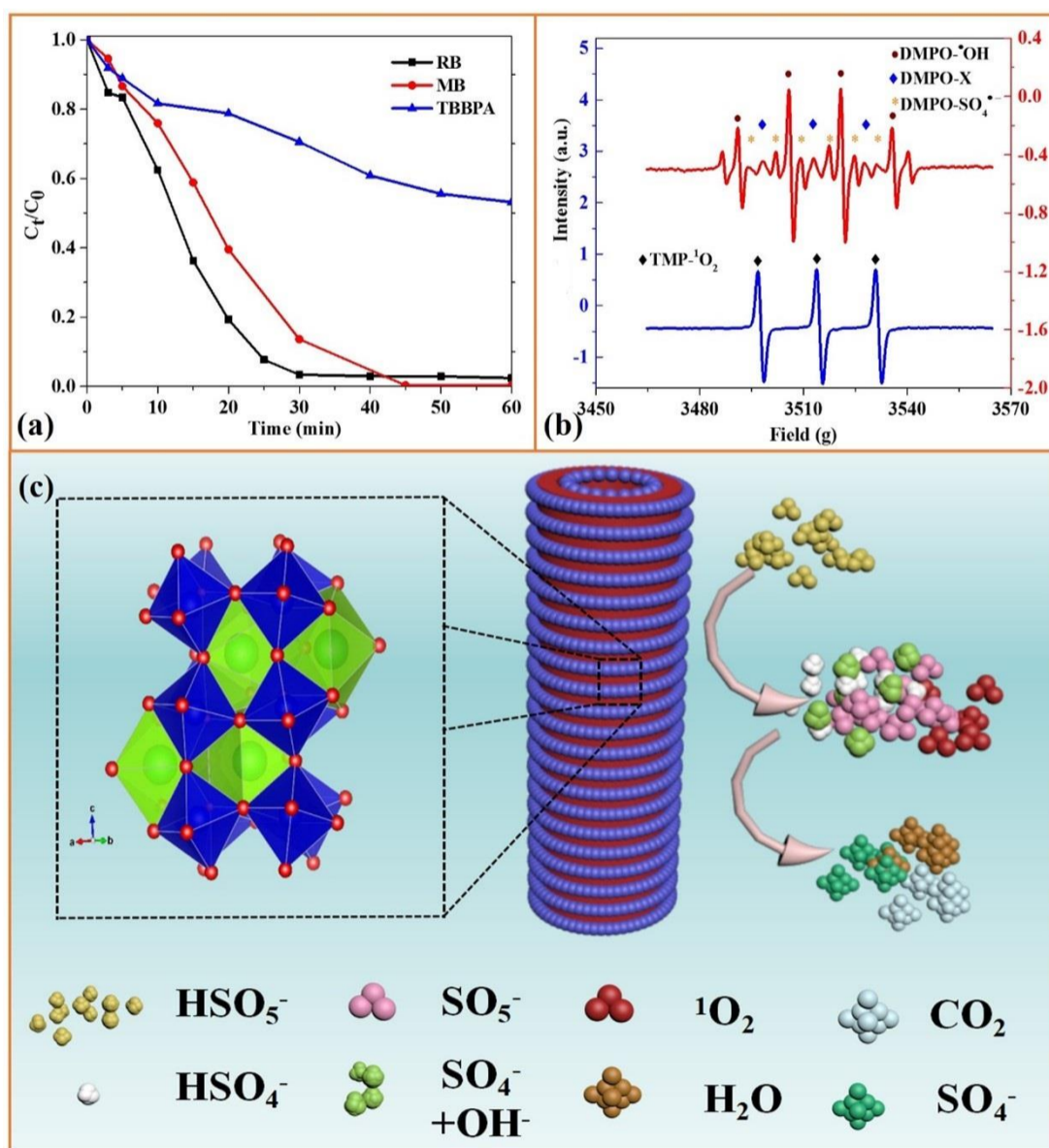


Figure 5.9. (a) Remove of various pollutants on LCFA/Al₂O₃. Conditions: 0.3 g/L PMS, pH=7, and test temperature 25 °C; (b) EPR tests in catalytic oxidation on LCFA/Al₂O₃



(Centerfield: 3510 G; sweep width: 100 G; modulation frequency: 100 GHz. Reaction conditions: catalyst loading = 0.5 g/L, PMS loading = 0.3 g/L, pH = 7.0, MB= 20 ppm, TMP = 1 mM, DMPO = 0.08 M); (c) Proposed mechanism of PMS activation and pollutants oxidation on a LCFA/Al₂O₃ composite hollow fibre catalyst.

Besides methylene blue, LCFA/Al₂O₃ composite hollow fibre also showed catalytic effect on some other organic pollutants such as rhodamine B (RB) and tetrabromobisphenol A (TBBPA) (Figure 5.9a). Approximately 100 % of RB and 40 % of TBBPA were degraded within one hour. It suggested that LCFA/Al₂O₃ was a highly efficient and versatile catalyst with the ability to degrade various pollutants under the catalyst/PMS system. The effective catalysis of LCFA/Al₂O₃ composite hollow fibre can be attributed to the following reasons: firstly, the redox reaction of Fe²⁺/Fe³⁺ in the system (especially under the basic condition) contributed to the pollutant degradation; secondly, the doping of nano-sized silver particles improved the conductivity of the composite catalyst, and thus boost the electron transfer between the catalyst and PMS; thirdly, the substitution of Ca brought the oxygen vacancy, which would act as the defective site to absorb PMS molecules and facilitate the redox reaction of Fe²⁺/Fe³⁺.

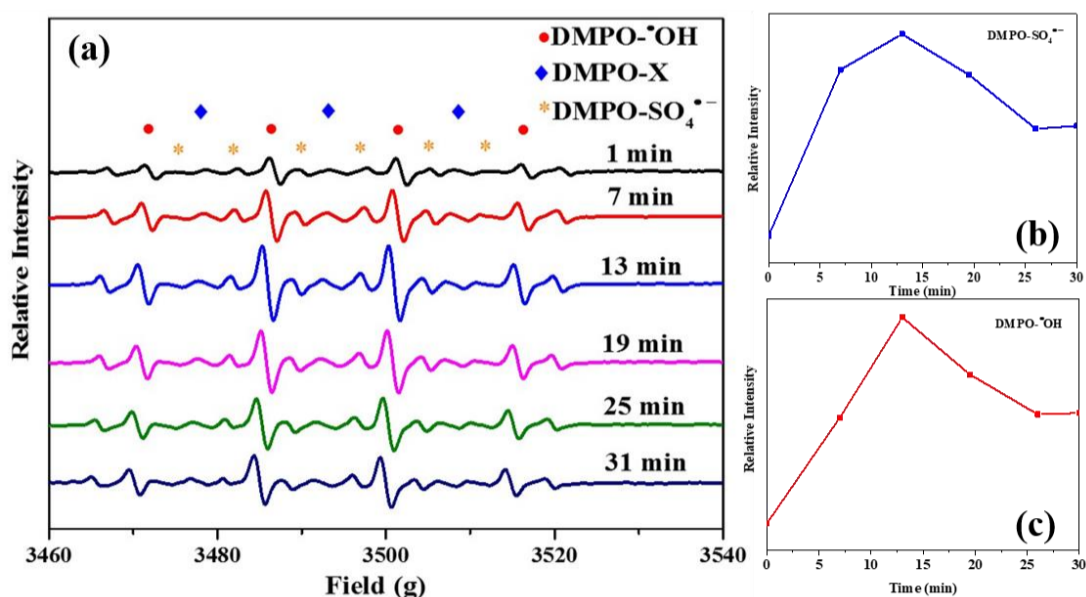


Figure 5.10. EPR test, free radicals in catalytic oxidation vs time. (a) DMPO-SO₄^{•-} and DMPO-[•]OH; (b) sulfate radical evolution; (c) hydroxyl radical evolution. Centerfield: 3510 G; sweep width: 100 G; modulation frequency: 100 GHz. Reaction conditions: catalyst loading = 0.5 g/L, PMS loading = 0.3 g/L, pH = 7.0, TMP = 1 mM, MB= 20 ppm, DMPO = 0.08 M.



In order to determine reaction mechanism, *in situ* electron paramagnetic resonance (EPR) experiments were performed to detect the radicals generated during PMS activation. Both $\text{DMPO}\cdot\text{SO}_4^{\bullet-}$ and $\text{DMPO}\cdot\text{OH}$ signals (consisting of a quartet with an intensity ratio of 1:2:2:1) could be observed with 5,5-dimethyl-1-pyrroline N-oxide (DMPO) as a radical spin trapping agent (Figure 5.9b), indicating that hydroxyl and sulfate radicals were produced during PMS activation. Besides, the signals of hydroxyl radicals were much stronger than those of sulfate radicals, and the intensities of hydroxyl radicals and sulfate radicals was the highest in the first 13 min during the reaction and then decreased which was conformed to the degradation rate of methylene blue (Figure 5.10a-c). It can be deduced that hydroxyl radicals and sulfate radicals played a great role in the MB degradation. Besides the free radicals above, singlet oxygen can be generated during the decomposition of PMS ($\text{HSO}_5^- + \text{SO}_5^{2-} \rightarrow \text{HSO}_4^- + \text{SO}_4^{2-} + {}^1\text{O}_2$). [40-42] Herein, three typical peaks assigned to singlet oxygen were found with 2,2,6,6-tetramethyl-4-piperidinol (TMP) as trapping agent of singlet oxygen and (Figure 5.9b, 10b and c), indicating that LCFA/ Al_2O_3 -PMS system also gave rise to the generation of ${}^1\text{O}_2$. [43-44] The intensity of singlet oxygen increased sharply in the first 6 min and then decreased, which accorded with the decomposition rate of methylene blue, suggesting that singlet oxygen also acted on the organic pollutant degradation.

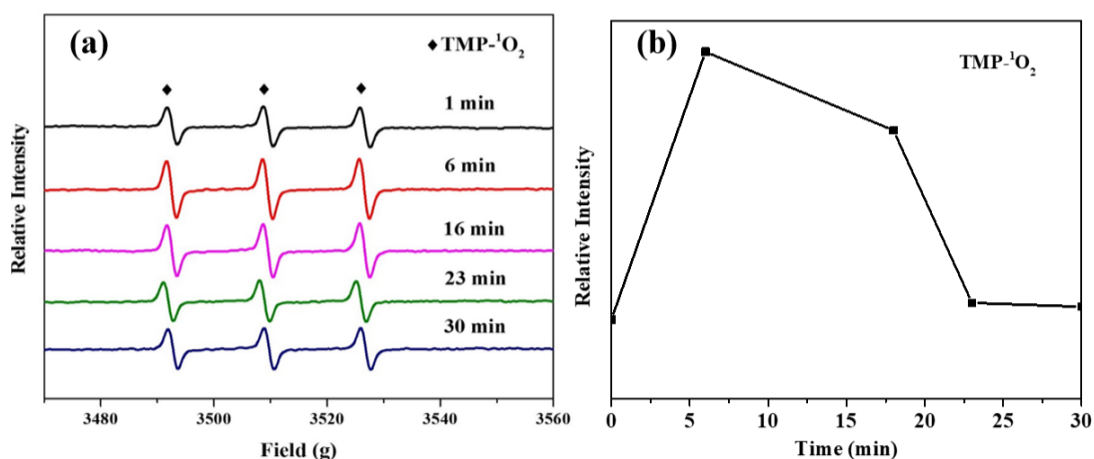
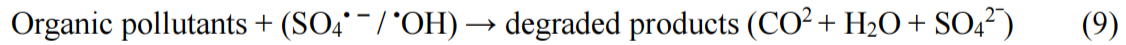
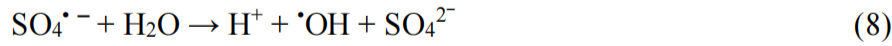
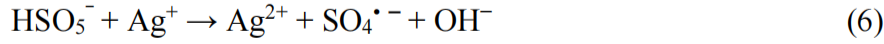
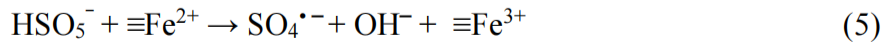
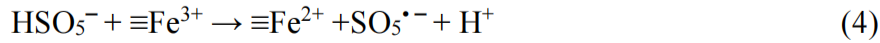


Figure 5.11. EPR test, (a) and (b) singlet oxygen in catalytic oxidation vs time. Centerfield: 3510 G; sweep width: 100 G; modulation frequency: 100 GHz. Reaction conditions: temperature = 25 °C, catalyst loading = 0.5 g/L, PMS loading = 0.3 g/L, MB= 20 ppm, pH = 7.0, TMP = 1 mM, DMPO = 0.08 M.

The mechanism of PMS activation by LCFA/ Al_2O_3 composite hollow fibre catalyst was

illustrated in Figure 5.9c and may follow the equations (4-9) as below:



* Organic pollutants are MB, RB, and TBBPA (in this work).

The degradation of organic pollutant *via* photocatalytic reaction by the composite hollow fibre was also investigated in this study. Figure 5.15a shows XRD patterns of Al_2O_3 hollow fibre and as-synthesized $\text{TiO}_2/\text{Al}_2\text{O}_3$ composite hollow fibres without calcination. The crystalline phase of the substrate hollow fibre is confirmed to be α - Al_2O_3 and after deposition, the particles growing on the outside surface of hollow fibres are identified as anatase TiO_2 . Due to the hydrophilic property of Al_2O_3 hollow fibres, the *in situ* growing TiO_2 coating adhered to the substrates surface excellently.[36]

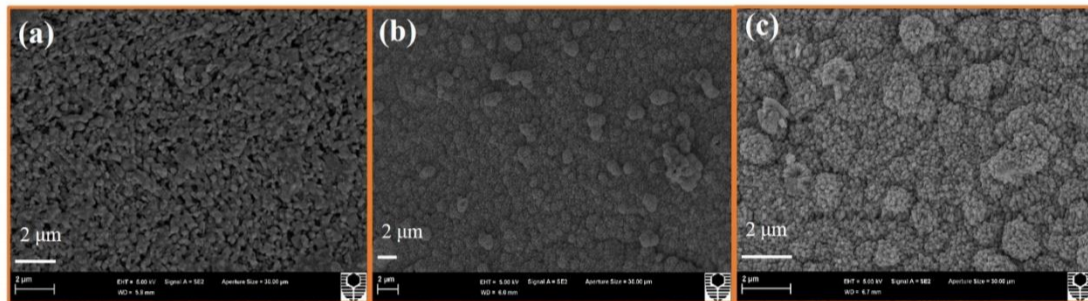


Figure 5.12. SEM surface views of the $\text{TiO}_2/\text{Al}_2\text{O}_3$ composite hollow fibres with different deposition time: (c) 48 h, (d) 72 h, and (e) 96 h.

From Figure 5.15b, we can see a thick layer consisted of fine grains distributing uniformly which were identified as TiO_2 . As the deposition time increased, the TiO_2 layer became denser (Figure 5.12) as more TiO_2 nanoparticles were grown on the support. After calcination in air at 250 °C, 450 °C and 650 °C, the coating layer was still anatase TiO_2 confirmed by XRD data in Figure 5.13 and the broad diffraction peaks indicated the small crystal size. The X-ray diffraction peaks locating at 25.4°, 37.8°, 48.0°, 54.3° and 62.7° were found corresponding to the crystal planes of (101), (004),

(200), (105), and (204), respectively. The higher intensity of TiO₂ calcinated at 450 °C in comparison with others suggested the better crystalline degree. The sub-micron crystal size of synthesized TiO₂ at different temperatures (25 °C, 250 °C, 450 °C, and 650 °C) were calculated based on Scherrer equation as 50.57 nm, 46.04 nm, 46.32 nm, and 38.95 nm, respectively (Figure 5.13).

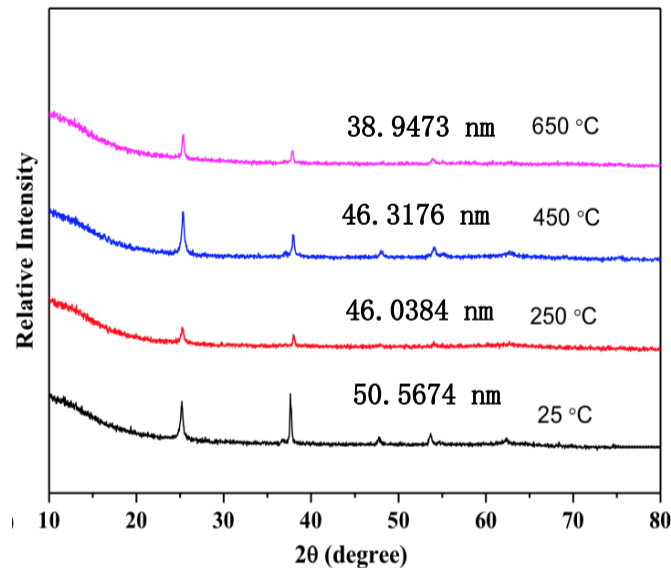


Figure 5.13. XRD patterns of as-synthesized TiO₂ and TiO₂ after heating at 250 °C, 450 °C and 650 °C.

The TiO₂ coating layer after annealing at 250 °C and 450 °C was still compact with millions of particles while some cracks occurred on the layer of TiO₂ annealed at 650 °C, probably due to the high tension during heating (Figure 5.14). The hollow fibres annealed at 450 °C were initially exposed to DI water to evaluate the permeation ability of composite hollow fibres. The calculated fibre flux was 56.6 L·m⁻²·h⁻¹·bar⁻¹ and dropped to 31.4 L·m⁻²·h⁻¹·bar⁻¹ while the fibres were exposed to methylene blue, with a 44.5% reduction compared to that of DI water. This indicates that MB in the solution formed a blocked layer on the fibre surface and thus may block the pores. However, the reduction was much less than nanostructured TiO₂ hollow fibre,[45] because the TiO₂ particles grew initially on the surface of the substrate and then filled up the pores between the Al₂O₃ grains in the hollow fibre surface gradually during the continuous deposition.[35] Denser surface and less surface area accounted for the slower reduction, which could also explain why the MB adsorption capacity of composite hollow fibre after coating decreased sharply compared with the fibres without coating (Figure 5.15c).

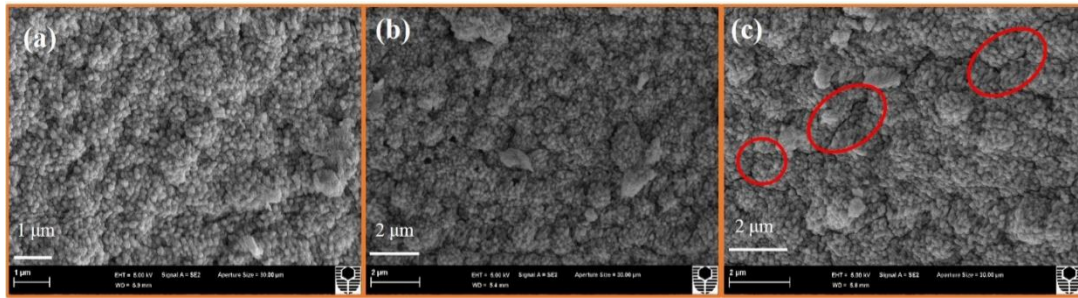


Figure 5.14. SEM images of the $\text{TiO}_2/\text{Al}_2\text{O}_3$ composite hollow fibres calcinated at different temperature (a) 250 °C, (b) 450 °C and (c) 650 °C.

The photocatalytic efficiencies of various fibres after coating in degradation of MB solutions were shown in Figure 5.15d. It was found that the fibres without calcination exhibited the worst photocatalytic effect compared with the calcinated ones, only 55.2 % degradation in 24 h. Approximately, 96.0 % of MB was degraded in 24 h by fibres annealed at 450 °C, showing the best photocatalytic efficiency among the samples. It could be explained as below: (1) Higher anatase TiO_2 crystalline phase formed after high temperature calcination (450 and 650 °C), comparing with TiO_2 calcinated at low temperature (25 and 250 °C). (2) High calcination temperature at 650 °C would induce the cracks on the coating layer and affect the density of surface layer of TiO_2 as confirmed above in Figure 5.14. The photodegradation efficiency was not satisfactory because the intensity of lamp we used in this study was small, only $848.3 \mu\text{W}/\text{cm}^2$. But it was still inspired that the $\text{TiO}_2/\text{Al}_2\text{O}_3$ composite hollow fibre owned the ability to decompose organic pollutants *via* photocatalysis, and the photocatalytic effect could be adjusted by calcination at various temperatures.

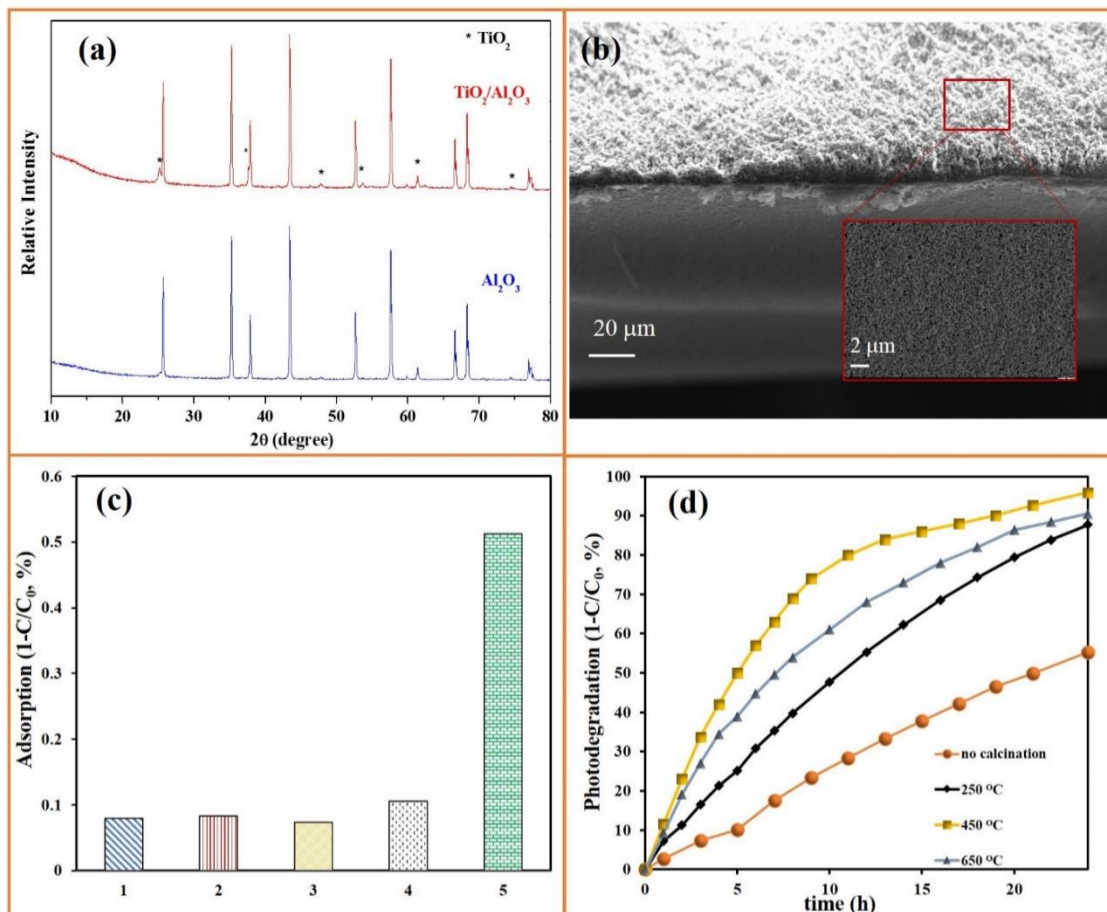


Figure 5.15. (a) XRD patterns for Al₂O₃ hollow fibre and TiO₂/Al₂O₃ composite hollow fibre ((* anataze TiO₂); (b) SEM images of cross-section and TiO₂ coating layer (insets) on the outside surface of the TiO₂/Al₂O₃ composite hollow fibres; (c) MB adsorption by hollow fibre before and after coating (1: without calcination; 2: calcination temperature at 250 °C; 3: calcination temperature at 450 °C; 4: calcination temperature 650 °C; 5: Al₂O₃ support); (d) Photo-degradation of MB using TiO₂/Al₂O₃ composite hollow fibres. ([MB] = 10 ppm; reaction temperature = 25 °C).

Reaction rate constant, k (min^{-1}) of the first-order kinetics in the following equation

$$\ln\left(\frac{C_t}{C_0}\right) = -kt$$

5.4 Conclusions

Catalyst/Al₂O₃ composite hollow fibres were obtained *via* in-site growth and dip coating methods. For Ag-La_{0.8}Ca_{0.2}Fe_{0.95}O_{3-δ}/Al₂O₃ composite hollow fibre, the complete degradation of MB (20 ppm) could be achieved in 10 min over 35 °C with PMS (0.3 g/L), due to the hydroxyl and sulfate radicals as well as singlet oxygen. The



redox cycle of $\text{Fe}^{2+}/\text{Fe}^{3+}$, oxygen vacancy and good conductivity of the composite hollow fibre facilitated the excellent catalytic effect. The pH value and reaction temperature exerted great influence on the catalytic effect of perovskite/ Al_2O_3 composite hollow fibre. For $\text{TiO}_2/\text{Al}_2\text{O}_3$, the compact anatase TiO_2 layer was successfully coated on the outer surface of the Al_2O_3 hollow fibre. The photocatalytic effect of $\text{TiO}_2/\text{Al}_2\text{O}_3$ composite hollow fibres could be adjusted by calcination at various temperatures. Catalyst/ Al_2O_3 composite hollow fibre enables the elimination of the secondary contamination effectively, compared to powder catalysts, which is of great significance to the industry applications.



References

1. The rise of graphene. *Nat. Mater.* 2007; 6(3):18391.
2. Zhu YW, Murali S, Cai WW, Li XS, Suk JW, Potts JR, et al. Graphene and graphene oxide: synthesis, properties, and applications. *Adv. Mater.* 2010; 22(35):3906-24.
3. Loh KP, Bao QL, Ang PK, Yang JX. The chemistry of graphene. *J. Mater. Chem.* 2010; 20(12):2277-89.
4. Su DS, Perathoner S, Centi G. Nanocarbons for the development of advanced catalysts. *Chem. Rev.* 2013; 113(8):5782-816.
5. Lai LF, Potts JR, Zhan D, Wang L, Poh CK, Tang CH, et al. Exploration of the active center structure of nitrogen-doped graphene-based catalysts for oxygen reduction reaction. *Energ. Environ. Sci.* 2012; 5(7):7936-42.
6. Duan X, Sun H, Wang Y, Kang J, Wang S. N-doping-induced nonradical reaction on single-walled carbon nanotubes for catalytic phenol oxidation. *ACS Catal.* 2014; 5(2):553-9.
7. Su DS, Zhang J, Frank B, Thomas A, Wang XC, Paraknowitsch J, et al. Metal-free heterogeneous catalysis for sustainable chemistry. *Chemsuschem.* 2010; 3(2):16980.
8. Chizari K, Deneuve A, Ersen O, Florea I, Liu Y, Edouard D, et al. Nitrogen-doped carbon nanotubes as a highly active metal-free catalyst for selective oxidation. *Chemsuschem.* 2012; 5(1):102-8.
9. Anipsitakis GP, Dionysiou DD. Degradation of organic contaminants in water with sulfate radicals generated by the conjunction of peroxymonosulfate with cobalt. *Environ. Sci. Technol.* 2003; 37(20):4790-7.
10. Anipsitakis GP, Dionysiou DD, Gonzalez MA. Cobalt-mediated activation of peroxymonosulfate and sulfate radical attack on phenolic compounds. Implications of chloride ions. *Environ. Sci. Technol.* 2006; 40(3):1000-7.



11. Anipsitakis GP, Stathatos E, Dionysiou DD. Heterogeneous activation of oxone using Co_3O_4 . *J. Phys. Chem. B.* 2005; 109(27):13052-5.
12. Liang HW, Sun HQ, Patel A, Shukla P, Zhu ZH, Wang SB. Excellent performance of mesoporous $\text{Co}_3\text{O}_4/\text{MnO}_2$ nanoparticles in heterogeneous activation of peroxydisulfate for phenol degradation in aqueous solutions. *Appl. Catal., B* 2012; 127:330-5.
13. Saputra E, Muhammad S, Sun HQ, Ang HM, Tade MO, Wang SB. Different crystallographic one-dimensional MnO_2 nanomaterials and their superior performance in catalytic phenol degradation. *Environ. Sci. Technol.* 2013; 47(11):5882-7.
14. Sun HQ, Liu SZ, Zhou GL, Ang HM, Tade MO, Wang SB. Reduced graphene oxide for catalytic oxidation of aqueous organic pollutants. *ACS Appl. Mater. Inter.* 2012; 4(10):5466-71.
15. Enoki T, Fujii S, Takai K. Zigzag and armchair edges in graphene. *Carbon.* 2012; 50(9):3141-5.
16. Frank B, Zhang J, Blume R, Schlogl R, Su DS. Heteroatoms increase the selectivity in oxidative dehydrogenation reactions on nanocarbons. *Angew. Chem. Int. Ed.* 2009; 48(37):6913-7.
17. Liu SZ, Peng WC, Sun HQ, Wang SB. Physical and chemical activation of reduced graphene oxide for enhanced adsorption and catalytic oxidation. *Nanoscale.* 2014; 6(2):766-71.
18. Peng WC, Liu SZ, Sun HQ, Yao YJ, Zhi LJ, Wang SB. Synthesis of porous reduced graphene oxide as metal-free carbon for adsorption and catalytic oxidation of organics in water. *J. Mater. Chem. A* 2013; 1(19):5854-9.
19. Zhang J, Liu X, Blume R, Zhang AH, Schlogl R, Su DS. Surface-modified carbon nanotubes catalyze oxidative dehydrogenation of n-butane. *Science.* 2008; 322(5898):73-7.



20. Sun HQ, Kwan C, Suvorova A, Ang HM, Tade MO, Wang SB. Catalytic oxidation of organic pollutants on pristine and surface nitrogen-modified carbon nanotubes with sulfate radicals. *Appl. Catal., B* 2014; 154:134-41.
21. Sun HQ, Wang YX, Liu SZ, Ge L, Wang L, Zhu ZH, et al. Facile synthesis of nitrogen doped reduced graphene oxide as a superior metal-free catalyst for oxidation. *Chem. Commun.* 2013;49(85):9914-6.
22. Hummers WS, Offeman RE. Preparation of graphitic oxide. *J. Am. Chem. Soc.* 1958;80(6):1339-.
23. Delley B. From molecules to solids with the DMol(3) approach. *J. Chem. Phys.* 2000; 113(18):7756-64.
24. Perdew JP, Burke K, Ernzerhof M. Generalized gradient approximation made simple. *Phys Rev Lett.* 1996;77(18):3865-8.
25. Grimme S. Semiempirical GGA-type density functional constructed with a long-range dispersion correction. *J. Comput. Chem.* 2006; 27(15):1787-99.
26. Qu LT, Liu Y, Baek JB, Dai LM. Nitrogen-doped graphene as efficient metal-free electrocatalyst for oxygen reduction in fuel cells. *ACS Nano.* 2010; 4(3):1321-6.
27. Su YZ, Zhang Y, Zhuang XD, Li S, Wu DQ, Zhang F, et al. Low-temperature synthesis of nitrogen/sulfur co-doped three-dimensional graphene frameworks as efficient metal-free electrocatalyst for oxygen reduction reaction. *Carbon.* 2013; 62:296-301.
28. Ferrari AC, Meyer JC, Scardaci V, Casiraghi C, Lazzeri M, Mauri F, et al. Raman spectrum of graphene and graphene layers. *Phys. Rev. Lett.* 2006; 97(18).
29. Choi CH, Park SH, Woo SI. Binary and ternary doping of nitrogen, boron, and phosphorus into carbon for enhancing electrochemical oxygen reduction activity. *ACS Nano.* 2012; 6(8):7084-91.



30. Berciaud S, Ryu S, Brus LE, Heinz TF. Probing the intrinsic properties of exfoliated graphene: raman spectroscopy of free-standing monolayers. *Nano Lett.* 2009; 9(1):346-52.
31. Casiraghi C, Pisana S, Novoselov KS, Geim AK, Ferrari AC. Raman fingerprint of charged impurities in graphene. *Appl. Phys. Lett.* 2007; 91(23):Doi 10.1063/1.2818692.
32. Kumar NA, Nolan H, McEvoy N, Rezvani E, Doyle RL, Lyons MEG, et al. Plasma-assisted simultaneous reduction and nitrogen doping of graphene oxide nanosheets. *J. Mater. Chem. A.* 2013; 1(14):4431-5.
33. Li XL, Wang HL, Robinson JT, Sanchez H, Diankov G, Dai HJ. Simultaneous nitrogen doping and reduction of graphene oxide. *J. Am. Chem. Soc.* 2009; 131(43):15939-44.
34. Kinoshita K. *Carbon: electrochemical and physicochemical properties* 1988. Medium: X; Size: Pages: 541 p.
35. Sheng ZH, Shao L, Chen JJ, Bao WJ, Wang FB, Xia XH. Catalyst-free synthesis of nitrogen-doped graphene via thermal annealing graphite oxide with melamine and its excellent electrocatalysis. *ACS Nano.* 2011; 5(6):4350-8.
36. Lin ZY, Waller G, Liu Y, Liu ML, Wong CP. Facile Synthesis of nitrogendoped graphene via pyrolysis of graphene oxide and urea, and its electrocatalytic activity toward the oxygen-reduction reaction. *Adv. Energ. Mater.* 2012; 2(7):884-8.
37. Wang CD, Zhou YA, He LF, Ng TW, Hong G, Wu QH, et al. In situ nitrogendoped graphene grown from polydimethylsiloxane by plasma enhanced chemical vapor deposition. *Nanoscale.* 2013; 5(2):600-5.
38. Long JL, Xie XQ, Xu J, Gu Q, Chen LM, Wang XX. Nitrogen-doped graphene nanosheets as metal-free catalysts for aerobic selective oxidation of benzylic alcohols. *ACS Catal.* 2012; 2(4):622-31.
39. Deng DH, Pan XL, Yu LA, Cui Y, Jiang YP, Qi J, et al. Toward n-doped graphene via solvothermal synthesis. *Chem. Mater.* 2011; 23(5):1188-93.



40. Kong XK, Sun ZY, Chen M, Chen CL, Chen QW. Metal-free catalytic reduction of 4-nitrophenol to 4-aminophenol by N-doped graphene. *Energ. Environ. Sci.* 2013; 6(11):3260-6.
41. Kong XK, Chen CL, Chen QW. Doped graphene for metal-free catalysis. *Chem. Soc. Rev.* 2014; 43(8):2841-57.
42. Saputra E, Muhammad S, Sun HQ, Wang SB. Activated carbons as green and effective catalysts for generation of reactive radicals in degradation of aqueous phenol. *Rsc Adv.* 2013; 3(44):21905-10.
43. Wang SB, Sun HQ, Ang HM, Tade MO. Adsorptive remediation of environmental pollutants using novel graphene-based nanomaterials. *Chem. Eng. J.* 2013; 226:336-47.
44. Liu HT, Liu YQ, Zhu DB. Chemical doping of graphene. *J. Mater. Chem.* 2011; 21(10):3335-45.
45. Gong KP, Du F, Xia ZH, Durstock M, Dai LM. Nitrogen-doped carbon nanotube arrays with high electrocatalytic activity for oxygen reduction. *Science.* 2009; 323(5915):760-4.

Every reasonable effort has been made to acknowledge the owners of copyright material. I would be pleased to hear from any copyright owner who has been omitted or incorrectly acknowledged.



Chapter 6 Catalytic performance of natural metal ore in peroxymonosulfate activation for soil remediation and its financial feasibility

Abstract

With the immense development of the human society, the accumulation of hazardous xenobiotic chemicals in soil has caused significant deleterious consequences for human health and ecosystems. Due to the characteristic low mobility, soil pollution and sediment contamination need to be paid special attention. This study investigates manganese ore (MO) /peroxymonosulfate-based advanced oxidation processes (AOPs) as in-situ remediation technology to degrade organic pollutants in soil. The experiments were conducted in a home-made liquid-solid reactor. The tetrabromobisphenol A (TBBPA) removal efficiency was systematically studied with varying pollutant amount, sand volume, natural ore catalyst loading dosage and water washing flow rate. Results show that TBBPA in the sand wash water could be effectively degraded by this MO/PMS system with extremely low cost in comparison with synthetic transition metal containing catalysts.



6.1 Introduction

With the continuous development of agriculture and chemical industry, the accumulation of human-made chemical pollutants in soil has become a global concern.[1] There are several categories of harmful chemicals involved in the land degradation such as petroleum hydrocarbons, pesticides and heavy metals.[2] Among these pollutants, hydrophobic organic compounds are extremely persistent over time, since they have low water solubility thus tend to fuse with soil matrix, leading to little mass transfer and low biodegradability.[3] Apparently, these contaminants will alter plant metabolism and reduce crop yields. More concerns over soil contamination arise fundamentally from the consequent health risks.[4] These permanent organic pollutants (POPs) have potential mutagenicity and carcinogenicity properties. And they become even more concentrated from life forms in the lower pyramid levels of the food chain to the top.[5] Exposure to POPs may cause congenital disorders and many other chronic health conditions.[6]

Various techniques have been developed for the remediation of POPs-contaminated soil and sediments. They can basically be divided into *in-situ* and *ex-situ* technologies. *In-situ* technologies include chemical reduction/oxidation, flushing and thermal treatment that allow the contaminated soil to be restored in place.[7] While *ex-situ* technologies require soil excavation, typically followed by soil washing, solidification, vapor extraction, or simple disposal into landfill.[8] To avoid the disturbance of soil texture, *in-situ* remediation approaches towards contaminated land are constantly evolving. Recently, advanced oxidation processes (AOPs) have attracted intensive attention for POPs degradation, which utilize oxidants like hydrogen peroxide, ozone and peroxymonosulfate (PMS) to generate reactive species such as hydroxyl radicals ($\cdot\text{OH}$), sulfate radicals ($\text{SO}_4^{\cdot-}$) or other highly active species.[9] In principal, PMS can be reduced by thermal activation, UV irradiation, ultra-sonication, and catalytic activation with transition metal oxides.[10] However, the high price of catalysts and strict reaction requirements challenge the practical application of PMS based AOPs in environment remediation. Therefore, the natural mineral catalysts used in previous chapters have obvious advantages and broad prospects in this field.

As a part of sustainable development, the carbon footprint of catalysts should also be taken into consideration. The raw materials for synthetic catalysts, i.e. commercial grade transition metals, require extremely high energy consumption. For example, one



ton of iron particles consumes an average energy of 793.4 MJ/t, which is equivalent to the emission of 58.5 kg CO₂. [11] Take Germany as an example, which is a pioneer in environmental protection, this country releases 408 grams of carbon dioxide with producing per kilowatt of electricity on average. [12] In a normal production process, every ten grams of synthetic catalyst need to consume tens of kilowatts of electricity due to the high temperature and high pressure preparation environment. Therefore, natural ore catalysts without complicated processing requirements are much more eco-friendly in terms of sustainable development.

On the other hand, Western Australia is the main mining area in Australia and abundant in mineral deposits such as magnetite, bauxite and ferromanganese, most of which contain various transition metal elements. [13] Actually, mining is a pillar industry in Western Australia, accounting for more than half of exports and providing with quantities of jobs. [14, 15] However, since COVID-19 and China-US trade war, the price of ore especially iron ore has been fluctuating greatly, with the highest price being more than three times of the bottom. [16, 17] Moreover, as the per capita share of metal in emerging markets such as China continues to increase and gradually approaches the level of developed countries, recycled metals will account for an increasing consumption proportion, and the demand for incremental metal ore will gradually decrease. [18] Meanwhile, driving by the goal of carbon neutrality, smelting industry has gradually reduced its production capacity due to the high energy consumption. [19] Therefore, in the medium and long term, the prospects of Western Australia's mining industry are not optimistic. For this reason, the development of new possible scenarios for ore utilization has become a significant forward-looking subject.

In order to explore the possibility of *in-situ* catalytic degradation of organic pollutants via metal ore/PMS composite, a soil reaction simulation system was constructed in this study. The system mimics the basic process of soil reaction in principle, which is similar to soil washing method. The influence of various environmental factors on the degradation rate was investigated. Besides using tetrabromobisphenol A (TPPBA) as a model pollutant, industrial herbicide quinclorac was chosen to test the feasibility of this metal ore/PMS catalytic system as well. Moreover, the financial feasibility study was conducted to highlight the huge advantages of natural metal ore compared with synthetic metal catalysts.



6.2 Experimental Section

Materials and Chemicals. The manganese ore (MO) was provided by Karara Mining Ltd., Australia and OM Manganese Pty. Ltd., Australia. The composition of received ore was provided by mining companies as shown in Table 6.1. The manganese ore used in this study is the sample No. 5 (labelled as MO-5) in Chapter 3. Prior to the experiment, the chosen materials were washed with ultrasonic cleaner, filtered and then dried overnight. Subsequently, the ore samples were crushed to powder and sieved to a particle size of 50–60 μm for further use.

Table 6.1 The composition of manganese ore (MO) as received.

Composition	Formula	Content (wt%)
Braunite	$4\text{MnO}_3 \cdot 3\text{MnO}_2 \cdot \text{SiO}_2$	30%
Psilomelane	$\text{Ba} \cdot \text{Mn} \cdot \text{Mn}_8\text{O}_{16}(\text{OH})$	30%
Pyrolusite	MnO_2	30%
Quartz	SiO_2	10%

The sand was purchased from Burnings Group (Australia), which was clean playground sand. After soaking in 1% hydrochloric acid for 10 min, the sand was rinsed with deionized water until the pH was neutral. Dry in an oven at 200°C for 8 h to ensure that the weighed density is the original density of 1.5 g/ml for further use.

All chemicals including methanol, Peroxymonosulfate (OXONE) ($\geq 42.8\%$) and tetrabromobisphenol A (TBBPA, $\geq 97.0\%$) were purchased from Sigma-Aldrich, Australia. Contaminants were diluted by deionized water to the designed concentration. Due to the low solubility of TBBPA under standard pH condition, sodium hydroxide solution was added into the solution to adjust the pH to 11.

The industrial herbicide, quinclorac, was purchased from BASF through Living Turf in Western Australia. The commercial name of this herbicide is Drive XL. according to the safety data sheet, its content 15.93% quinclorac, 75% ethyleneglycol and 5% dimethylamine.

Soil contaminant degradation in liquid-solid reactor. As shown in Figure 6.1, the main body of the reactor was made of a 40 mm diameter round PVC pipe with a length of about 80 cm. There was a filter support device at the bottom of the reactor pipe to



fix the filter paper during the experiment. The ore catalyst and PMS were placed in the middle centre above the sand to simulate the rain infiltration effect under natural conditions. The targeted pollutants to be degraded were placed at the bottom of beaker. Contaminated solution was continuously circulated by a peristaltic pump to the top of the reactor, and then returned to the beaker after being catalytically degraded. 1 mL of solution was periodically withdrawn, while the concentration of TBBPA was measured by a JASCO UV–visible spectrophotometer at 464 nm.

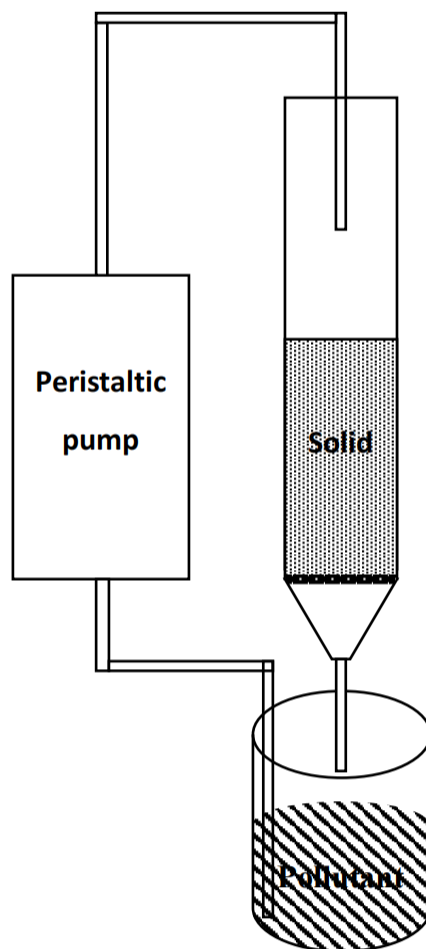


Figure 6.1 Schematic diagrams of the home-made pollutant degradation liquid-solid reactor.

Long-term degradation reactor: In order to study the catalytic degradation in the actual environment, another form of experiment was conducted.

The sand was soaked in the industrial herbicide quinclorac solution for 24 h. 15 g of the soaked solid particles were placed in a 20 ml glass vial and mixed with different quantity of PMS and natural metal ore. The vials were sealed and placed in an outdoor environment under direct sunlight for four weeks in order to explore the feasibility of



quinclorac degradation. A blank control group was also made to determine the photolysis of the herbicide. After four-week degradation procedure, 10 ml deionized water was mixed with the solid in glass vial. Then 1 mL of solution was withdrawn, filtered by 0.45 μm PEFT membrane, and then immediately mixed with 0.5 mL of methanol to quench the oxidation. The residual concentration of quinclorac was measured with an ultrahigh performance liquid chromatograph (UHPLC, Thermo Fisher Scientific UltiMate 3000) with a UV detector set at 240 nm.

6.3 Results and Discussion

As shown in the Figure 6.2 the natural metal mineral catalyst has an obvious catalytic degradation effect on organic pollutant TBBPA. At 30 minutes, the adsorption and PMS only curves hardly changed, meanwhile the ore/PMS curve has achieved a pollutant removal rate of more than 20%. The pollutants are almost completely degraded after 120 minutes of catalytic reaction. At the same time, PMS and MO act separately on the soil reactor has no obvious degradation results for the TBBPA pollutant. Which is basically point out that the PMS-natural ore system has the possibility apply in the in-situ solid remediation. The solid reactor was mimicking a rain-solid circle system in the lab. Even it was not fully considered about the soil dynamics.

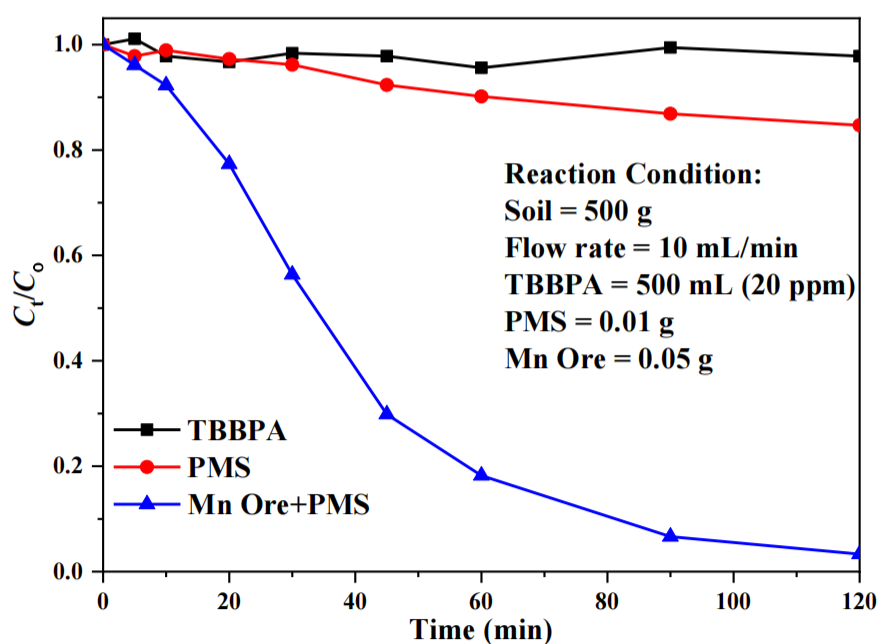


Figure 6.2 The AOP degradation of TBBPA by Mo/PMS system in a solid reactor.



The pollutant volume has an observable effect on the pollutant degradation rate in first hour, as shown in Figure 6.3. However, after 90 min, more than 90% pollutants were degraded. It can be seen from the degradation curve that the amount of pollutant has a negligible effect on the degradation effect. This negligible effect is advantageous for large-scale in-situ soil remediation, which means that the system has acceptable adaptability to different concentrations of pollutants.

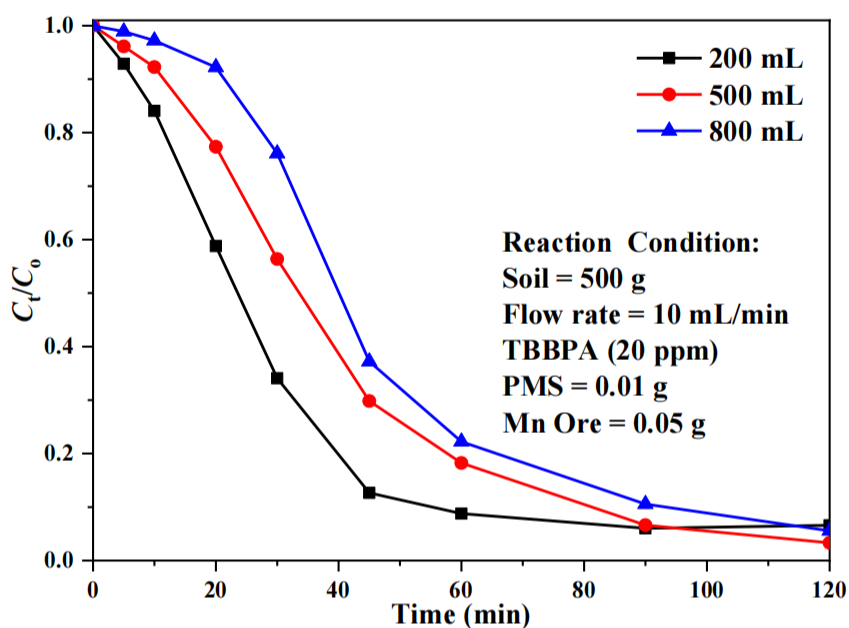


Figure 6.3 The effect of the volume of pollutants in solid reactor

As Figure 6.4 shows, the mass of the sand has no significant effect on the reaction rate. Although there was a ten-fold mass difference, the maximum concentration difference after degradation was less than 20% in the first half an hour. The pollutant concentration curve crosses at about 40 min and reaches a minimum at 60 min. The reason for this phenomenon may be that the initial small sand volume is beneficial to the diffusion of catalyst and PMS in the system. However, when the diffusion was complete, the less soil volume causes the reaction contact surface to become smaller, which leads to a lower degradation rate than the larger volume group. In the end, different volumes of soil can degrade more than 90% of the pollutants, indicating that the degradation efficiency of the reaction system in in-situ soil remediation is slightly affected by the volume of the sand, but it did not affect the final degradation results.

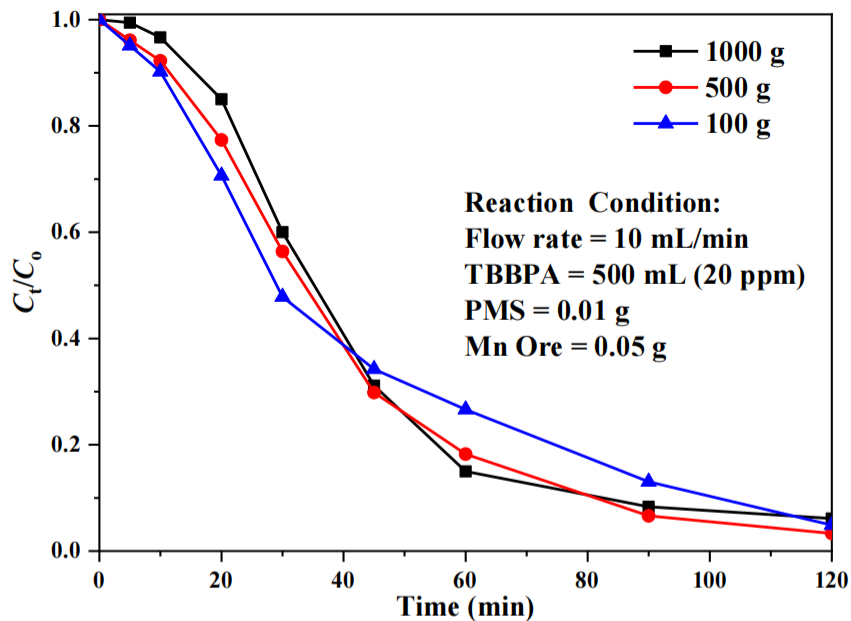


Figure 6.4 The effect of the volume of solid in liquid-solid reactor.

The degradation efficiency shows a significant difference in Figure 6.5 when the weight of the catalyst changes. At 30 min, the residual concentration of 0.1 g catalyst was nearly 50% higher than that of 0.025 g, and the concentration of pollutants in the 0.05 g experimental group was roughly in the middle of the two, indicating that the catalyst has a direct and relatively linear influences of degradation rate. As the concentration of pollutants decreases, the three sets of degradation curves tend to be consistent. This can be regarded as a decrease in the concentration of pollutants leading to a decrease in the degradation rate. Similar trends have appeared in the previous groups of this studies. Although the number of catalysts has a significant effect on the degradation rate, most of the pollutants are eventually removed from the system. This shows that even a small amount of catalyst can achieve feasible effects in large-scale in-situ soil remediation.

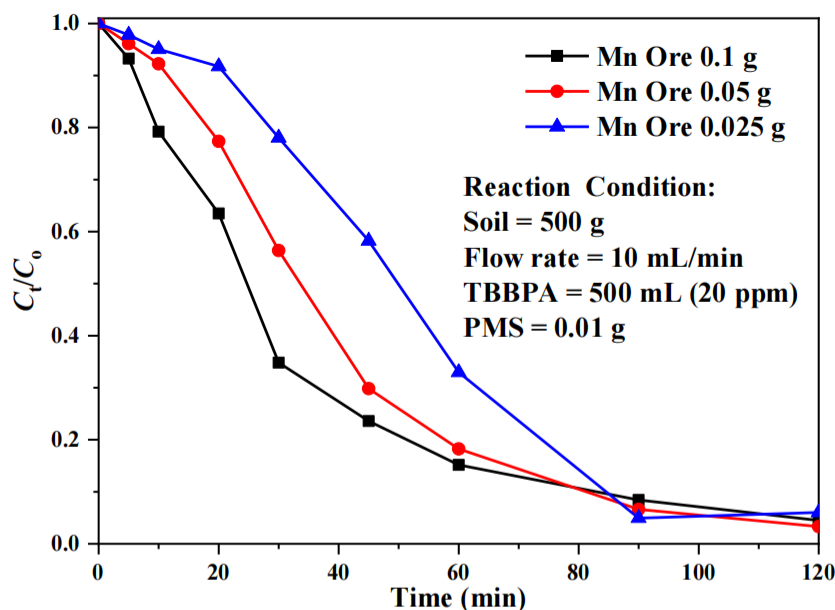


Figure 6.5 The dosage effect of the catalyst on TBBPA degradation.

The influence of flow rate on pollutant degradation was studied Figure 6.6. In the first 20 min, the difference in reaction rate basically obeys the difference in flow rate. However, as the concentration of pollutants decreases, the difference in reaction rate gradually becomes close. The response curves of the 20 ml/min group and the 10 ml/min group tended to be the same after 60 min. At the same time, the response curve of 1 ml/min group continued to decrease. We believe the reason of that is the pollutant concentration plays a leading role in the degradation rate at this stage. Although the small flow group only removed about 80% of the pollutants in 2 h, its degradation curve still had a significant downward trend, so it is reasonable to speculate that eventually more than 90% of the pollutant would be removed like the large flow group. From this experiment, it can be concluded that although the rainwater flow has a significant influence in this system. However, the rate in the late stage of the reaction is mainly determined by the concentration of pollutants. Therefore, even in a drier area, as long as a certain degree of basic rainfall or artificial labour can be guaranteed, the system could play a role in in-situ soil remediation, and it will have a better effect in humid climate areas.

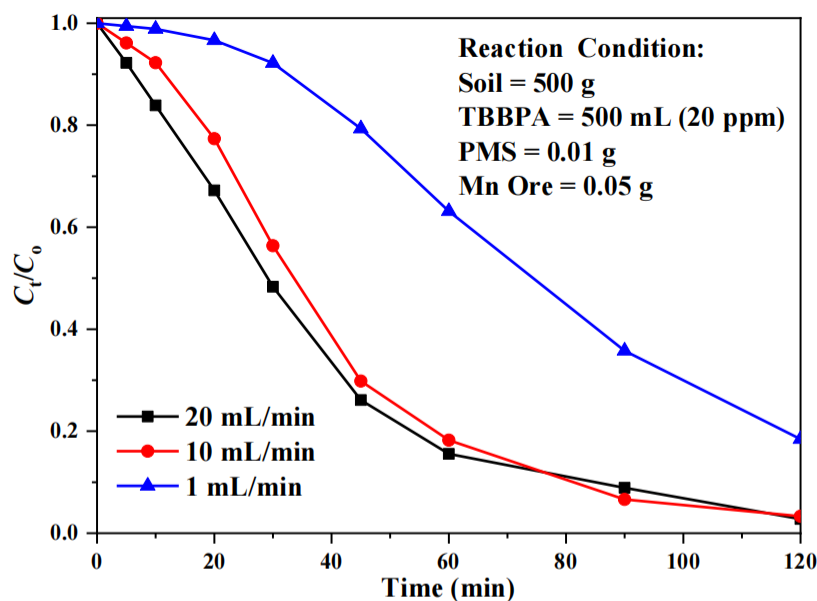


Figure 6.6 The effect of flow rate on TBBPA degradation in the liquid-solid reactor.

According to Figure 6.2, the PMS-natural metal ore system shows a potential possibility for in-situ soil remediation. This system has extremely low demand for PMS and ore catalysts and has excellent adaptability to pollutant concentrations. There is no obvious requirement for the volume of the soil of the plot and it can be applied in a semi-arid climate with low rainfall. Therefore, we believe that this is a very promising research direction in the field of soil in-situ remediation.

In order to further explore the potential of this technology in the field of soil remediation, the herbicide Drive XL, with active constituent of 180 g/L quinclorac, was used for long-term degradation studies. According to the user instruction, 4.6 L Drive XL was diluted with 400 L water, which produced around 10000 ppm of Drive XL. The concentration of active quinclorac would be 1593 ppm. Considering the dilution caused by subsequent experiments and extraction, we thought that the stock concentration of 10000 ppm was enough. The sand was soaked in Drive XL diluted to 10000, 5000, 2500, and 1000 ppm for 24 h to use in further research. The concentration of the soaking solution in the control group was further diluted to 10 ppm. 15 g of soaked sand was sealed in a 20 ml glass vial and placed in direct sunlight for 4 weeks. In the experimental group, the soil was mixed with various amounts of PMS and natural ore catalysts to explore the effect of degradation. However, when the glass vials extracted by 10 ml water to analysis by HPLC after four weeks, there was no quinclorac detected, even in the control group. We believe that there are several possible reasons may cause this



situation. The first possibility is that the herbicide was over-diluted and out of the detectable range during the soaking and extraction process. The amount of pollutants that the sand can adsorb during the soaking process was unable to predict. Secondly, it is possible that other components of the herbicide, the ethanol that quenched the reaction, and the mobile phase caused the HPLC detection to fail. The third reason may be that industrial herbicides are used instead of pure pollutants. There may be a degradable mechanism in the design, which makes the main components unable to be detected in long-term experiments.

To demonstrate the comparative advantages of natural ore and synthetic transition-metal catalysts in large-scale soil in-situ remediation, a financial feasibility study was carried out and results are shown in Table 6.2. The price of chemical products mainly derives from the price of metal elements provided by Sigma to represent the approximate cost of the basic raw materials required for the laboratory synthetic catalyst. Metal prices refer to the time-sharing average price of the spot trading market in China, which is the largest producer of steel and metal finished products. Metal smelting products are generally used as industrial raw materials. In this study, it represents the lowest raw material price of laboratory-grade synthetic catalysts after the completion of industrialized large-scale production conversion. The price of ore was taken from the approximate price of the international ore futures trading market. Due to the classification of ore with different purity, we used the highest purity refined ore as the price index. This action can ensure that our ore price is higher than the actual situation. As shown in Table 6.2, the price of chemicals is two orders of magnitude higher than that of industrial metal smelting products. Even cobalt, which is a rare element, has a chemical price four times higher than that of metal. The price of common metals is five times that of bulk refined ore. And the price of the rare metal cobalt ore is only 3% of its metal price. In the process of making synthetic metal catalysts, many additional chemical products are required. Therefore, the actual catalyst raw material price difference must be greater than data shown in Table 6.2 because most of the industrial or laboratory chemicals used in this process are more expensive than ordinary metal products. For example, the raw material cost of the synthetic catalyst used in Chapter 5 exceeds 2,000 Australian dollars, while the finished product we synthesized was less than 500 g. In addition, synthetic catalysts require a lot of chemical experiment equipment including but not limited to muffle furnace, high pressure reactor, fume hood,



etc. Considering the cost of various consumables and equipment in the process, the current price of transition-metal catalysts is about thousands of Australian dollars per kilogram. Even if industrialized production can greatly reduce its manufacturing costs, its price will still be hundreds of times that of natural metal ore catalysts. Therefore, natural metal ore catalysts have incomparable financial advantages in activating PMS to degrade organic pollutants in large-scale soil remediation.

Table 6.2 The price of the main components of the transition-metal catalyst.

Price (AUD/kg)	Fe	Mn	Co
Analytical reagents	71	238	1088
Metal	0.60	2	267.5
Ore	0.15	0.41	7.94

To achieve an environmentally sustainable society, a significantly reduced carbon footprint needs to be achieved. As we all know, whether it is industrial product of metals or chemicals, the source of raw materials is metal ore. In the process of purifying metal ore, high temperature is indispensable therefore metal smelting is an industry with high energy consumption and high pollution. These industries have shifted from developed countries to developing countries in the past few decades due to high pollution. In the past ten years, 1.8 tons of carbon dioxide were emitted for every ton of steel produced. Even without considering the carbon emission in the purification of metal raw materials, only the high temperature and high pressure conditions required in the synthetic catalyst process creates a large amount of carbon footprint. In the process of synthesis of Chapter 5 synthetic catalyst, only the power consumption in drying process emits several kilograms carbon dioxide. Taking into account the various materials and equipment required for the production of synthetic catalysts, the full cycle carbon footprint may be as high as tens of kilograms, or even hundreds of kilograms per kilogram of catalyst depends on the synthesis method. In-situ soil remediation is an important part of environmental protection, and the environmental impact in the process needs to be fully considered. Therefore, considering the level of global carbon



neutrality, natural metal ore catalysts have a non-negligible advantage over synthetic catalysts.

6.4 Conclusions

Manganese natural metal ore catalyst was used in the simulation study of in-situ soil remediation and achieved good results. The catalyst and PMS content required to achieve effective remediation is extremely low, which can be as low as one hundredth or even one thousandth of the weight of the soil. The system has excellent adaptability to the concentration of pollutants. Although the application of in-situ soil remediation requires the participation of water, rainfall only affects the degradation rate and does not affect the final desirable degradation effect, so the system can be adapted to different climatic environments. At the same time, research on financial feasibility and carbon footprint shows that natural metal ore catalysts have unparalleled significant advantages over synthetic catalysts in terms of finance and environmental protection. This study fully illustrates the great potential of natural transition-metal ore catalysts in replacing synthetic transition-metal catalysts for large-scale in-situ soil remediation. However, soil dynamics is an extremely complex field, and further research is needed to conduct in order to accomplish the PMS-transition metal ore catalyst system in large-scale in-situ soil remediation.



References

1. Delang, C.O., *Causes and distribution of soil pollution in China*. Environmental & Socio-economic Studies, 2017. **5**(4): p. 1-17.
2. Cabral-Pinto, M.M., et al., *Human health risk assessment due to agricultural activities and crop consumption in the surroundings of an industrial area*. Exposure and Health, 2020. **12**(4): p. 629-640.
3. Rabani, M.S., A. Habib, and M.K. Gupta, *Polycyclic Aromatic Hydrocarbons: Toxic Effects and Their Bioremediation Strategies*, in *Bioremediation and Biotechnology, Vol 4*. 2020, Springer. p. 65-105.
4. Steffan, J., et al., *The effect of soil on human health: an overview*. European journal of soil science, 2018. **69**(1): p. 159-171.
5. Thompson, L.A. and W.S. Darwish, *Environmental chemical contaminants in food: review of a global problem*. Journal of toxicology, 2019. **2019**.
6. Yilmaz, B., et al., *Endocrine disrupting chemicals: exposure, effects on human health, mechanism of action, models for testing and strategies for prevention*. Reviews in endocrine and metabolic disorders, 2020. **21**(1): p. 127-147.
7. Cagnetta, G., J. Huang, and G. Yu, *A mini-review on mechanochemical treatment of contaminated soil: From laboratory to large-scale*. Critical Reviews in Environmental Science and Technology, 2018. **48**(7-9): p. 723-771.
8. Sun, S., et al., *Pesticide pollution in agricultural soils and sustainable remediation methods: a review*. Current Pollution Reports, 2018. **4**(3): p. 240-250.
9. Gaur, N., K. Narasimhulu, and Y. PydiSetty, *Recent advances in the bio-remediation of persistent organic pollutants and its effect on environment*. Journal of cleaner production, 2018. **198**: p. 1602-1631.
10. Kundu, P. and I.M. Mishra, *Treatment and reclamation of hydrocarbon-bearing oily wastewater as a hazardous pollutant by different processes and technologies: a state-of-the-art review*. Reviews in Chemical Engineering, 2019. **35**(1): p. 73-108.
11. Lv, W., Z. Sun, and Z. Su, *Life cycle energy consumption and greenhouse gas emissions of iron pelletizing process in China, a case study*. Journal of Cleaner Production, 2019. **233**: p. 1314-1321.
12. Icha, P., T. Lauf, and G. Kuhs, *Development of specific carbon dioxide emissions of the German electricity mix in the years 1990-2020*. 2021.
13. Maxwell, P., *The end of the mining boom? A Western Australian perspective*. Mineral Economics, 2018. **31**(1): p. 153-170.
14. government, W.A.s. *Western Australia's economy and international trade*. 2021; Available from: <https://www.wa.gov.au/government/publications/western-australias-economy-and-international-trade>.
15. Flint, D., et al., *The importance of iron ore to Western Australia's economy*. AusIMM Bulletin, 2018(Jun 2018).
16. Löf, A. and O. Löf, *This Year's Iron Ore Report Looks Much Better Than Many Expected*. Engineering and Mining Journal, 2020. **221**(11): p. 28-33.
17. Jones, O., *Coronavirus and its current impact on the mining industry*. Gold Mining Journal, 2021. **1**(144): p. 12-13.



18. Burke, P.J., *Metal footprint linked to economy*. Nature Geoscience, 2018. **11**(4): p. 224-225.
19. Azadi, M., et al., *Transparency on greenhouse gas emissions from mining to enable climate change mitigation*. Nature Geoscience, 2020. **13**(2): p. 100-104.

Every reasonable effort has been made to acknowledge the owners of copyright material. I would be pleased to hear from any copyright owner who has been omitted or incorrectly acknowledged.



Chapter 7 Conclusions and recommendations

7.1 Conclusions

To summarise, many remediation technologies have been developed for wastewater and soil contaminants removal. Advanced oxidation processes (AOPs) are able to oxidise basically any organic pollutants present in the water matrix through in-situ production of highly reactive oxygen species. All previous studies focus on synthesizing catalysts via multistep and complicated fabrication procedures therefore limit the adaption of AOPs on a large scale. Finding economic catalyst for AOPs, this PhD tends to employ natural ores to deliver environmentally responsible solution for effective contaminants degradation. From the experimental results presented in the thesis, conclusions can be drawn as follows.

Firstly, the catalytic performance of manganese ore has been investigated to reduce peroxomonosulfate (PMS) for hydroxyl radicals ($\cdot\text{OH}$) and sulfate radicals ($\text{SO}_4^{\cdot-}$) production. One of the major compounds of manganese ore is manganese dioxide (MnO_2). The combination of commercial-grade ore and PMS effectively oxidized tetrabromobisphenol A (TBBPA) and rhodamine B (RB) without discrimination. This shows the great potential of transition metal containing ores in the field of environmental protection.

Secondly, we observed effective activation of PMS by bauxite ore, largely composed of a mixture of hydrous aluminium oxides and two iron oxides goethite ($\text{FeO}(\text{OH})$) and haematite (Fe_2O_3). The results of the EPR demonstrate that $\cdot\text{OH}$ and $\text{SO}_4^{\cdot-}$ are the main active radicals for persistent organic pollutants degradation.

Thirdly, we evaluated the catalytic performance of the synthetic $\text{TiO}_2/\text{Al}_2\text{O}_3$ composite hollow fiber in PMS based advanced oxidation of organic pollutants. It is found that the catalytic efficiency of natural metal minerals in the AOP process is within an acceptable range compared with synthetic $\text{TiO}_2/\text{Al}_2\text{O}_3$ composite hollow fibres. The study of catalytic influencing factors also performed that the natural ore/PMS system has strong adaptability under most temperature and pH environments, which shows reasonable catalytic efficiency under different conditions. At the same time, the secondary contamination study also shows that the potential pollution caused by the system was within the law limit.



Fourthly, we attempted to investigate the possibility of large-scale application of natural ore/PMS system for in-situ soil remediation and explored some factors such as flow rate, soil value, catalyst that may influence its efficiency.

Finally, the financial feasibility study demonstrates the huge cost advantage of natural metal ore catalysts compared to synthetic catalysts. Carbon footprint research illustrates the potential environmental advantages of natural ore catalysts compared to biomass carbon-based catalysts produced after high temperature burning.

In this PhD thesis, natural ores were extensively studied to present their advantages over other synthetic catalysts. The overall results prove that natural transition metal ore is an efficient and low-cost alternative to metal catalysts. The strategy developed in this thesis can pave the road for further adaption of AOPs which is still in the early stage and need more investigation to reduce the cost. The following recommendations can help to mature this novel chemical treatment procedure.

7.2 Perspectives and suggestions for future research

Regarding the applications of natural ores for AOPs, more studies need to be carried out to deeply investigate their shortcomings and potentials. Here are some recommendations for future works:

1. Because of the heterogeneity of the ore, the degradation efficiencies showed fluctuation even when the ore samples came from the same batch. Although this study tried to accurately determine the composition of ore and find a feasible way to predict the catalytic effectiveness, this goal was not achieved due to constrained sample size. Pilot scale test should be carried out to improve the assessment accuracy.
2. Except for PMS, other primary oxidants such as hydrogen peroxide (H_2O_2) and peroxydisulfate (PDS) can be conjugated with natural ores for more economic in situ chemical oxidation.
3. $\cdot\text{OH}$ and $\text{SO}_4^{\cdot-}$ can kill waterborne pathogens like bacteria and viruses, which makes primary oxidant/ore system a constructive solution to microorganism contamination problems.

All in all, natural ores need more development before competing with the synthetic catalysts. With the experiences of manganese and bauxite ores, it is believed that



AOPs might show great potential in terms of degradation performance and economics.

Every reasonable effort has been made to acknowledge the owners of copyright material. I would be pleased to hear from any copyright owner who has been omitted or incorrectly acknowledged.



Appendix I: Attribution Tables

Paper: Efficient removal of organic pollutants by ceramic hollow fibre supported composite catalyst. Ning Han., Zhengxin Yao., Heng Ye., Chi Zhang., Ping Liang., Hongqi Sun., Shaobin Wang., Shaomin Liu. Sustainable Materials and Technologies, 2019, 20, e00108.

	Conception and design	Experiments conduction & data acquisition	Data processing & analysis	Interpretation & discussion	Manuscript writing, revision and finalisation	Final Approval
Zhengxin Yao	×	×	×	×	×	
I acknowledge that these represent my contribution to the above research output. Sign:						
Ning Han	×	×	×	×	×	
I acknowledge that these represent my contribution to the above research output. Sign:						
Heng Ye		×				
I acknowledge that these represent my contribution to the above research output. Sign:						
Chi Zhang			×			
I acknowledge that these represent my contribution to the above research output. Sign:						
Ping Liang	×				×	
I acknowledge that these represent my contribution to the above research output. Sign:						
Hongqi Sun			×			×
I acknowledge that these represent my contribution to the above research output. Sign:						
Shaobin Wang			×			×
I acknowledge that these represent my contribution to the above research output. Sign:						
Shaomin Liu	×				×	×
I acknowledge that these represent my contribution to the above research output. Sign:						



Appendix II: Copyright Permission Statements

Chapter 1

Figure 1.1 (a) & (b):

<https://ourworldindata.org/water-access#the-global-distribution-of-deaths-from-unsafe-water>

- To reach universal access within 10 years (the current gap is 26%) we need to see a 13 percentage point increase every five years. That's 3.25 times higher than the 4 percentage point increase we've seen in the last five years.
- Spence, M., Annez, P. C., & Buckley, R. M. (2009). *Urbanization and growth: commission on growth and development*. Available [online](#).
- World Bank & WHO/UNICEF Joint Monitoring Programme (JMP) for Water Supply and Sanitation. World Development Indicators Metadata. Available [online](#).

Reuse our work freely

All visualizations, data, and code produced by Our World in Data are completely open access under the [Creative Commons BY license](#). You have the permission to use, distribute, and reproduce these in any medium, provided the source and authors are credited.

The data produced by third parties and made available by Our World in Data is subject to the license terms from the original third-party authors. We will always indicate the original source of the data in our documentation, so you should always check the license of any such third-party data before use and redistribution.

All of our [charts can be embedded](#) in any site.


Chapter 2


Figure 2.1:

License Number	5197410390690	Printable Details
License date	Nov 27, 2021	
Licensed Content		Order Details
Licensed Content Publisher	Elsevier	Type of Use
Licensed Content Publication	Chemical Engineering Journal	reuse in a thesis/dissertation figures/tables/illustrations
Licensed Content Title	Chemistry of persulfates in water and wastewater treatment: A review	Number of figures/tables/illustrations
Licensed Content Author	Stanislaw Wacławek, Holger V. Lutze, Klaudiusz Grübel, Vinod V.T. Padil, Miroslav Černík, Dionysios.D. Dionysiou	Format
Licensed Content Date	Dec 15, 2017	both print and electronic
Licensed Content Volume	330	Are you the author of this Elsevier article?
Licensed Content Issue	n/a	No
Licensed Content Pages	19	Will you be translating?
		No
About Your Work		Additional Data
Title	Natural metal/oxides for catalytic oxidation of persistent organic pollutants (POPs) in contaminated water and soil	Portions
Institution name	Curtin University	Figure 2
Expected presentation date	Nov 2021	



Chapter 5

Home ? Help ✉ Email Support 👤 Sign in 👤 Create Account



Efficient removal of organic pollutants by ceramic hollow fibre supported composite catalyst

Author: Ning Han,Zhengxin Yao,Heng Ye,Chi Zhang,Ping Liang,Hongqi Sun,Shaobin Wang,Shaomin Liu

Publication: Sustainable Materials and Technologies

Publisher: Elsevier

Date: July 2019

© 2019 Elsevier B.V. All rights reserved.

Journal Author Rights

Please note that, as the author of this Elsevier article, you retain the right to include it in a thesis or dissertation, provided it is not published commercially. Permission is not required, but please ensure that you reference the journal as the original source. For more information on this and on your other retained rights, please visit: <https://www.elsevier.com/about/our-business/policies/copyright#Author-rights>

BACK

CLOSE WINDOW